Long-term Climate Variability of the Baltic Sea Region

Kumulative Dissertation
zur Erlangung des akademischen Grades
doctor rerum naturalium (Dr. rer. nat.)
der Mathematisch-Naturwissenschaftlichen Fakultät
der Universität Rostock
vorgelegt von

Florian Börgel
geb. am 22.02.1991 in Münster

Juni 2020

https://doi.org/10.18453/rosdok_id00002798

Gutachter*innen:
1. Gutachter
Prof. Dr. H.E. Markus Meier
Leibniz-Institut für Ostseeforschung Warnemünde
2. Gutachterin
Prof. Dr. Anna Rutgersson
Uppsala University
3. Gutachter
Prof. Dr. Arne Biastoch
Geomar Helmholtz-Zentrum für Ozeanforschung Kiel

Datum der Einreichung: 15.06.2020
Datum der Verteidigung: 14.10.2020

Thesis advisor: Prof. Dr. H. E. Markus Meier Florian Börgel

Long-term Climate Variability of the Baltic Sea Region

Abstract

This thesis analyzes the impact of the Atlantic Multidecadal Oscillation (AMO) on North European climate and traces the AMO signal into the Baltic Sea region. With a frequency of 50 - 90 years, effects of the AMO are difficult to evaluate, since observations are limited to about 150 years. To overcome this lack of observational data, a combination of a general circulation model (GCM) and a regional climate model (RCM) is used to analyze the pre-industrial period from 950 - 1800. Further, the importance of the AMO for the more recent period 1850 - 2008 is discussed.

This work can be separated into three different topics: First, the impact of the AMO on the Baltic Sea is shown. This study reveals that AMO-related changes of the atmospheric circulation affect precipitation over the Baltic Sea region, which in turn alter the river runoff and consequently the salinity of the Baltic Sea. A persistent coherence between the AMO and the mean salinity of the Baltic Sea is found, which suggests that the Baltic Sea is under the constant influence of the AMO.

Second, it is found that the AMO changes the zonal position of the North Atlantic Oscillation (NAO). Using a RCM it is shown that the AMO changes the spatial structure of the NAO. The spatial position of the NAO plays a crucial role for its regional importance. It either reduces or enhances the NAO's influence on regional climate variables of the Baltic Sea such as sea surface temperature (SST), ice extent or river runoff.

Third, the SST variability of the Baltic Sea during the period 1850 - 2008 is analyzed. It is shown that the main driver of the SST is the air temperature. By analyzing the importance of large-scale climate variability it is found that the AMO is responsible for 60 % of the Baltic Sea SST variability on decadal time scales. Hence, the often reported strong SST trend during 1982 - 2006 in the Baltic Sea can be explained by an AMO shift from a negative towards a positive phase.

In summary, this work shows that the AMO plays an important and often neglected role for the climate of the Baltic Sea.

Zusammenfassung

Diese Arbeit untersucht die Auswirkungen der Atlantischen Multidekaden-Oszillation (AMO) auf das nordeuropäische Klima und verfolgt das AMO-Signal in der Ostseeregion. Beobachtungsdaten sind auf etwa 150 Jahre begrenzt. Aufgrund der AMO-Frequenz von 50 bis 90 Jahren ist es daher unmöglich, konkrete Aussagen über den Effekt der AMO zu treffen, da kaum zwei volle AMO-Zyklen erfasst werden. Um dieses Problem zu vermeiden, werden in dieser Arbeit numerische Modelle verwendet: Mit einer Kombination aus einem globalen Zirkulationsmodell (GCM) und einem regionalen Klimamodell (RCM) wird der vorindustrielle Zeitraum von 950 bis 1800 analysiert. Darüber hinaus wird die Bedeutung der AMO für den Zeitraum von 1850 bis 2008 diskutiert.

Diese Arbeit kann in drei verschiedene Themenbereiche unterteilt werden:

Erstens werden die Auswirkungen der AMO auf die Ostsee anhand eines regionalen Klimamodells untersucht. Diese Analyse hat gezeigt, dass AMO-bedingte Veränderungen der atmosphärischen Zirkulation sich auf die Niederschläge im Ostseeraum auswirken. Diese verändern wiederum den Frischwassereintrag in die Ostsee und folglich auch den Salzgehalt der Ostsee. Außerdem wird mit Hilfe einer Wavelet-Kohärenz gezeigt, dass die Ostsee während des gesamten Modellzeitraums durchgehend durch die AMO beinflusst wird.

Zweitens wird gezeigt, dass die AMO die zonale Position der Nordatlantikoszillation (NAO) verändert. Die räumliche Position der NAO ist entscheidend für ihre regionale Bedeutung für das Klima der Ostsee. Abhänging von ihrer Entfernung von Europe reduziert oder verstärkt sich der Einfluss der NAO auf regionale Klimavariablen der Ostsee wie die Meeresoberflächentemperatur (SST), Eisausdehnung oder Frischwassereintrag.

Drittens wird die Variabilität der SST im Zeitraum 1850 bis 2008 analysiert. Dabei wird gezeigt, dass hauptsächlich die Lufttemperatur für Veränderungen der SST verantwortlich ist. Änderungen in der SST werden auf dekadischer Skala maßgeblich durch die AMO beeinflusst. Mit rund 60 % hat die AMO damit den größten Einfluss auf Änderungen der SST Variabilität. Daher kann der starke SST-Trend der Ostsee von 1982 bis 2006 durch einen Übergang von einer negativen in eine positive AMO Phase erklärt werden.

Zusammenfassend zeigt diese Arbeit, dass die AMO eine wichtige und oftmals nicht berücksichtigte Rolle für das Klima der Ostsee spielt.

Contents

Publications

Publications for the cumulative dissertation

A Börgel, F., *Frauen, C., Neumann, T., Schimanke, S., and Meier, H. E. M.* (2018). Impact of the Atlantic Multidecadal Oscillation on Baltic Sea variability. Geophysical Research Letters, 45, 9880– 9888. https://doi.org/10.1029/2018GL078943

B Börgel, F., *Frauen, C., Neumann, T and Meier, H. E. M.* (2020). The Atlantic Multidecadal Oscillation controls the impact of the North Atlantic Oscillation on North European climate. Environmental Research Letters, (under review)

C *Kniebusch, M., Meier, H. E. M., Neumann, T.,* and Börgel, F. (2019). Temperature variability of the Baltic Sea since 1850 and attribution to atmospheric forcing variables. Journal of Geophysical Research: Oceans, 124, 4168– 4187. https://doi.org/10.1029/2018JC013948

Other peer-reviewed publications

- *Meier H. E. M,* Börgel F., *Frauen C. and Radtke H.* (2020) Commentary: Lake or Sea? The Unknown Future of Central Baltic Sea Herring. Front. Ecol. Evol. 8:55. doi: http://10.3389/fevo.2020.00055
- *Radtke, H.,* Börgel, F., *Brunnabend, S.-E., Eggert, A., Kniebusch, M., Meier, H.E.M., Neumann, D., Neumann, T. and Placke, M.*, (2019). Validator – a Web-Based Interactive Tool for Validation of Ocean Models at Oceanographic Stations. Journal of Open Research Software, 7(1), p.18. doi: http://doi.org/10.5334/jors.259

Conferences

- Impact of the Atlantic Multidecadal Oscillation on Baltic Sea variability
  Börgel, F., *Frauen, C., Neumann, T., Schimanke, S., and Meier, H. E. M*
  Poster | EGU General Assembly 2019 | Vienna, Austria | 12.04.2019

- Impact of the Atlantic Multidecadal Oscillation on Baltic Sea variability
  Börgel, F., *Frauen, C., Neumann, T., Schimanke, S., and Meier, H. E. M*
  Talk | 2nd Baltic Earth Conference | Helsingør, Denmark | 14.06.2018

- The Impact of Sea Ice on Baltic Inflows
  Börgel, F. *and Neumann, T.*
  Poster | Baltic Sea Science Congress 2017 | Rostock, Germany | 15.06.2017

Listing of figures

Abbrevations

AH	Azores High
AMO	Atlantic Multidecadal Oscillation
BP	Before Present
CWT	Continuous Wavelet Transformation
ENSO	El Niño / Southern Oscillation
EOF	Empirical Orthogonal Function
GCM	General Circulation Model
HadISST	Hadley Centre Sea Ice and Sea Surface Temperature
IL	Icelandic Low
IPCC	Intergovernmental Panel on Climate Change
MOM	Modular Ocean Model
NAO	North Atlantic Oscillation
NH	Northern Hemisphere
RCA3	Rossby Centre Atmosphere Model 3
RCM	Regional Climate Model
RCO	Rossby Centre Ocean Model
SAT	Surface Air Temperature
SLP	Sea Level Pressure
SSS	Sea Surface Salinity
SST	Sea Surface Temperature
WTC	Wavelet Coherence

Come on kid, this is your dream.

Acknowledgments

If I said that my doctoral thesis has determined my life during the past months or so I'd be lying. Within a year everything in my life changed since becoming a father. Nevertheless, I am incredibly grateful to have the opportunity to pursue a PhD.

I guess I could just thank everyone and get to the interesting stuff, however, I feel that I need to stress what this means to me. I remember when I started my bachelors, I was not even interested in my field of study or anything else. Right now, I feel that I work in a field that I love and I'll probably never be bored. Therefore, thank you Marie for pushing me to do something that I am passionate about. I know that pursuing a PhD is about getting ready for a career in academia and I really enjoyed the process. It showed me that research and especially climate research matters. I am working in a field that is shaping our future as I type. I feel that I have the responsibility to communicate that. So, yeah, good choice to quit engineering, I guess.

A big part of this process was my supervisor Markus. Thank you for your support during that time. I always had and have the feeling that you care. Also thank you for replying to mails at 1 am. Claudia, my second supervisor, was also always there to help. I enjoyed working with you and it is a pity that you left IOW for DKRZ in Hamburg. A special thanks goes out to Thomas who also took a lot of time to listen to my problems I was facing during my PhD.

One of the best parts working at IOW was having such nice and supportive colleagues. Thank you Marvin, Anja, Hagen, Madline, Peter, Knut, Daniel, Fatemeh, Ulf, Celine, Jen-Ping, and Jan and all the others. Thanks Lolle for the support from underneath my desk.

Mama und Papa, danke für eure Unterstützung. Ich weiß, ich wiederhole mich, aber das ist wahrscheinlich die letzte Danksagung, die ich schreibe. Danke, dass ihr mir immer das Gefühl gebt, dass ich alles richtig mache, egal wie abwegig meine Entscheidung ist.

Auch wenn ich jetzt nicht alle Freunde aufzählen will, möchte ich doch Gregor, Michi, Yeşim und Luis danken. Gut, dass wir euch als Patenonkel und -tante für immer an uns gebunden haben.

Zum Schluss, danke Marie - für alles. Ich hatte jetzt seit über 7 Jahren keinen schlechten Tag und das nur dank dir. Hey Leo, dein Papa ist jetzt bald Doktor!

Those who do not move, do not notice their chains.

Rosa Luxemburg

1 Introduction

What drives our climate system? Ultimately, the main driver of the climate system is the sun. Climate variations can be caused by external forcing such as changes in the solar radiation, volcanic eruptions, or greenhouse gas emissions. Changes in the climate system may also result from internal interactions between the components of the climate system itself, such as the atmosphere and the ocean. The Earth's climate system is never in equilibrium. There is a constant exchange of mass, momentum, and energy between all of its components. Although many processes are non-linear, these interactions are predictable to a certain degree (Libardoni et al., 2019). Understanding the key mechanisms of natural climate variations is essential to further improve predictions of changes in the earth system. However, understanding internal variability and its influence on climate is challenging. While the response time of the atmosphere is relatively fast, ranging from days to weeks, the response of the ocean is much slower due to the large heat capacity of the ocean (IPCC, 2013). Long time scales make it even more difficult to understand changes in the climate, since measurement

data are only available to a limited extent. A common approach to deal with the problem of undersampling is to use numerical models. The ability of global climate models (GCMs) to simulate historical climate change, regional modes of variability, and variations on different time scales has improved immensely over the past years. Still, even the most advanced GCMs have their limitations when it comes to confident statements of future climate projections (IPCC, 2013). Besides GCMs, regional climate models (RCM) play a particularly important role. They cover a smaller area and can have a higher spatial resolution, which allows to analyze climate variability on a regional scale that is not captured by the GCM. However, the quality of the projection is still determined by the GCM, since RCMs are driven by GCMs.

Coastal seas such as the Baltic Sea are among the most socioeconomically used areas on the planet. They are under the permanent influence of both anthropogenic pressure and natural climate variability. The Baltic Sea is a very prominent example for coastal seas since it responds very sensitively to external forcing. Therefore, the Baltic Sea can be viewed as a laboratory to analyze the impact of internal variability on its ecosystem which then could be projected onto other coastal seas (Reusch et al., 2018). The most important climate mode for the climate of the Baltic Sea is the North Atlantic Oscillation (NAO). Therefore, studies about the climate of the Baltic Sea often only consider the impact of the NAO. However, the impact of another important climate mode in the Northern Hemisphere – the Atlantic Multidecadal Oscillation (AMO) – is neglected, since its impact is mostly relevant on multidecadal time scales.

Up to this point no study has been able to show whether a teleconnection between the AMO and the Baltic Sea region exists. Therefore, this work aims at analyzing the impact of the AMO on the Baltic Sea region, using global and regional climate models. In a second step the interaction between two of the most dominant climate modes in the Northern Hemisphere, the NAO and the AMO, is analyzed. Can the state of the AMO alter the spatial position of the NAO, moving its centers towards Europe? And does the position of the NAO centers affect the NAO's regional importance for the Baltic Sea?

Although the AMO is a mode of natural climate variability, a better understanding helps

to grasp how it affected the climate of the past. This allows to assess its future impact on anthropogenic climate change. This means understanding the AMO's spatial and temporal pattern will provide information about whether it will amplify or dampen anthropogenic climate change in the coming decades. Finally, this all leads to the question: What is the role of the AMO for the climate of Northern Europe and especially for the Baltic Sea? The AMO fluctuates on multidecadal time scales. Therefore, trend estimates shorter than a full AMO cycle are likely biased by this multidecadal climate mode.

In the following the reader will be introduced to modes of climate variability with a focus on both climate modes that are analyzed in this work – the NAO and the AMO. Then a brief overview over the characteristics of the Baltic Sea is given. Following, the data used and a description of the relevant methods is summarized in the chapter 'Data & Methods'. In chapter 4, the three publications and their main results are presented. Finally, the significance of these results for regional climate research and especially the Baltic Sea region is discussed.

Why quantum mechanics? And why turbulence?

Werner Heisenberg

2

Modes of climate variability

Atmosphere, ocean, cryosphere, and continental hydrology exchange mass, momentum, and energy causing fluctuations in global- or regional-scale climate variables, such as sea surface temperature (SST), precipitation, and sea surface pressure (de Viron et al., 2013). Time scales of these fluctuations vary from days to centennials and can be summarized as modes of climate variability. Identifying climate modes helps to understand our climate system. They simplify high-dimensional systems and provide a better predictive capacity (Wang and Schimel, 2003). According to the World Meteorological Organization the average weather, better known as climate, is defined as periods longer than 30 years. Hence, the term climate variability aims at explaining variations in the mean state and other statistics of the climate "on all spatial and temporal scales beyond that of individual weather events" (IPCC, 2013). Examples of climate variability can be found throughout time: During the last 500,000 years there were only four full glacial cycles, caused by changes to the Earth's orbital parameters. The last glacial period (115,000 BP - 11,700 BP) was characterized by strong temperature variations while the past

10,000 years have seen more constant temperatures. The past 1,000 years were dominated by a warm period from the 11th to the 13th century, followed by a cold period from the 16th to the 19th century. These periods are commonly known as the Medieval Climate Anomaly (MCA) and the Little Ice Age (LIA; Mann et al., 2009). Regional patterns of climate are typically much more variable than global climate, and the involved time scales are shorter. Regional climate modes are found by decomposing the spatio-temporal variability of the atmosphere or the ocean into spatial patterns that change in magnitude over time. While some modes affect the climate of large parts of the Earth, others have smaller-scale effects, affecting only local climate conditions. It is striking how some climate modes affect the weather halfway across the globe. These long-distance effects are called teleconnections. The most prominent climate mode, the so called El Niño / Southern Oscillation (ENSO), is associated with SST changes in the central equatorial Pacific Ocean. It affects weather all over the globe from Peru to North America and from Australia to east Africa. If climate modes and their teleconnections are interpreted correctly, the predictability of regional climate conditions can be increased. However, one difficulty regarding reliable predictions is that the temporal variability of a climate mode can change stochastically. Further, the effect of one climate mode can be either compensated for or enhanced by another climate mode. Another difficulty is that the temporal variability of climate modes can be affected by the interaction between two modes. Therefore, when studying regional climate, it is necessary to understand how relevant climate modes interact. In the following, two dominant modes of the climate of the Northern Hemisphere are introduced; First, the North Atlantic Oscillation (NAO) and second, the Atlantic Multidecadal Oscillation (AMO). In addition, current research results on how they influence European climate and the Baltic Sea region are discussed.

2.1 North Atlantic Oscillation

During winter the most dominant and recurrent mode of climate variability in the Northern Hemisphere (NH) is the NAO. The NAO is primarily an atmospheric phenomenon and is characterized by a sea level pressure (SLP) difference between the subpolar low-pressure system near Iceland (Icelandic Low) and the subtropical anticyclone in the Atlantic near the Azores (Azores High; Hurrell et al., 2003). The spatial pattern of the NAO is shown in Fig-

ure 2.1. It can be seen that in the case of ECHO-G the NAO accounts for 38.17 % of the SLP variability in the model domain.

There are several ways to define the NAO. One way is the winter SLP difference between Lisbon and Reykjavik (e.g. Jones et al., 1997). A more advanced approach is the Empirical Orthogonal Function (EOF) analysis (see Figure 2.1). A detailed description of this method is given in chapter 4. The underlying idea of this linear concept is to find atmospheric patterns that fluctuate between positive and negative states, which applies to the NAO.

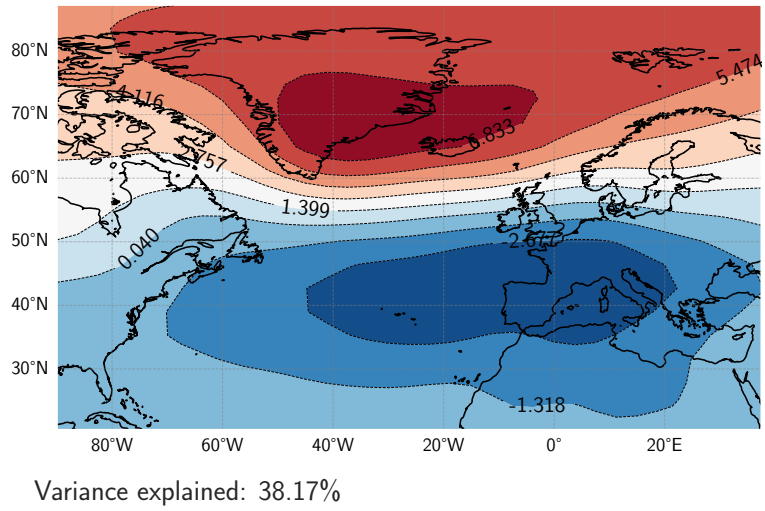

Figure 2.1: North Atlantic Oscillation (EOF1) for the period 950 - 1800 as simulated by the global circulation model ECHO-G. Monthly sea level pressure anomalies (20°N - 80°N; 90°W - 40°E) of the winter season (December, January, February, and March) are used. 38.17% variance explained. Data: OETZI2 ECHO-G (Hünicke et al., 2010)

The positive NAO state (NAO+) is characterized by a pronounced Icelandic Low (IL) and Azores High (AH) resulting in large pressure differences between the two centers. Positive NAO states (NAO+) are associated with strong westerlies, transporting moist air masses from the North Atlantic to Europe (Jaagus, 2009). The opposite negative NAO state (NAO-) is characterized by a weak Icelandic Low and Azores High. The resulting smaller gradient between the two pressure centers leads to reduced westerlies and consequently to lesser moisture transport decreasing precipitation over Northern Europe.

The NAO shows a large interannual variability fluctuating between NAO+ and NAO- states as shown in Figure 2.2. However, it also exhibits an interdecadal variability. For exam-

ple, with the turn of the 20th century, the NAO+ state was mostly positive until the 1930s when a negative NAO state prevailed. During 1970 - 1998 the NAO accounts for more than 80 % of the SLP variability in the Baltic Sea region and for about 40 % of the SLP variability for the whole NH (Kauker and Meier, 2003). It has been linked to a variety of climate variations, e.g. storm tracks, temperature, and precipitation over North America and Europe (Delworth and Zeng, 2016, Scaife et al., 2008, Ricardo et al., 2002).

In this work the NAO is defined in two different ways. In Börgel et al. (2020) it is defined as the first EOF calculated from the monthly SLP anomalies (20°N - 80°N; 90°W - 40°E). In Kniebusch et al. (2019a) it is defined as winter SLP differences between Reykjavik, Iceland, and Gibraltar, Spain (Jones et al., 1997). Both methods show similar results for the period 1899 - 2018 with a correlation of 0.88. However, only the EOF analysis can capture the spatial variability of the NAO which is necessary for the analysis performed in Börgel et al. (2020).

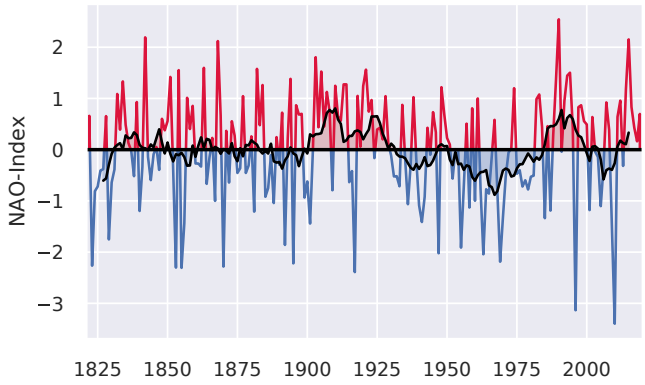

Figure 2.2: NAO index for boreal winter (December, January, February, and March) 1823/1824 - 2019/2020 calculated as the difference between the normalized station pressures of Gibraltar and Iceland (Jones et al., 1997). Index baseline period 1951 - 1980.

2.2 Atlantic Multidecadal Oscillation

Temperature variability in the North Atlantic is traditionally defined as the spatially averaged SST anomaly over the whole North Atlantic domain (0° - 60°N, 0° - 80°W) and is called North Atlantic SST index (NASSTI; Wills et al., 2019). The NASSTI resembles a basin wide monopole SST pattern (see Figure 2.3).

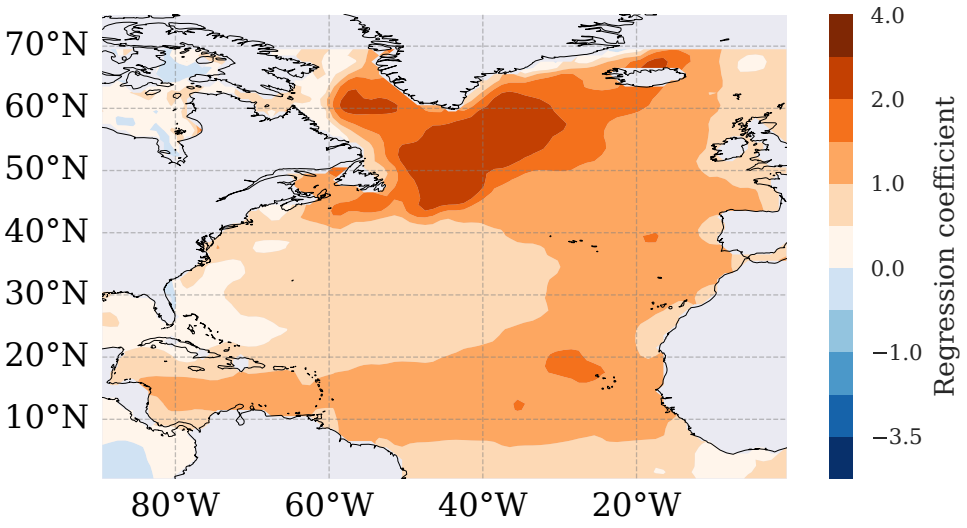

Figure 2.3: Regression of Atlantic sea surface temperature anomalies on NASSTI. Data: Hadley Centre Global Sea Ice and Sea Surface Temperature (HadISST) (Rayner et al., 2003).

The NASSTI has a dominant low-frequency component and is therefore often low-pass filtered. This low-pass filtered signal is more commonly known as the Atlantic Multidecadal Oscillation (AMO). The AMO has a frequency of about 50 - 90 years and describes an alternation between warm and cold SST temperatures in the North Atlantic (Knight et al., 2006). However, the frequency of the AMO may change on centennial or longer times scales (Knudsen et al., 2011).

The influence of the AMO on regional climate has been analyzed in several studies. They show that the AMO has an impact not only on European summer climate, precipitation over Europe, and cold weather episodes in European winters, but also on the weather in Africa and North America (Enfield et al., 2001, Knight et al., 2006, Börgel et al., 2018, Sutton and Hodson, 2005, Ting et al., 2011, Casanueva et al., 2014, Ruprich-Robert et al., 2017, Peings and Magnusdottir, 2014).

While several regions have been shown to be impacted by the AMO the origin of the

AMO is still not fully understood. Recent work indicates that the interaction between the atmosphere and ocean in the North Atlantic plays a key role influencing the frequency of the AMO. Wills et al. (2019) argued that the interaction between the NAO and Atlantic Meridional Overturning Circulation (AMOC) leads to a low-frequency response of the ocean which was then historically defined as the AMO. This agrees with numerous other studies (Delworth and Zeng, 2016, Delworth et al., 2017, Sun et al., 2015).

In contrast, Clement et al. (2015) argued that the AMO is the response to stochastic forcing from the NAO. By analyzing a suite of slab ocean models, they found that the ocean itself does not play an important role for the AMO variability. However, Wills et al. (2019) argued in their work that slab ocean models cannot be used for a physical interpretation, since the mechanism of the AMO differs between observational data and slab ocean models.

Traditionally, the AMO was defined by removing the influence of global warming by linear detrending (Enfield et al., 2001). However, as linear detrending has no physical reason, it is not possible to differentiate between variations of the AMO caused by anthropogenic impacts and variations that are part of natural variability of the North Atlantic. Therefore, Trenberth and Shea (2006) proposed to remove the global SST signal, as it is associated with global processes and thus related to global warming in recent decades. Frankcombe et al. (2010a) also showed that the amplitude and phase of the AMO are sensitive to the chosen method of detrending. This becomes clear by comparing the two methods of Enfield et al. (2001) and Trenberth and Shea (2006) (see Figure 2.4).

In Figure 2.4 (a) the annual SST anomalies of the North Atlantic and a linear trend fit are shown. Figure 2.4 (b) shows the resulting detrended AMO index (Enfield et al., 2001). The definition of Trenberth and Shea (2006) is shown in Figure 2.4 (c), (d). Figure 2.4 (c) shows the annual global SST anomalies which are subtracted by the annual SST anomalies of the North Atlantic in Figure 2.4 (d). By comparing Figure 2.4 (b) and (d) it is found that the AMO index differs most from 1870 - 1900. The stronger positive phase in (b) is an artifact of the linear detrending. Summarizing, the method of Trenberth and Shea (2006) can extract pure Atlantic variability as the global SST signal is removed. Further, the approach of Enfield et al. (2001) was chosen to analyze recent periods when the climate is affected by anthropogenic impacts. However, the present study focuses on pre-industrial periods without

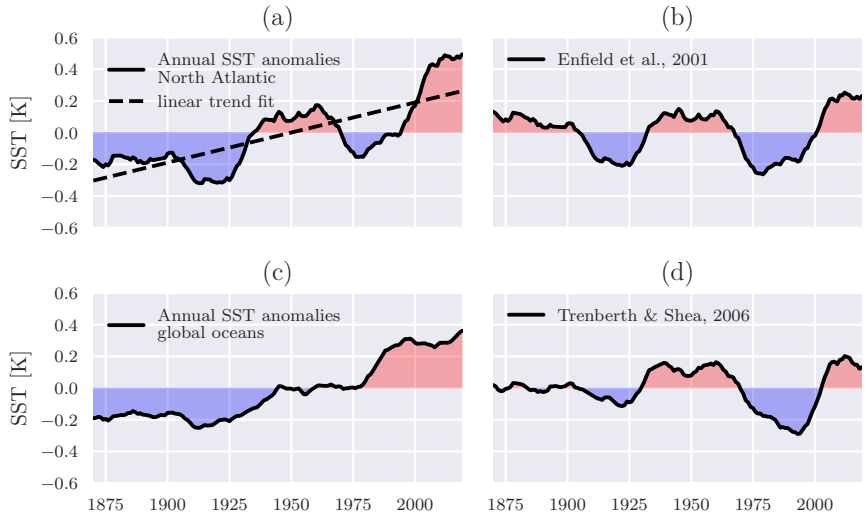

Figure 2.4: 10-year rolling mean of (a) annual SST anomalies averaged over the North Atlantic with the corresponding linear fit (dashed), (b) annual SST anomalies over the North Atlantic but with the linear trend of (a) removed, (c) annual SST anomalies averaged over the global oceans, (d) annual SST anomalies averaged over the North Atlantic but with the global mean SST (c) removed. Data: Hadley Centre Global Sea Ice and Sea Surface Temperature (HadISST) (Rayner et al., 2003).

significant anthropogenic emissions. Therefore, in this study the AMO is defined according to Trenberth and Shea (2006).

Even if you never have the chance to see or touch the ocean, the ocean touches you with every breath you take, every drop of water you drink, every bite you consume.

Sylvia Earle, from her book 'The World is Blue'

3 Baltic Sea

The Baltic Sea is a semi-enclosed sea and is connected to the world ocean through the shallow and narrow Danish Straits. It is a prominent example when analyzing coastal oceans, since it has been shown to respond very sensitively and fast to external forcing (Belkin, 2009). Stigebrandt and Gustafsson (2003) went even further, describing the state of the Baltic Sea as the result of external forcing.

3.1 Dynamics of the Baltic Sea

Salinity, temperature, and oxygen are important parameters used to describe the physical state of the Baltic Sea. The salinity of the Baltic Sea is mainly driven by freshwater supply from rivers and precipitation and saltwater inflows from the North Sea. Therefore, water masses in the Baltic Sea can be understood as a mixture of the saline water of the North Sea and freshwater (Döös et al., 2004). In most parts of the Baltic Sea, its sea surface salinity (SSS) varies

between 0 - 10 g kg^{-1} (see Figure 3.1). Consequently, all other ecosystem variables tend to show strong gradients as well. The freshwater input into the Baltic Sea comes either as river runoff or a positive net precipitation (precipitation minus evaporation) over the sea surface. The net precipitation accounts for 11 % and the river input for 89 % of the total freshwater input (Meier and Döscher, 2002). The river runoff accumulates over the Baltic drainage basin and is therefore a result of precipitation minus evaporation over land. The north-eastern part of the Baltic Sea is the farthest away from its connection with the North Sea. In addition, most of the rivers are located in the north-eastern part. This results in strong meridional salinity gradients with lower salinities in the northern part which gradually increase towards the transition area of the Danish Straits (see Figure 3.1). Salinity has a large ecological relevance and defines the distribution of Baltic Sea species and other ecosystem variables (Remane and Schlieper, 1971).

On average, the Baltic Sea has a water surplus with respect to the open ocean, which can be expressed as a pressure gradient driving a nearly permanent barotropic outflow of low saline water at the surface (see Figure 3.2). This outflow is compensated for by a corresponding inflow of denser saline water just above the sea floor originating from the North Sea.

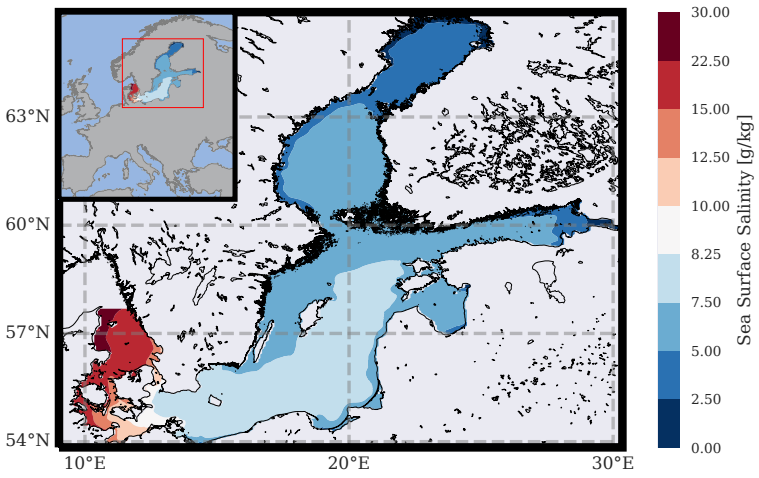

Figure 3.1: Mean sea surface salinity of the Baltic Sea during the period 950 - 1800 in the Baltic Sea (Schimanke and Meier, 2016). Overview map with the study area marked by a red rectangle in the top left corner.

Saltwater inflows can be divided into barotropic and baroclinic inflows (Meier et al.,

2006). Stronger barotropic inflows are characterized by periods of easterly wind, pushing the water masses out of the Baltic Sea into the North Sea, followed by strong westerly winds reversing the pressure gradient and causing a higher relative sea level in the North Sea. The saltwater inflows happen on time scales of about 20 days (Schimanke and Meier, 2016). Very strong inflows are called Major Baltic Inflows (MBI; Matthäus and Franck, 1992, Fischer and Matthäus, 1996, Mohrholz, 2018). They transport oxygen-rich water into the deeper parts of the Baltic Sea, since the surface water entering from the North Sea has not only a higher oxygen content, but also a higher salinity and consequently a higher density. Therefore, the inflow plumes are moving eastward along the bottom into the deeper parts of the Baltic Sea. During these MBI events the average sea level of the Baltic Sea can vary between -60 cm and +60 cm (Matthäus and Franck, 1992). Baroclinic inflows are caused by density gradients between the Kattegat and the Baltic Sea and usually occur during summertime. These saline inflows are also important for the oxygen supply of the deeper layers of the Baltic Sea as it is heavily stratified and only the layers above the permanent halocline are supplied with oxygen from the atmosphere (Mohrholz et al., 2015).

The restricted water exchange with the open ocean makes the Baltic Sea naturally susceptible to hypoxic conditions. Hypoxia may be summarized as low-oxygen conditions (<2 mg L^{-1}) which are unable to support most marine life (Carstensen et al., 2014). As of 2016, the spread of hypoxia in the Baltic Sea covers approximately 70.000 km^2 – 19 % of its total area (Meier et al., 2018a). Even though hypoxia occurred naturally during different phases of the Baltic Sea history, present-day hypoxia is a result of increased eutrophication and supported by climate warming (Meier et al., 2019).

3.2 Variability of the Baltic Sea

Defining parameters of the Baltic Sea, such as salinity, temperature, and oxygen, are affected by both natural variability and anthropogenic influences. It remains challenging to disentangle both types of variation. However, numerical models of the Baltic Sea have brought great advances in understanding the impact of natural variability.

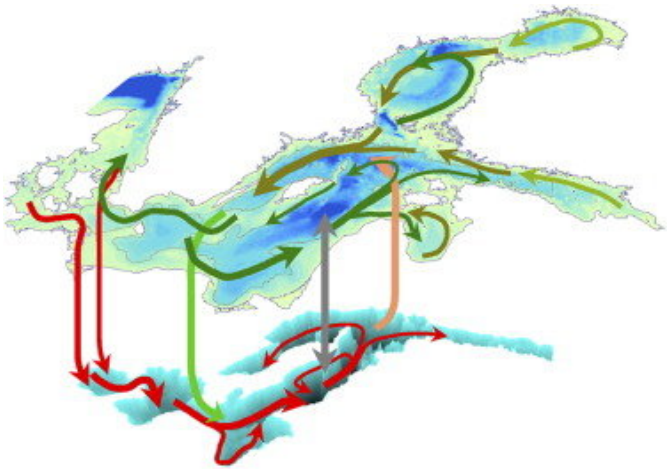

Figure 3.2: Diagram of the large-scale circulation in the Baltic Sea (Elken and Matthäus, 2008). Green (brackish surface water) and red (saline bottom water) arrows show the surface and bottom layer circulation, respectively.

3.2.1 Salinity

Meier and Kauker (2003) showed that decadal salinity variations of about 1 g kg^{-1} are caused, inter alia, by annual runoff variations. Further, Meier and Kauker (2003) showed that about 50 % of the decadal salinity variability can be explained by variations in freshwater input into the Baltic Sea. Freshwater variations can be caused by the NAO as it is linked to large-scale precipitation patterns over the Baltic Sea. Therefore, the NAO influences the river runoff and consequently the salinity of the Baltic Sea. Besides freshwater variations, long-term changes in westerly winds have also been linked to the decadal salinity variability of the Baltic Sea and account for the other half of decadal salinity variability. Zorita and Laine (2000) showed that stronger westerlies lead to lower salinities in both upper and lower layers in the Baltic Sea. This increase in westerlies is caused by an NAO-like pattern. Meier (2006) found an e-folding time scale of about 20 years for the response of salinity to atmospheric and hydrological changes in the Baltic Sea. Longer forcing anomalies will drive the Baltic Sea into a new state with a permanently changed salinity.

There are numerous studies analyzing salinity variability in the Baltic Sea on decadal time scales but salinity variations on multidecadal or even centennial time scales have not been analyzed in depth. In a study simulating the period 950 - 1800 Schimanke and Meier (2016)

showed that 66 % of multi-decadal salinity variability can be explained by combining river runoff, precipitation, wind, temperature, and the NAO. Further, they found that the mean salinity is varying on time scales of about 100 years, but they did not provide a physical explanation for the origin of this effect. Kniebusch et al. (2019b) found that low-frequency oscillations in wind and runoff of about 30 years have been dominating the variability of the SSS since 1850. In addition, by analyzing the period from 1920 - 2008, they found a significant positive trend in the latitudinal SSS gradient. This trend can be attributed to a regional increase in river runoff in the northern basins while the mean SSS has increased over the last century.

3.2.2 Temperature

The Baltic Sea experiences strong seasonal temperature variations. The mean SST varies between 4°C in winter and about 18°C in summer (Placke et al., 2018). The Baltic Sea is affected by exceptionally strong SST trends. From 1982 - 2006 the Baltic Sea warmed by 1.31 K, corresponding to a warming of 0.56 - 0.57 K decade^{-1} (Lehmann et al., 2011, Belkin, 2009). This is seven times faster than the global rate and is the highest warming rate among all oceans. Possible reasons of the exceptional warming of the Baltic Sea have been postulated by Lehmann et al. (2011). They related the SST increase in the Baltic Sea to an increase in air temperature. Other studies found an increase in warm summer inflow events, transporting warmer water masses from the North Sea into deeper parts of the Baltic Sea (Meier, 2006, Mohrholz et al., 2006).

The NAO is also contributing to SST changes, depending on the season, with the strongest impact during winter (Lehmann et al., 2011, Stramska and Białogrodzka, 2015). Positive NAO phases are associated with mild temperatures and increased precipitation whereas negative NAO phases are characterized by warm summers, cold winters, and less precipitation. Increasing winter temperatures in the Baltic Sea have also been linked to an observed shift in the storm tracks (BACC II Author Team, 2015).

Kniebusch et al. (2019a) analyzed the SST variations in the Baltic Sea in depth. In this

work it was shown that the Baltic Sea SST mainly follows variations in surface air temperature but is also driven by large-scale climate variability indices such as the NAO and AMO.

3.2.3 Oxygen

The hypoxic area in the Baltic Sea is constantly varying. Carstensen et al. (2014) found a 10-fold increase of hypoxia during the last century (1898 - 2012), which was mainly linked to an increase in nutrient loads. Meier et al. (2018b) confirmed these findings. They found that without increased nutrient loads, hypoxia would not have occurred at all during the 20th and 21th century. Further, studies of Meier et al. (2017) supported these findings as the impact of eustatic sea level rise on hypoxia is considerably low. However, a recent reduction of nutrient loads did not result in the expected decrease of the hypoxic areas. Neumann et al. (2017) argued that a large residence time for phosphate and a positive feedback mechanism (Vahtera et al., 2007) – increased phosphate release from sediments under hypoxic conditions – could explain the slow decline of the hypoxic area. The importance of this vicious cycle was stressed by Meier et al. (2019) as they found that it has played an important role in the development of hypoxia in the past. Hypoxic areas are also influenced by dense saltwater inflows transporting in oxygen into the bottom waters. Depending on their intensity and frequency areas located further east in the Baltic Sea are ventilated (Neumann et al., 2017). However, saltwater inflows are also increasing the stratification of the water column, so oxygen can be depleted more quickly due to lower diffusion into the bottom layer (Conley, 2002).

All models are wrong, but some are useful.

George Box

4 Data and Methods

4.1 Data

Studying multidecadal variability is often limited by the lack of observational data. Therefore, the studies by Börgel et al. (2018, 2020) were based on the model results of Schimanke and Meier (2016). Their study used a multi-centennial paleoclimate simulation performed with the GCM ECHO-G focusing only on the last millennium (Hünicke et al., 2010). ECHO-G is a coupled ocean-atmosphere model. The atmospheric model has a horizontal resolution of approximately 3.75° x 3.75° and 19 vertical levels. The ocean component has a resolution of 2.8° x 2.8° and 20 vertical levels. Variations in orbital parameters, solar irradiance and greenhouse gases were used to force the ECHO-G Holocene simulation. In the case of ECHO-G, the Baltic Sea consists of only 5 x 5 grid points which is too coarse to capture all of the complex climate dynamics within the Baltic Sea area. To overcome this limitation a dynamical downscaling was performed with the regional circulation model Rossby Centre regional cli-

mate model (RCA3; Samuelsson et al., 2011), using ECHO-G at the lateral boundaries. The downscaling covers the period 950 - 1800. RCA3 has a horizontal resolution of 0.44° x 0.44° with 24 vertical levels and a 30-minute time step, covering nearly the whole area of Europe (33.0°W - 58.52°E; 26.0°N - 71.76°N). The difference between both resolutions is shown in Figure 4.1. It illustrates the need for regional climate modeling, since the spatial information in GCMs is limited.

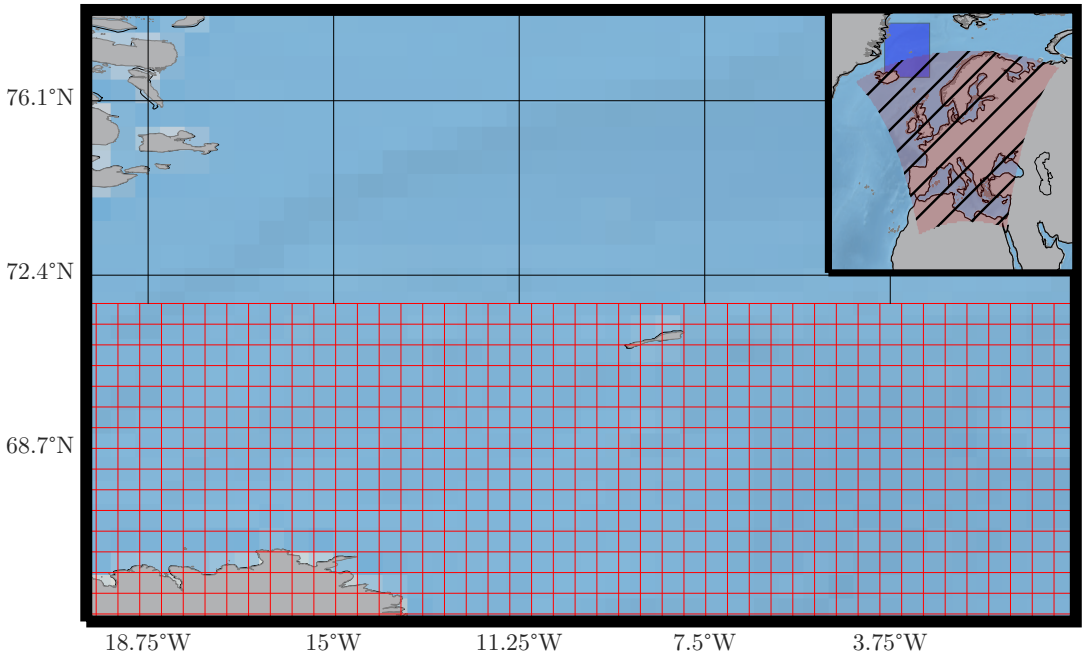

Figure 4.1: Resolution difference between the global circulation model ECHO-G (black) and the regional climate model Rossby Centre Atmosphere model (RCA3; red). Overview map with the RCA3 domain (hatched red) and the zoomed area marked by a blue rectangle in the top right corner.

Finally, RCA3 was used to force the regional ocean model Rossby Centre Ocean (RCO) which has a horizontal resolution of 3.7 km x 3.7 km and consists of 83 levels, with a thickness of 3 m each. RCO is a Bryan-Cox-Semtner primitive equation circulation model (e.g. Meier et al., 2003). The work of Kniebusch et al. (2019a) also used RCO to simulate the period 1850 - 2008 but used the Modular Ocean Model (MOM) in addition. MOM has a resolution of 5 km x 5 km with a vertical resolution of 2 m and a maximum depth of 268 m. Further, Kniebusch et al. (2019a) used a MOM box model setup. The box model uses a rectangular

basin with 3 x 3 grid points and is located in the Gotland Basin (19.5°E - 20.5 °E, 57°N - 57.5°N; see Figure 4.2). It consists of a flat bottom with a depth of 100 m. Horizontal ocean currents were set to zero to omit horizontal advection. However, to guarantee a realistic vertical stratification, the salinity profile was reinitialized at the beginning of every year.

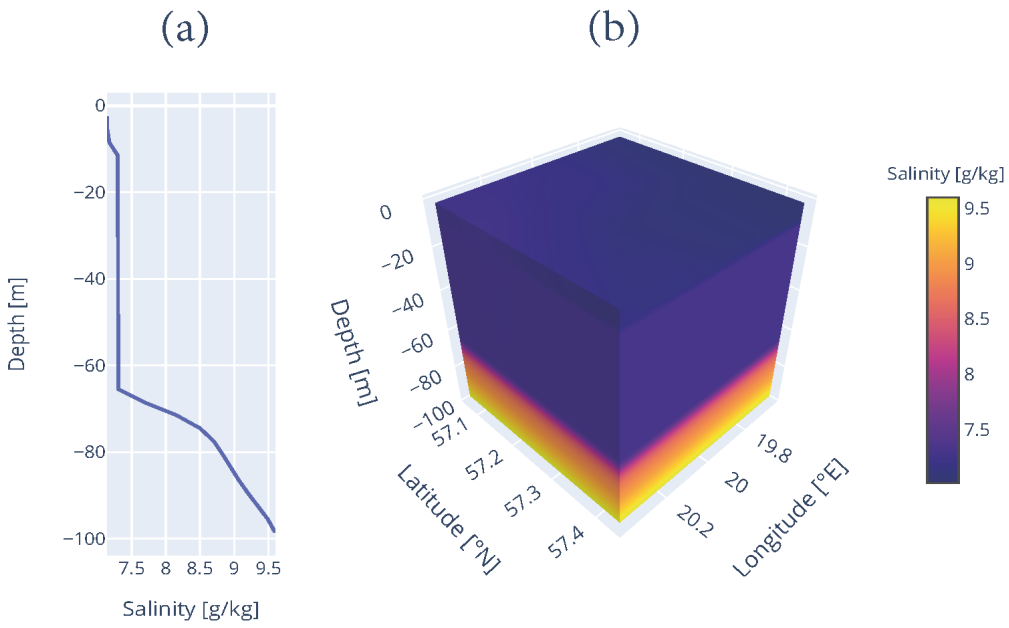

Figure 4.2: MOM box model setup: (a) the horizontally averaged salinity profile and (b) the model domain.

4.2 Methods

Two relevant methods for this work are wavelet analysis and empirical orthogonal functions (EOFs), which will be presented in the following.

4.2.1 Wavelet analysis

The first question that comes to mind when analyzing the spectral components of a signal is: Why not use Fourier analyzes? Fourier decomposition may give all the spectral components of a time series, but it does not provide any information about when they are present. The power spectrum is usually used to evaluate a time series and shows the distribution of power over frequencies. One common application is to search for a seasonal signal in the data. If so, the spectrum will show peaks at the seasonal frequencies. The power spectrum $S_{xx}(f)$ of a time series $x(t)$ is defined as:

$$S_{xx}(f) = |\tilde{x}(f)|^2 \tag{4.1}$$

with

$$\int_{-\infty}^{\infty} |x(t)|^2 dt = \int_{-\infty}^{\infty} |\tilde{x}(f)|^2 df \tag{4.2}$$

$$\tilde{x}(f) = \int_{-\infty}^{\infty} e^{-2\pi i f t} x(t) dt \tag{4.3}$$

The importance of retaining temporal information when analyzing a time series is illustrated in Figure 4.3. The upper left part of Figure 4.3 (a) shows a time series in which two sines with different frequencies were concatenated together in time, whereas the upper right shows a time series in which the two sinusoidal signals were added (b). The lower row shows the resulting power spectra and the limitation of the power spectrum. Both series have virtually the same power spectrum, since temporal information is lost. It is obvious, however, that this information is needed to interpret these results. For example, by applying these results to the temperature change in the Baltic Sea region, one would argue that the internal dynamics in the system changed, whereas the other time series suggest that the system remained stable over time.

The continuous wavelet transform (CWT) expands a time series into a time-frequency space. This reveals time localized oscillations and areas with high power. Therefore, CWT is a good choice, if one is interested in studying periodic phenomena that change over time. The most common wavelet function is the Morlet wavelet (Torrence and Compo, 1998).

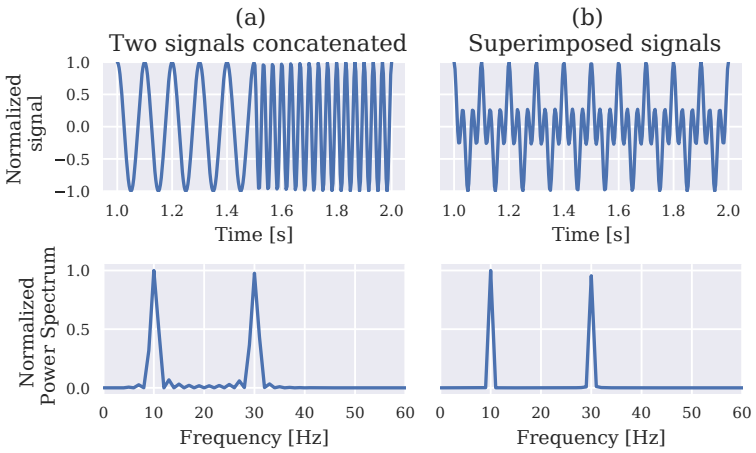

Figure 4.3: Example for the limitation of the power spectrum: (a) time series concatenated of two sine signals and the resulting power spectrum and (b) superimposed signals and the resulting power spectrum.

$$\psi(t) = \pi^{-1/4} e^{i\omega t} e^{-t/2} \tag{4.4}$$

The Morlet wavelet transform is defined as the convolution between a set of Morlet wavelet functions and the discrete time series x(t). This set of wavelet functions was generated by shifting the wavelet by τ and scaling it by s.

$$\mathrm{CWT}(\tau, s) = \sum_t x(t) \frac{1}{\sqrt{s}} \psi^* \left(\frac{t - \tau}{s} \right) \tag{4.5}$$

The position of a wavelet function is defined by the time parameter τ that is shifted by the time increment dt. The scaling factor s defines the temporal width of the wavelet, which determines the frequency of oscillation due to its fixed shape. Like the power spectrum, the wavelet power spectrum is defined as

$$\mathrm{Power}(\tau, s) = \frac{1}{s} |\mathrm{CWT}(\tau, s)|^2 \tag{4.6}$$

Summarizing, the CWT allows to analyze the frequency spectrum and its energy while retaining the time information. The advantage of the wavelet power spectrum is shown in Figure 4.4 using the same time series as in Figure 4.3.

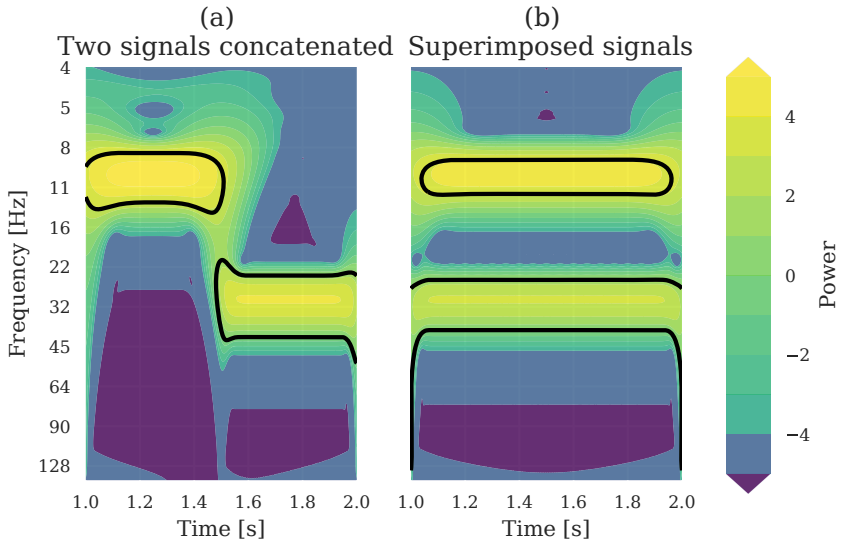

Figure 4.4: Added value of wavelet analysis. (a) The wavelet power spectrum of the concatenated signals, (b) wavelet power spectrum of the superimposed signal (cf. Figure 4.3).

The CWT reveals that one signal consists of two timeseries that are joined in time, whereas the other time series consists of two sine signals that are added onto each other.

This study also uses wavelet coherence (WTC) which can be understood as the local correlation between two CWTs, revealing locally phase-locked behavior (Grinsted et al., 2004).

4.2.2 Empirical Orthogonal Functions (EOF)

Climate variability is characterized by complex dynamics. Persistent spatial and temporal patterns are often hidden by small-scale processes (Dawson, 2016). However, when analyzing climate data, one is often trying to answer the question: What are the important patterns that appear in this field and how much of the variance is explained by them? Empirical Orthogonal Functions are a popular method to identify large-scale patterns of variability. In climate science, the data usually consists of three-dimensional fields F, with two dimensions in space and one dimension in time. For the calculation of an EOF, the spatial dimensions are joined into a single location vector $\vec{s}$, resulting in the space-time field X(t,s). Then the anomaly field is defined as

$$X'(t,s) = X(t,s) - \overline{X}_t(s) \tag{4.7}$$

with $\overline{X}_t(s)$ as the time average of the field. With the anomaly data matrix, the covariance matrix is defined as

$$C = \frac{1}{n-1} X'^T X'. \tag{4.8}$$

The covariance matrix is a symmetric matrix describing the covariance between the time series of the field and any pair of grid points (Hannachi et al., 2007). The aim of an EOF is to find the linear combination of all variables that explains a maximum variance. This results in an eigenvalue problem

$$Ca = \lambda a. \tag{4.9}$$

The k'th eigenvector of a_k of C represents the k'th EOF. The eigenvalue λ_k represents the explainend variance of the k'th EOF. When projecting the anomaly field X' onto the k'th EOF one obtains the k'th principal component

$$c_k(t) = \sum_{s=1}^{p} X'(t,s) \cdot a_k(s) \tag{4.10}$$

with p as number of grid points.

Both the EOFs and the principal components are orthogonal between the modes. It should be noted that EOFs represent patterns in which often a combination of a few explains most of the observed variance. However, a physical interpretation is not trivial. EOF analysis is a statistical method and the spatial modes need not be related to individual physical processes. Further, physical processes are not necessarily orthogonal even if they are independent. Therefore, the interpretation of EOFs should be performed with care. One problem that is addressed in this work is that EOFs aim at finding patterns of maximum variance for a given period. These spatial patterns are then interpreted and related to modes of climate variability. In the Northern Hemisphere the North Atlantic Oscillation (NAO) is such a pattern of maximum variance in the sea level pressure, showing a dipole-like structure (see Figure 2.1). Spatial patterns identified by EOFs such as the NAO are often discussed under the as-

sumption that its spatial structure does not change. However, this is not the case when the time scales change significantly, e.g. patterns identified over decadal time-scales may change over multi-centennial time scales. To analyze the change of the spatial position of the NAO an EOF analysis with overlapping time windows was performed. The idea of this concept is similar to a centered moving average. For each time step t an EOF is calculated considering time steps [t-n, t+n] of the SLP anomalies. The next EOF is then calculated for a window of the same length but shifted along the time axis by a time increment dt (see Figure 4.5).

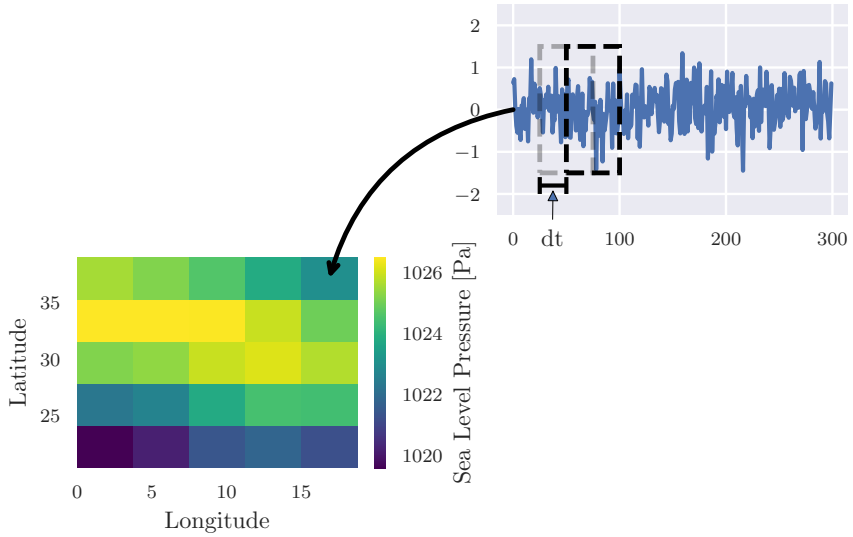

Figure 4.5: Concept of the overlapping Empirical Orthogonal Function for a 3-dimensional array.

Shifting the time window for the EOF calculation by dt creates a series of EOFs for every time step. A k-Means cluster algorithm is then used to identify the centers of maximum variance for each EOF pattern. The difference in the spatial position of the maxima between consecutive overlapping intervals is defined as the movement of the NAO centers.

What we call results are beginnings.

Ralph Waldo Emerson

5

Long-term variability and its impact on regional climate

5.1 Impact of the Atlantic Multidecadal Oscillation on Baltic Sea variability

Several studies showed that the AMO impacts regional climate all around the world. However, for the first time it was shown that the Baltic Sea variability is exposed to the remote forcing of the AMO (Börgel et al., 2018). By using a regional climate model it was shown that the AMO changes the atmospheric circulation, influencing the precipitation over the Baltic Sea region. Ultimately, this impacts the river runoff into the Baltic Sea, affecting the mean salinity of the Baltic Sea. The AMO constantly influenced the Baltic Sea during the whole model simulation of the pre-industrial period from 950 - 1800, which provides strong evidence for long-term changes in the Baltic Sea as a result of alternating AMO phases.

5.1.1 Analyzing the characteristics of the AMO in ECHO-G

The SST fields for the calculation of the AMO index were extracted from the global circulation model ECHO-G for the period 950 - 1800 (Figure 5.1 a). It fluctuates between positive AMO (AMO+) and negative AMO (AMO-) phases, indicated by red and blue areas. This means that AMO+ phases correspond to anomalous warm SSTs in the North Atlantic. During the MCA the AMO tends to stay in a positive phase, which was confirmed by studies of Landrum et al. (2013) and Mann et al. (2009), while the LIA has more frequent AMO- phases. To analyze the AMO signal a continuous wavelet transform (CWT) was used (Figure 5.1 b). The CWT revealed that the AMO concsists of two persistent low-frequency components: From 1150 - 1400 the AMO shows significant power in the frequency range of 120 - 180 years. This period approximately coincides with the MCA, defined as a time of warm climate in the North Atlantic region. The exceptionally persistent frequency of the AMO during the MCA differs from the literature's definition of 60 - 90 years, however, studies of e.g. Frankcombe et al. (2010b) or Wei et al. (2012) showed that the AMO's frequency can be modulated by background climate conditions. From 1400 - 1700 the AMO shows significant power in the frequency range of 60 - 90 years. This second low-frequency component coincides with the LIA (1400 - 1700), a period of strong cooling after the MCA. Summarizing, the representation of the AMO in ECHO-G is sufficient.

5.1.2 The relationship between the AMO and the Baltic Sea

The AMO pattern was then linked to the mean salinity of the Baltic Sea. As the river runoff is responsible for over 50 % of the decadal salinity variations, the same analysis was repeated for the river runoff. To analyze non-stationary coherence a WTC was applied between first the AMO and the mean salinity and second the AMO and the river runoff of the Baltic Sea (Figure 5.2). In other words, the WTC between the AMO and the two other signals should reveal a significant coherence between both low-frequency components where the AMO has significant power – the MCA and the LIA.

It was found that both mean salinity and river runoff have a significant coherence with the AMO signal for both low-frequencies components. For the MCA in the frequency range of 120 - 180 years and for the LIA in the frequency range of 60 - 90 years. This leads to the

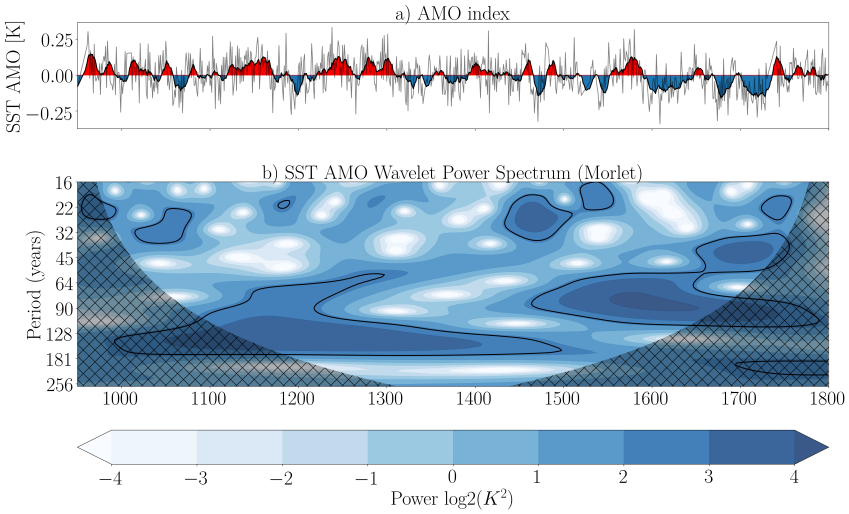

Figure 5.1: Calculated AMO index (a) and corresponding continuous wavelet transform of the AMO index (b). The black contour lines show statistical significance according to Grinsted et al. (2004). The cone of influence where edge effects might influence the results is hatched (Grinsted et al., 2004). AMO = Atlantic Multidecadal Oscillation; SST = sea surface temperature (Börgel et al., 2018).

conclusion that the low-frequency variability of the river runoff is very likely driving the low-frequency variability of the mean salinity of the Baltic Sea.

5.1.3 Physical attribution

The WTC showed that the AMO impacts the Baltic Sea by changing the river runoff and consequently its mean salinity. However, one question that still needed to be addressed is how the AMO signal propagates into the Baltic Sea. Precipitation over the Baltic Sea catchment area is a good estimate for the river runoff flowing into the Baltic Sea, since it is directly related to the freshwater budget of the Baltic Sea (Kauker and Meier, 2003, their Figure 14). Therefore, in the next step the seasonal precipitation was analyzed. To estimate the impact of the AMO the difference in precipitation between AMO+ and AMO- for each season was calculated (Figure 5.3). The outcome was normalized to show the percentual increase of precipitation per season caused by the AMO.

While all seasons indicate that AMO+ phases increase the precipitation over the Baltic Sea, only winter and spring show a statistically significant increase of precipitation for the

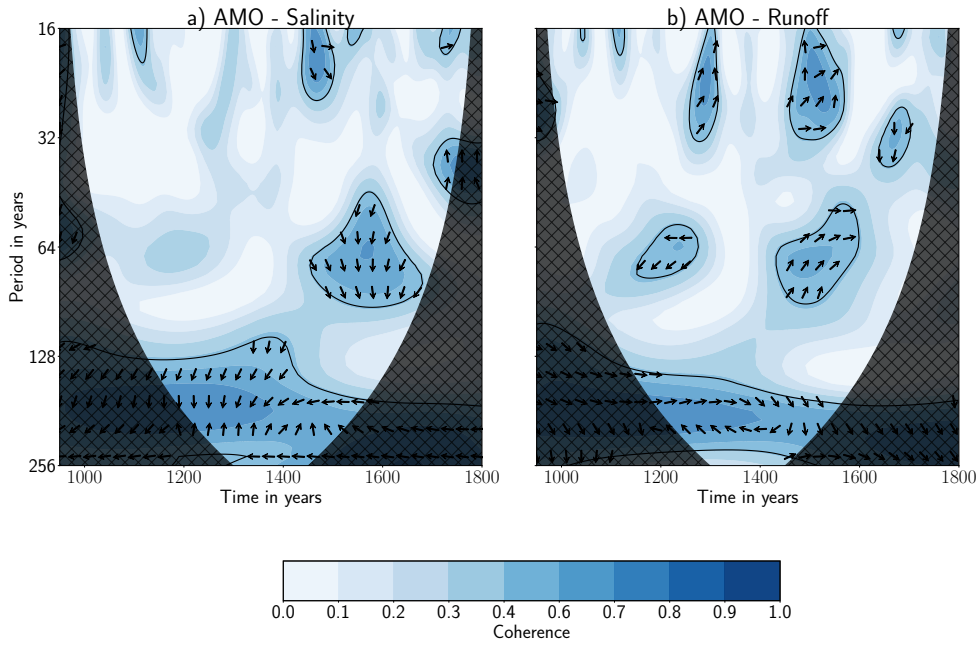

Figure 5.2: Wavelet coherence of the AMO index and the mean salinity of the Baltic Sea (a) and AMO index and river runoff into the Baltic Sea (b). The black contour lines show the 95 % significance level (Grinsted et al., 2004). The arrows in the significant regions indicate the phase relationship between the signals: pointing right (left) in phase (antiphase), and AMO leading (lagging) straight up (down) (Börgel et al., 2018).

entire Baltic Sea catchment area. During winter and spring, local differences account for up to 10 % of the seasonal mean precipitation. In the mean, AMO+ phases show an increase of about 3.5 % of the seasonal mean precipitation and during spring the precipitation is even increased by 4.4 %. Annually an increase of 2.5 % is found. The increased precipitation during AMO+ phases then leads to higher river runoff into the Baltic Sea. The observed changes in the precipitation pattern can be linked to changes in the atmospheric circulation caused by the AMO (Figure 5.4). Since only winter and spring show a significant change in precipitation, only the SLP fields for these two seasons were considered. The left panel (Figure 5.4a and c) shows the mean state during winter and spring respectively. Both seasons are characterized by a low-pressure system in the North (Icelandic Low) and a high-pressure system in the South

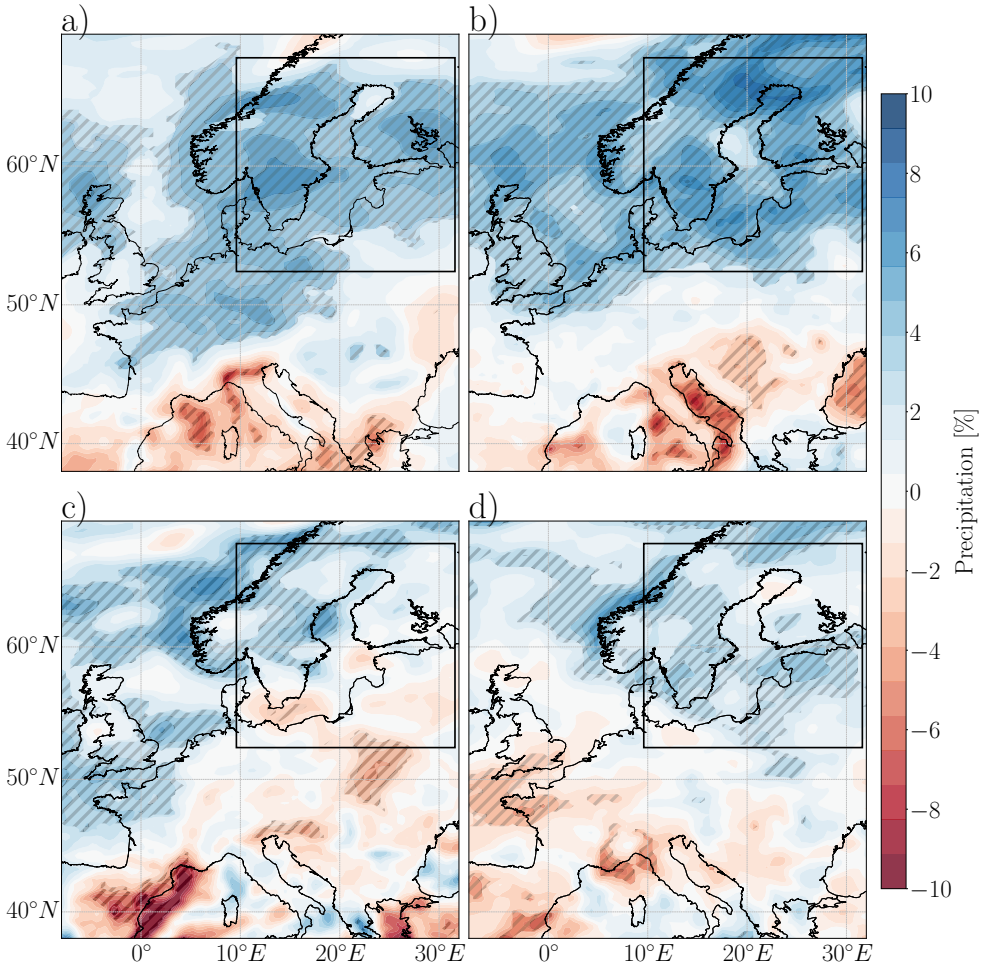

Figure 5.3: Difference in precipitation between AMO+ and AMO−. (a) Winter (December, January, February), (b) Spring (March, April, May), (c) Summer (June, July, August), (d) Autumn (September, October, November). The scale shows the relative difference to the local seasonal mean. Statistical significance is hatched and calculated with a two-tailed Student's t test (α = 0.05), in which the calculated differences are compared against seasonal fluctuations. The rectangular indicates the defined Baltic Sea catchment area (9.6°E - 32°E and 52.4°N - 67.4°N), which accumulates all of the freshwater input into the Baltic Sea (Börgel et al., 2018).

(Azores High). The right panel shows the difference in SLP between AMO+ and AMO- phases. During winter and spring the AMO+ tends to increase the SLP difference between the Icelandic Low and Azores High. This affects the wind fields over the Baltic Sea region resulting in stronger westerlies. Enhanced mean westerlies increase the transport of moist

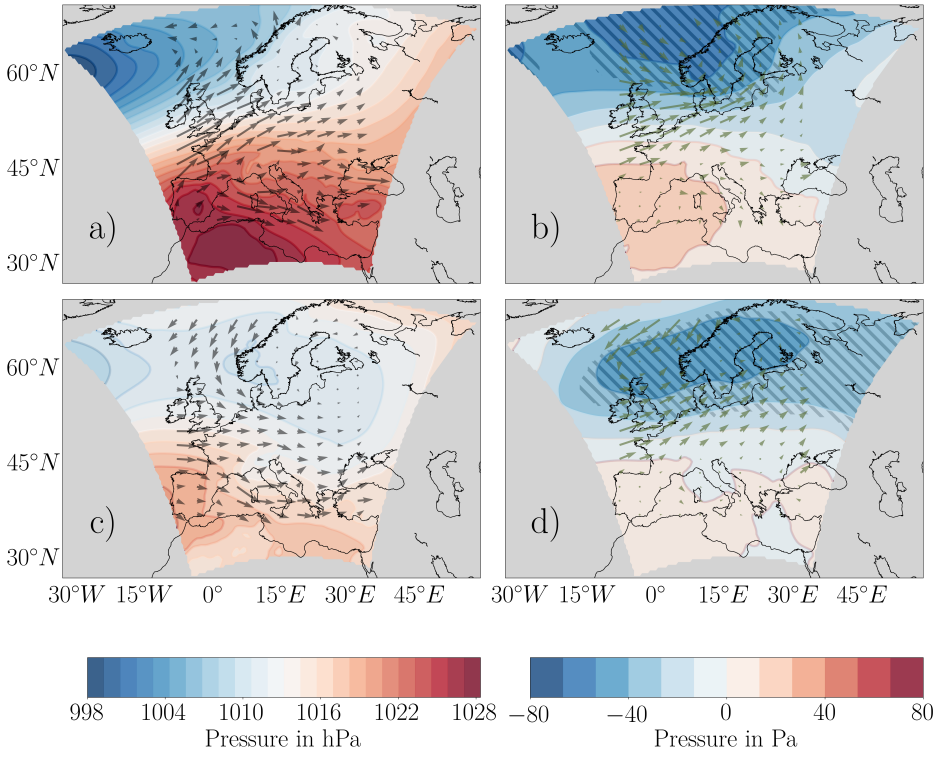

Figure 5.4: Mean sea level pressure (SLP) during winter in hPa (a), SLP difference between AMO+ and AMO− during winter in Pa (b), mean SLP during spring in hPa (c), SLP difference between AMO+ and AMO− during spring in Pa (d). The arrows indicate the wind direction. Statistical significance is hatched and calculated with a two-tailed Student's t test (α = 0.05) where the calculated differences are compared with seasonal fluctuations (Börgel et al., 2018).

air masses from the Atlantic into the Baltic Sea region. Consequently, this leads to higher precipitation in the Baltic Sea catchment area.

Summarizing, this work confirmed that the Baltic Sea is influenced by the quasi-global climate mode AMO. It was found that the AMO has a constant impact on the Baltic Sea throughout the simulation. While this work focused on the mean salinity, other parameters such as SST and sea ice cover also showed a significant coherence with the AMO. Since AMO+ phases are likely to last longer than 30 years, an increase of 2.5 % in precipitation per year during AMO+ phases plays a significant role for the state of the Baltic Sea, resulting in multi-decadal salinity variations of up to 0.7 g kg^{-1}. The findings of this work lead to the conclusion that the state of the AMO should be considered when the state of the Baltic Sea

is discussed.

5.2 The Atlantic Multidecadal Oscillation controls the impact of the North Atlantic Oscillation on North European climate

The aim of this study was to show the influence of the AMO on the spatial structure of the NAO (Börgel et al., 2020). The NAO is often used to explain changes in regional climate variables, assuming a constant spatial pattern. However, the results of this study showed that the AMO changes the zonal position of the NAO. This is of great importance for studies discussing regional climate and demonstrates that the assumption of a constant spatial structure of the NAO does not hold.

Using the Baltic Sea as an example for the impact of the NAO on North European climate, it was found that the correlation between regional climate variables and the NAO varies on multidecadal time scales. For example, the correlation between the NAO and SST varies immensely with correlations ranging from 0.0 - 0.8. In this study a combination of a GCM (ECHO-G) and a regional climate model (RCA3) was used (see Data and Methods). The SLP fields and the SST fields were taken from ECHO-G. Wind fields and SLP fields for the calculation of the storm tracks were taken from RCA3.

5.2.1 Analyzing the characteristics of the AMO and its relationship with the NAO

As this study focused on the interaction between the AMO and the NAO, their relationship in ECHO-G was analyzed using CWT and WTC. Both the AMO and the NAO alternate between positive and negative states. During the MCA they tend to stay in a positive state, while during the LIA the number of positive and negative states is more balanced (Figure 5.5 a). The CWT (Figure 5.5 b) revealed that the AMO has two persistent low-frequency components with significant power: During the MCA in the frequency range from 90 - 180 years and during the LIA from 60 - 90 years. The relationship between the AMO and the NAO was analyzed in Figure 5.5 (c). The WTC showed a significant coherence in the frequency range that can be attributed to the AMO. Summarizing, in ECHO-G a significant coherence

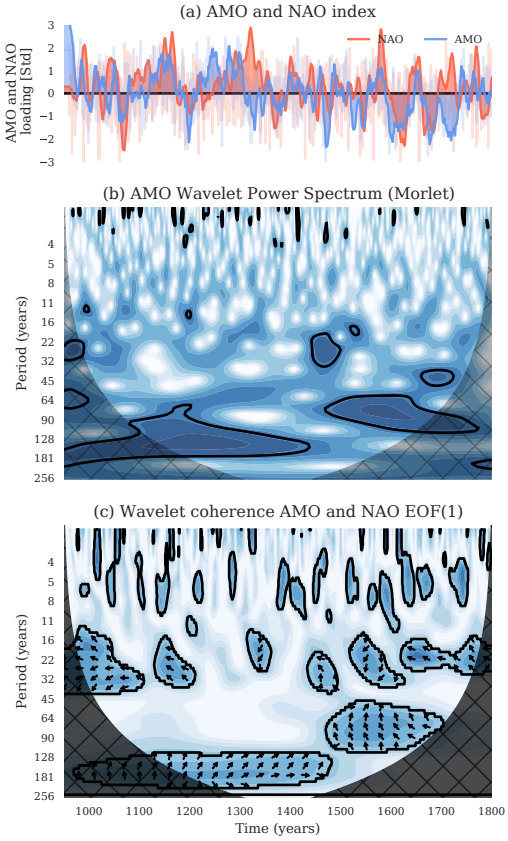

Figure 5.5: Calculated AMO and NAO indices (a), wavelet power spectrum of the AMO (b) and the wavelet coherence between the AMO and the NAO (c). The black contour lines show statistical significance. The cone of influence where edge effects might influence the results is hatched (Grinsted et al., 2004). The arrows show the phase relationship between the signals: pointing right (left) in phase (antiphase), and AMO leading (lagging) up (down). (Börgel et al., 2020).

between the AMO and the NAO was found and therefore it is assumed that ECHO-G can represent the interaction between the AMO and the NAO.

To capture the spatial variability of the NAO an EOF analysis with overlapping time windows of 30 years was performed. As the wavelet analysis revealed that the AMO experiences a frequency shift between the MCA and the LIA both climate states were discussed separately. Figure 5.6 shows the spatial variability of the IL and the AH during the MCA and the LIA. It was found that the MCA and the LIA show similar results. The IL is located further west during AMO+ phases and further east during AMO- phases. For the AH the opposite case

was found: The AH is located further west (east) during AMO+ (AMO-) phases. However, the impact of the AMO on the position of the IL increases during the LIA.

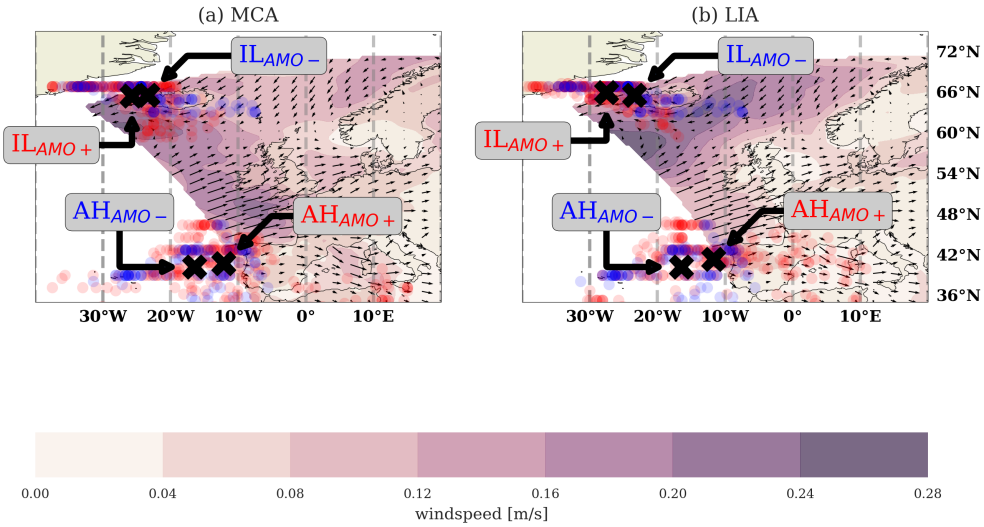

Figure 5.6: Spatial shift of the Icelandic Low and the Azores High sorted by AMO+ and AMO- phases during MCA (a) and LIA (b). Each dot corresponds to the center position obtained by the EOF analysis with overlapping time windows. Red (blue) dots indicate AMO+ (AMO-) phases. The black markers show the mean position of both NAO centers of action (AH and IL) during AMO+ and AMO- phases. The arrows represent the mean wind field and are scaled to m/s. The purple contour shows the windspeed difference between AMO+ and AMO- phases. MCA = Medieval Climate Anomaly; LIA = Little Ice Age; IL = Icelandic Low; AH = Azores High (Börgel et al., 2020).

5.2.2 Regional importance of the spatial position of the NAO

The regional importance of the NAO for Northern Europe was analyzed using the example of the Baltic Sea. Studies have shown that the importance of the NAO for the Baltic Sea region changes over time (Vihma and Haapala, 2009, Omstedt and Chen, 2001, Hünicke and Zorita, 2006, Chen and Hellström, 1999, Meier and Kauker, 2002, Beranová and Huth, 2008). Figure 5.7 (a) shows the 30-year running correlation between the NAO and important regional climate variables such as SST, sea ice extent, and runoff compared to the zonal position of the IL. All climate variables show strong multidecadal variability. To analyze the importance of the zonal position of the IL for the Baltic Sea region the correlation between the running correlation and the position of the IL was computed. A correlation of 0.5 for the SST, a cor-

relation of 0.42 for the sea ice extent, and a correlation of 0.35 for the river runoff is found. The same analysis was repeated for the AH. However, it was found that the position of the AH does not have a significant impact on the climate of the Baltic Sea.

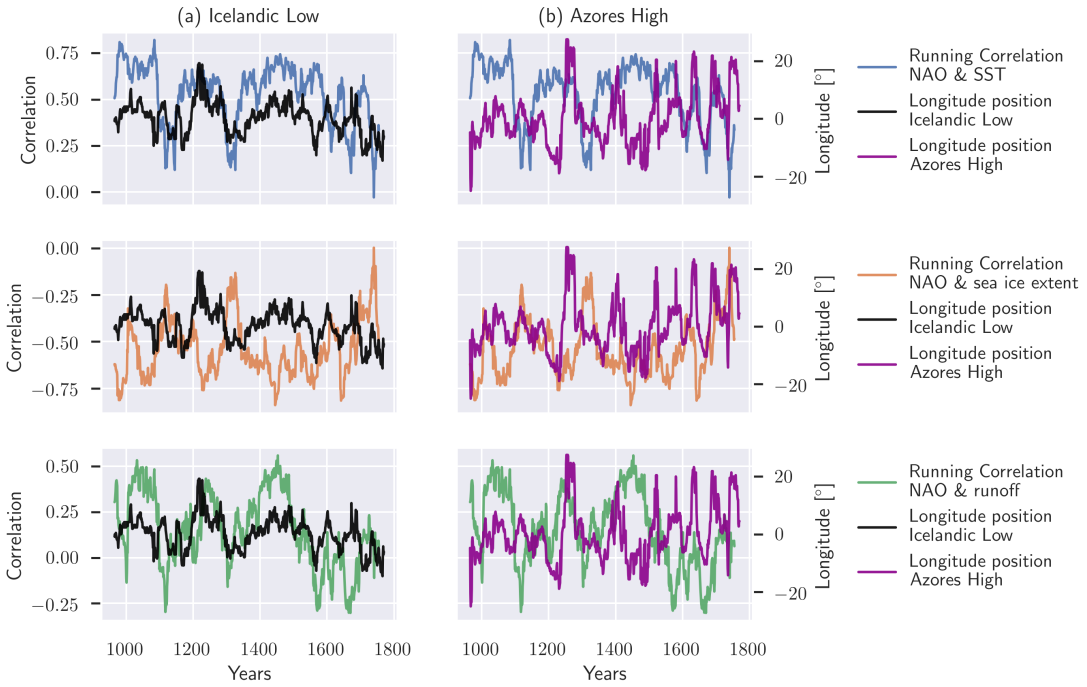

Figure 5.7: Comparison of the longitudinal position of the IL (a) and the AH (b) with the 30-year running correlation between the NAO and regional climate variables of the Baltic Sea, namely, sea ice extent, river runoff, and SST. NAO = North Atlantic Oscillation; SST = sea surface temperature; IL = Icelandic Low; AH = Azores High (Börgel et al., 2020).

5.2.3 Summary and regional importance for the Baltic Sea

In this work it was shown that the AMO influences the spatial pattern of the NAO on multi-decadal time scales. The state of the AMO influences the zonal position of the IL causing it to shift westward during AMO+ states. A westward shift of the IL reduces the regional importance of the NAO for the North European climate. The impact of the AMO on the spatial position of both NAO centers of action (IL and AH) was analyzed for the MCA and the LIA. Independent of the respective climate state it was found that during AMO+ states, the

Icelandic Low moves further towards North America while the Azores High moves further towards Europe and vice versa for AMO- states. Luo et al. (2010) argued that the position of the Atlantic storm tracks likely influences the position of both NAO centers of action. However, it was found that the multidecadal spatial variability of the IL and the AH is not affecting the mean storm track density (Börgel et al., 2020, their Figure 3).

The shift of the IL and the AH is of great importance for the climate in Northern Europe and is often neglected in studies discussing global and regional climate. The Baltic Sea is exposed to a variety of anthropogenic pressures. However, this study focused only on the impact of natural variability because it may be even more important than anthropogenic climate change in the near future, as approximately 60 % of the decadal variability of the mean SST can be attributed to the AMO (Kniebusch et al., 2019a). While Beranová and Huth (2008) found a higher correlation between the NAO and the European climate when the NAO centers of action are located farther east. However, this study showed that only the location of the IL is relevant for the regional correlation between the NAO and North European climate. Summarizing, the AMO influences the east-west position of the IL and the AH, with a NW and SE shift respectively during AMO+ phases. Therefore, it is important to consider the respective state of the AMO since it indicates whether the correlation between the NAO and regional climate will increase or decrease.

5.3 Temperature variability of the Baltic Sea since 1850 and attribution to atmospheric forcing variables

The Baltic Sea is under the constant influence of anthropogenic pressures and climate change and is one of the fastest warming seas in the world (Belkin, 2009). However, the observed warming trends depend on the chosen period. The warming trend considering the period 1957 - 2006 was weaker than considering only the period 1982 - 2006. This leads to the questions: What drives the temperature trends in the Baltic Sea? This work provides an in-depth analysis of why the Baltic Sea was warming the fastest (Kniebusch et al., 2019a). The following summary focuses on the attribution of the SST trends to the atmospheric forcing and oceanographic variables. The analysis was based on two different regional ocean circulation

models, RCO and MOM, validated by available observational. In addition, a MOM box model setup was used.

5.3.1 Atmospheric drivers affecting SST trends

The SST is mainly driven by the air temperature. Calculating the explained variance between the SST and the surface air temperature (SAT) showed that the SAT explains about 80 % of the SST variance (Figure 5.8). However, explained variance or in other words R^2 does not necessarily imply causation or a physical relationship of any kind. Therefore, to isolate the effect of the SAT on the SST a box model without horizontal ocean currents was used, excluding any advectional processes such as wind. For the box model two different approaches were chosen, since the vertical stratification of the Baltic Sea is highly variable. MOMbox1 used a constant salinity profile for the whole period while MOMbox2 used the salinity profile at Gotland extracted from the original RCO simulation. Figure 5.9 shows that the long-term variability of the SST is not affected by omitting advectional processes in the MOM box model.

In addition, the results of MOMbox1 showed that processes such as inflows from the North Sea and changes in stratification are not affecting the long-term variability of the SST as well. The SST differences between the MOM and the MOM box model can be explained by differences in the spatial mean. Therefore, the MOMbox confirmed the results of the statistical analysis identifying the air temperature as the main driver of the SST.

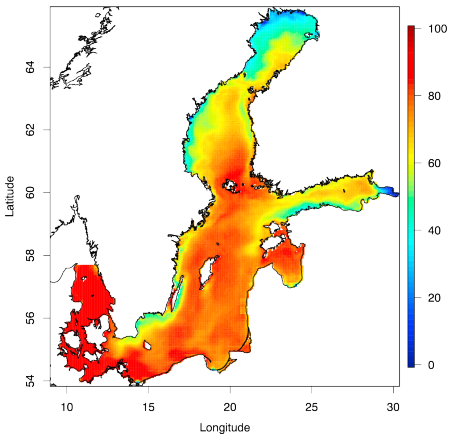

Figure 5.8: Explained variance (in percent) between the simulated annual mean sea surface temperature (RCO) and the forcing air temperature (HiResAFF) for the whole simulated period (Kniebusch et al., 2019a).

To analyze the contribution of the other atmospheric drivers, the SAT was filtered by using a linear model regressing the SAT onto the SST. The residuals represent the remaining variability explained by the other atmospheric

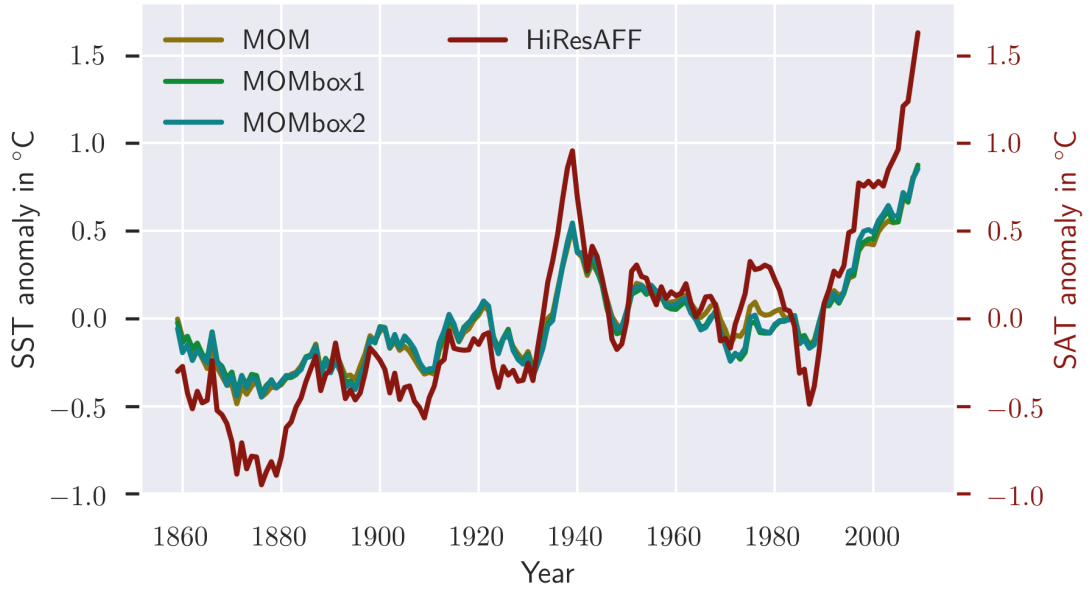

Figure 5.9: Ten-year running mean of simulated time series. SAT (HiResAFF) and SST anomalies at Gotland Deep. SAT = surface air temperature; SST = sea surface; HiResAFF data (Rayner et al., 2003)

drivers. A cross-correlation analysis of the residuals with the other atmospheric drivers showed that the latent heat flux is the second most important driver of the SST with an explained variance of 30 % to 50 % of the residual time series (see Figure 5.10). The third most important driver is either cloudiness or meridional wind, depending on the location under consideration. Meridional wind plays an important role on the Western and Northern coast of the Baltic Sea, which can be linked to wind-induced upwelling in coastal areas. The cloudiness plays an important role in the open sea and can be interpreted as a measure of the radiation budget. However, the explained variance of both drivers is relatively low with below 4 %.

5.3.2 What is the reason for the observed warming in the Baltic Sea?

The air temperature has been identified as the main driver for the SST in the Baltic Sea. Consequently, air temperature trends in the Northern Hemisphere are responsible for the observed warming in the Baltic Sea. Figure 5.11 attributes the SST variability to the climate

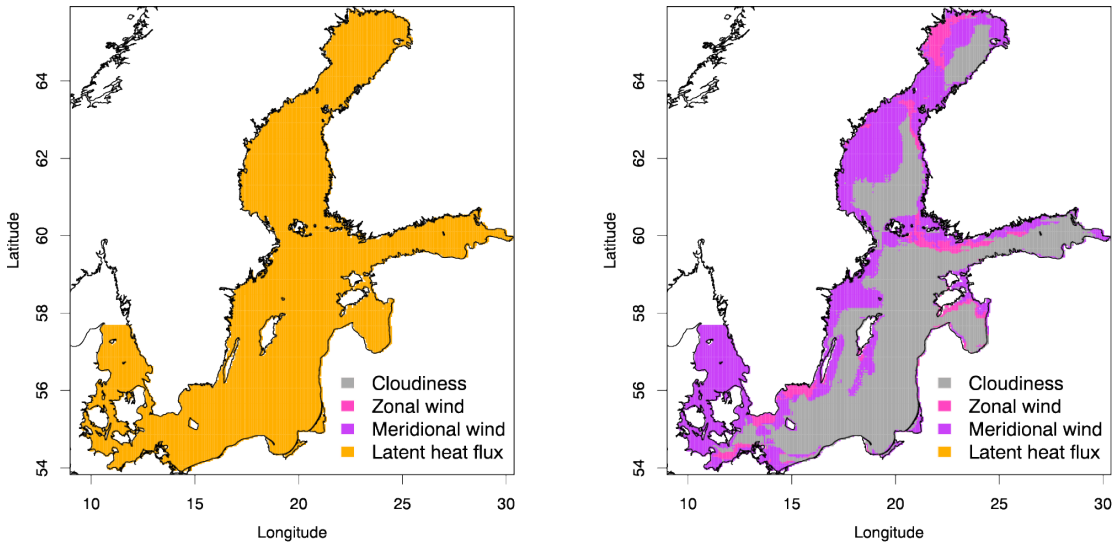

Figure 5.10: Results of the cross-correlation analysis of the detrended SST (2-day output of the RCO model is used) with the wind components, latent heat flux, and cloudiness. Maps of atmospheric drivers (top row) with the highest (left column) and second highest (right column) cross correlations (Kniebusch et al., 2019a).

modes NAO and AMO. The NAO shows a higher impact on an annual scale with about 14 % of explained variance, the AMO explains about 60 % on decadal time scales. This suggests that the high SST values during the 1930s and the cold period in the 1980s can be explained by the AMO. Furthermore, the strong SST trends since the 1980s can be explained by the combination of anthropogenic climate change and a transition from a negative to a positive AMO phase. Summarizing, the AMO is an important driver for the observed SST trends in the Baltic Sea.

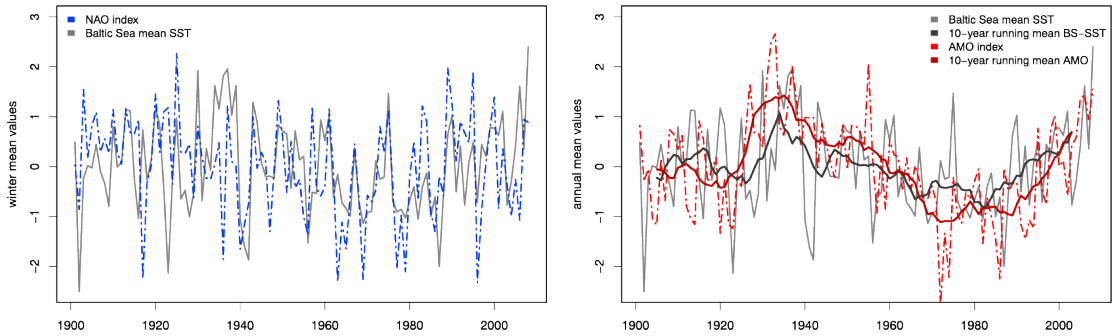

Figure 5.11: Detrended and normalized time series of the Baltic Sea annual mean SST and two climate indices. (left) Winter (December - February) mean NAO. (right) Annual and 10-year running mean AMO and SST. SST = sea surface temperature; NAO = North Atlantic Oscillation; AMO = Atlantic Multidecadal Oscillation. (Kniebusch et al., 2019a).

Remember, with great knowledge
comes great responsibility.

Uncle Ben, Spiderman 2002

6 Conclusion

The AMO has been shown to impact many different areas all over the world, impacting decade-long temperature and rainfall trends. This work for the first time revealed an impact of the AMO on the climate of the Baltic Sea. It is shown, that the AMO affects the mean salinity and the SST of the Baltic Sea. In addition, it affects the spatial pattern of the NAO changing the importance of the NAO for the Baltic Sea. Therefore, the findings of this work show that the state of the AMO should be considered when discussing the climate of Northern Europe and its impact on the Baltic Sea. A possible shortcomming of this study could be that the impact of the AMO on Northern European climate is solely based on one model simulation. To simulate the climate, models need to discretize and parameterize physical processes which always introduce uncertainty. Using a multi-model ensemble where discretization and parametrization differs would increase the robustness of these findings. Like the model uncertainty the forcing data also acts as a source of uncertainty. For example, the estimated temperature difference between MCA and LIA ranges between 0.87 K (Schimanke

et al., 2012) and about 2 K (Kabel et al., 2012). Including different forcing data sets would certainly increase the accuracy of this work. However, a Grand Ensemble of multiple models and multiple forcing data sets requires a huge amount of computational power. Nevertheless, to confirm the study of Börgel et al. (2020), one could analyze the spatial shift of the NAO by using the Paleoclimate Modelling Intercomparison Project (PMIP3) ensemble.

Based on this work a further research question is: Which role does the AMO play for the biogeochemistry of the Baltic Sea? The observed changes in salinity are likely to affect the biodiversity of the Baltic Sea on long time scales. The distribution of freshwater species and marine species in the Baltic Sea can be described according to Remane's species minimum concept (Remane and Schlieper, 1971). This concept defines the number of species along a salinity gradient, where at salinities between 5 - 7 g kg^{-1} the number of freshwater and marine species are at their minimum (Vuorinen et al., 2015). Since most rivers are in the Northern part of the Baltic Sea, higher river runoff will cause increased horizontal surface salinity gradients within the Baltic Sea. This changes the natural habitat of some species. Fresher conditions would force marine species to migrate southward while more freshwater species would populate the North (Vuorinen et al., 2015). the present work focuses on the effect the AMO has on the freshwater supply into the Baltic Sea. However, the other main driver of the salinity of the Baltic are saltwater inflows from the North Sea. Therefore, another open question that needs to be addressed is: Does the AMO impact the frequency and intensity of saltwater inflows into the Baltic Sea? Saltwater inflows happen irregularly and need special meteorological conditions. However, are there any pre-conditions that increase or decrease the frequency of saltwater inflows? It is conceivable that the AMO, which has been proven to lead to more precipitation in the Baltic Sea region during AMO+ phases, which in turn leads to more river runoff, ultimately also influences the intensity of inflow events. Higher river runoffs are likely to lead to a dilution of the water masses in the Danish Straits. This would probably decrease the intensity of the following saltwater inflows.

In this dissertation it was shown that the AMO has a much greater impact on the Baltic Sea than previously thought. Its impact may be even more important than anthropogenic climate change in the near future, as 58 % of the decadal variability in the Baltic Sea mean

SST can be explained by the AMO (Kniebusch et al., 2019a). However, further questions about the influence of the AMO on the Baltic Sea are still waiting to be answered.

References

Birgit Hünicke, Eduardo Zorita, and Susanne Haeseler. Baltic Holocene Climate and regional sea-level change: A statistical analysis of observations, reconstructions and simulations within present and past as analogues for future changes. *GKSS Reports*, 2010.

P. D. Jones, T. Jonsson, and D. Wheeler. Extension to the North Atlantic oscillation using early instrumental pressure observations from Gibraltar and south-west Iceland. *International Journal of Climatology*, 17(13):1433–1450, 1997.

N. A. Rayner, D. E. Parker, E. B. Horton, C. K. Folland, L. V. Alexander, D. P. Rowell, E. C. Kent, and A. Kaplan. Global analyses of sea surface temperature, sea ice, and night marine air temperature since the late nineteenth century. *Journal of Geophysical Research: Atmospheres*, 108(D14), 2003. doi: 10.1029/2002JD002670. URL https://agupubs.onlinelibrary.wiley.com/doi/abs/10.1029/2002JD002670.

Semjon Schimanke and H. E. Markus Meier. Decadal-to-Centennial Variability of Salinity in the Baltic Sea. *Journal of Climate*, 29(20):7173–7188, 2016. doi: 10.1175/JCLI-D-15-0443.1. URL https://doi.org/10.1175/JCLI-D-15-0443.1.

Jüri Elken and W. Matthäus. Baltic Sea oceanography. *Assessment of Climate Change for the Baltic Sea Basin. BALTEX Publication*, 01 2008.

A. Grinsted, J. C. Moore, and S. Jevrejeva. Application of the cross wavelet transform and wavelet coherence to geophysical time series. *Nonlinear Processes in Geophysics*, 11(5/6):561–566, 2004. doi: 10.5194/npg-11-561-2004. URL https://www.nonlin-processes-geophys.net/11/561/2004/.

Florian Börgel, Claudia Frauen, Thomas Neumann, Semjon Schimanke, and H. E. Markus Meier. Impact of the Atlantic Multidecadal Oscillation on Baltic Sea Variability. *Geophysical Research Letters*, 45(18):9880–9888, 2018. doi: 10.1029/2018GL078943. URL https://agupubs.onlinelibrary.wiley.com/doi/abs/10.1029/2018GL078943.

Florian Börgel, Claudia Frauen, Thomas Neumann, and H. E. Markus Meier. The Atlantic Multidecadal Oscillation controls the impact of the North Atlantic Oscillation on North European climate. *Environmental Research Letters (under review)*, 2020. doi: underreview.

Madline Kniebusch, H.E. Markus Meier, Thomas Neumann, and Florian Börgel. Temperature Variability of the Baltic Sea Since 1850 and Attribution to Atmospheric Forcing Variables. *Journal of Geophysical Research: Oceans*, 124(6):4168–4187, 2019a. doi: 10.1029/2018JC013948. URL https://agupubs.onlinelibrary.wiley.com/doi/abs/10.1029/2018JC013948.

Alex G. Libardoni, Chris E. Forest, Andrei P. Sokolov, and Erwan Monier. Underestimating internal variability leads to narrow estimates of climate system properties. *Geophysical Research Letters*, 46(16):10000–10007, 2019. doi: 10.1029/2019GL082442. URL https://agupubs.onlinelibrary.wiley.com/doi/abs/10.1029/2019GL082442.

IPCC. *Summary for Policymakers*, book section SPM, page 1–30. Cambridge University Press, Cambridge, United Kingdom and New York, NY, USA, 2013. ISBN ISBN 978-1-107-66182-0. doi: 10.1017/CBO9781107415324.004. URL www.climatechange2013.org.

Thorsten B. H. Reusch, Jan Dierking, Helen C. Andersson, Erik Bonsdorff, Jacob Carstensen, Michele Casini, Mikolaj Czajkowski, Berit Hasler, Klaus Hinsby, Kari Hyytiäinen, Kerstin Johannesson, Seifeddine Jomaa, Veijo Jormalainen, Harri Kuosa, Sara Kurland, Linda Laikre, Brian R. MacKenzie, Piotr Margonski, Frank Melzner, Daniel Oesterwind, Henn Ojaveer, Jens Christian Refsgaard, Annica Sandström, Gerald Schwarz, Karin Tonderski, Monika Winder, and Marianne Zandersen. The Baltic Sea as a time machine for the future coastal ocean. *Science Advances*, 4(5), 2018. doi: 10.1126/sciadv.aar8195. URL https://advances.sciencemag.org/content/4/5/eaar8195.

O. de Viron, J. O. Dickey, and M. Ghil. Global modes of climate variability. *Geophysical Research Letters*, 40(9):1832–1837, 2013. doi: 10.1002/grl.50386. URL https://agupubs.onlinelibrary.wiley.com/doi/abs/10.1002/grl.50386.

Guiling Wang and David Schimel. Climate change, climate modes, and climate impacts. *Annual Review of Environment and Resources*, 28(1):1–28, 2003. doi: 10.1146/annurev.energy.28.050302.105444. URL https://doi.org/10.1146/annurev.energy.28.050302.105444.

Michael E. Mann, Zhihua Zhang, Scott Rutherford, Raymond S. Bradley, Malcolm K. Hughes, Drew Shindell, Caspar Ammann, Greg Faluvegi, and Fenbiao Ni. Global Signatures and Dynamical Origins of the Little Ice Age and Medieval Climate Anomaly. *Sci-*

ence, 326(5957):1256–1260, 2009. ISSN 0036-8075. doi: 10.1126/science.1177303. URL http://science.sciencemag.org/content/326/5957/1256.

J. W. Hurrell, Y. Kushnir, G. Ottersen, and M. Visbeck. The North Atlantic Oscillation: Climatic Significance and Environmental Impact. *GEOPHYSICAL MONOGRAPH SERIES*, 134:279 pp, 2003 2003. doi: 10.1029/GM134.

Jaak Jaagus. Regionalisation of the precipitation pattern in the Baltic Sea drainage basin and its dependence on large-scale atmospheric circulation. *Boreal Environment Research*, 14(1): 31–44, 2009. ISSN 12396095.

F. Kauker and H. E. M. Meier. Modeling decadal variability of the Baltic Sea: 1. Reconstructing atmospheric surface data for the period 1902–1998. *Journal of Geophysical Research: Oceans*, 108(C8), 2003. doi: 10.1029/2003JC001797. URL https://agupubs.onlinelibrary.wiley.com/doi/abs/10.1029/2003JC001797.

Thomas L. Delworth and Fanrong Zeng. The Impact of the North Atlantic Oscillation on Climate through Its Influence on the Atlantic Meridional Overturning Circulation. *Journal of Climate*, 29(3):941–962, 2016. doi: 10.1175/JCLI-D-15-0396.1. URL https://doi.org/10.1175/JCLI-D-15-0396.1.

Adam Scaife, Chris Folland, Lisa Alexander, Anders Moberg, and Jeff Knight. European climate extremes and the North Atlantic Oscillation. *Journal of Climate*, 21(1): 72–83, 2008. doi: doi:10.1175/2007JCLI1631.1. URL http://ams.allenpress.com/perlserv/?request=get-document&doi=10.1175%2F2007JCLI1631.1.

Trigo Ricardo, J. Osborn Timothy, and M. Corte-Real Joao. The North Atlantic Oscillation influence on Europe: climate impacts and associated physical mechanisms. *Climate Research*, 20(1):9–17, 2002. doi: http://www.jstor.org/stable/24866789.

Robert C. J. Wills, Kyle C. Armour, David S. Battisti, and Dennis L. Hartmann. Ocean–Atmosphere Dynamical Coupling Fundamental to the Atlantic Multidecadal Oscillation. *Journal of Climate*, 32(1):251–272, 2019. doi: 10.1175/JCLI-D-18-0269.1. URL https://doi.org/10.1175/JCLI-D-18-0269.1.

Jeff R. Knight, Chris K. Folland, and Adam A. Scaife. Climate impacts of the Atlantic Multidecadal Oscillation. *Geophysical Research Letters*, 33(17), 2006. ISSN 1944-8007. doi: 10.1029/2006GL026242. URL http://dx.doi.org/10.1029/2006GL026242.

Mads Knudsen, Marit-Solveig Seidenkrantz, Bo Jacobsen, and Antoon Kuijpers. Tracking the Atlantic Multidecadal Oscillation through the last 8,000 years. *Nature communications*, 2:178, 02 2011. doi: 10.1038/ncomms1186.

David B. Enfield, Alberto M. Mestas-Nuñez, and Paul J. Trimble. The Atlantic Multidecadal Oscillation and its relation to rainfall and river flows in the continental U.S. *Geophysical Research Letters*, 28(10):2077–2080, 2001. ISSN 1944-8007. doi: 10.1029/2000GL012745. URL http://dx.doi.org/10.1029/2000GL012745.

Rowan T. Sutton and Daniel L. R. Hodson. Atlantic Ocean Forcing of North American and European Summer Climate. *Science*, 309(5731):115–118, 2005. ISSN 0036-8075. doi: 10.1126/science.1109496. URL https://science.sciencemag.org/content/309/5731/115.

Mingfang Ting, Yochanan Kushnir, Richard Seager, and Cuihua Li. Robust features of Atlantic multi-decadal variability and its climate impacts. *Geophysical Research Letters*, 38 (17), 2011. ISSN 1944-8007. doi: 10.1029/2011GL048712.

A. Casanueva, C. Rodríguez-Puebla, M. D. Frías, and N. González-Reviriego. Variability of extreme precipitation over Europe and its relationships with teleconnection patterns. *Hydrology and Earth System Sciences*, 18(2):709–725, 2014. doi: 10.5194/hess-18-709-2014. URL https://www.hydrol-earth-syst-sci.net/18/709/2014/.

Yohan Ruprich-Robert, Rym Msadek, Frederic Castruccio, Stephen Yeager, Tom Delworth, and Gokhan Danabasoglu. Assessing the Climate Impacts of the Observed Atlantic Multidecadal Variability Using the GFDL CM2.1 and NCAR CESM1 Global Coupled Models. *Journal of Climate*, 30(8):2785–2810, 2017. doi: 10.1175/JCLI-D-16-0127.1. URL https://doi.org/10.1175/JCLI-D-16-0127.1.

Yannick Peings and Gudrun Magnusdottir. Forcing of the wintertime atmospheric circulation by the multidecadal fluctuations of the North Atlantic ocean. *Environmental Research Letters*, 9(3):034018, 2014. URL http://stacks.iop.org/1748-9326/9/i=3/a=034018.

Thomas L. Delworth, Fanrong Zeng, Liping Zhang, Rong Zhang, Gabriel A. Vecchi, and Xiaosong Yang. The Central Role of Ocean Dynamics in Connecting the North Atlantic Oscillation to the Extratropical Component of the Atlantic Multidecadal Oscillation. *Journal of Climate*, 30(10):3789–3805, 2017. doi: 10.1175/JCLI-D-16-0358.1. URL https://doi.org/10.1175/JCLI-D-16-0358.1.

Cheng Sun, Jianping Li, and Fei-Fei Jin. A delayed oscillator model for the quasi-periodic multidecadal variability of the NAO. *Climate Dynamics*, 45(7):2083–2099, Oct 2015. ISSN 1432-0894. doi: 10.1007/s00382-014-2459-z. URL https://doi.org/10.1007/s00382-014-2459-z.

Amy Clement, Katinka Bellomo, Lisa N. Murphy, Mark A. Cane, Thorsten Mauritsen, Gaby Rädel, and Bjorn Stevens. The Atlantic Multidecadal Oscillation without a role for ocean circulation. *Science*, 350(6258):320–324, 2015. ISSN 0036-8075. doi: 10.1126/science.aab3980. URL https://science.sciencemag.org/content/350/6258/320.

Kevin E. Trenberth and Dennis J. Shea. Atlantic hurricanes and natural variability in 2005. *Geophysical Research Letters*, 33(12), 2006. ISSN 1944-8007. doi: 10.1029/2006GL026894. URL http://dx.doi.org/10.1029/2006GL026894. L12704.

Leela M. Frankcombe, Anna von der Heydt, and Henk A. Dijkstra. North Atlantic multidecadal climate variability: An investigation of dominant time scales and processes. *Journal of Climate*, 23(13):3626–3638, 2010a. ISSN 08948755. doi: 10.1175/2010JCLI3471.1.

Igor M. Belkin. Rapid warming of Large Marine Ecosystems. *Progress in Oceanography*, 81 (1):207 – 213, 2009. ISSN 0079-6611. doi: /10.1016/j.pocean.2009.04.011. URL http://www.sciencedirect.com/science/article/pii/S0079661109000317.

Anders Stigebrandt and Bo G. Gustafsson. Response of the Baltic Sea to climate change - Theory and observations. *Journal of Sea Research*, 49(4):243–256, 2003. ISSN 13851101. doi: 10.1016/S1385-1101(03)00021-2.

Kristofer Döös, H E Markus Meier, and Ralf Döscher. The Baltic haline conveyor belt or the overturning circulation and mixing in the Baltic. *Ambio*, 33(4-5):261–6, 2004. URL http://www.ncbi.nlm.nih.gov/entrez/query.fcgi?db=PubMed&cmd=Retrieve&list_uids=15264606&dopt=Citation.

Markus Meier and Ralf Döscher. Simulated water and heat cycles of the Baltic Sea using a 3D coupled atmosphere-ice - ocean model. *Boreal environment research*, 7(4):327–334, 2002.

A. Remane and C. Schlieper. Biology of Brackish Water. *E. Schweiserbart'sche Verlagsbuchhandlung*, (7):34–74, 1971.

Markus Meier, Rainer Feistel, Piechura Jan, Lars Arneborg, Hans Burchard, Fiekas Volker, Golenko Nikolay, Kuzmina Natalia, Volker Mohrholz, Nohr Christian, Vadim Paka, Adolf Stips, and Zhurbas Victor. Ventilation of the baltic sea deep water: A brief review of present knowledge from observations and models. *Oceanologia*, 48, 06 2006.

Wolfgang Matthäus and Herbert Franck. Characteristics of major baltic inflows—a statistical analysis. *Continental Shelf Research*, 12(12):1375 – 1400, 1992. ISSN 0278-4343. doi: https://doi.org/10.1016/0278-4343(92)90060-W. URL http://www.sciencedirect.com/science/article/pii/027843439290060W.

Hartmut Fischer and Wolfgang Matthäus. The importance of the Drogden Sill in the Sound for major Baltic inflows. *Journal of Marine Systems*, 9(3):137 – 157, 1996. ISSN 0924-7963. doi: https://doi.org/10.1016/S0924-7963(96)00046-2. URL http://www.sciencedirect.com/science/article/pii/S0924796396000462.

Volker Mohrholz. Major Baltic Inflow Statistics – Revised. *Frontiers in Marine Science*, 5:384, 2018. ISSN 2296-7745. doi: 10.3389/fmars.2018.00384. URL https://www.frontiersin.org/article/10.3389/fmars.2018.00384.

V. Mohrholz, M. Naumann, G. Nausch, S. Krüger, and U. Gräwe. Fresh oxygen for the Baltic Sea — An exceptional saline inflow after a decade of stagnation. *Journal of Marine Systems*, 148:152 – 166, 2015. ISSN 0924-7963. doi: https://doi.org/10.1016/j.jmarsys.2015.03.005. URL http://www.sciencedirect.com/science/article/pii/S0924796315000457.

Jacob Carstensen, Jesper H. Andersen, Bo G. Gustafsson, and Daniel J. Conley. Deoxygenation of the Baltic Sea during the last century. *Proceedings of the National Academy of Sciences*, 111(15):5628–5633, 2014. ISSN 0027-8424. doi: 10.1073/pnas.1323156111. URL https://www.pnas.org/content/111/15/5628.

Markus Meier, Kari Eilola, Elin Almroth-Rosell, Semjon Schimanke, Madline Kniebusch, A. Höglund, Per Pemberton, Ye Liu, Germo Väli, and S. Saraiva. Disentangling the impact of nutrient load and climate changes on baltic sea hypoxia and eutrophication since 1850. *Climate Dynamics*, 06 2018a. doi: 10.1007/s00382-018-4296-y.

H. E. Markus Meier, Moa Edman, Kari Eilola, Manja Placke, Thomas Neumann, Helén C. Andersson, Sandra-Esther Brunnabend, Christian Dieterich, Claudia Frauen, René Friedland, Matthias Gröger, Bo G. Gustafsson, Erik Gustafsson, Alexey Isaev, Madline Kniebusch, Ivan Kuznetsov, Bärbel Müller-Karulis, Michael Naumann, Anders Omstedt, Vladimir Ryabchenko, Sofia Saraiva, and Oleg P. Savchuk. Assessment of Uncertainties in Scenario Simulations of Biogeochemical Cycles in the Baltic Sea. *Frontiers in Marine Science*, 6:46, 2019. ISSN 2296-7745. doi: 10.3389/fmars.2019.00046. URL https://www.frontiersin.org/article/10.3389/fmars.2019.00046.

H. E. Markus Meier and Frank Kauker. Modeling decadal variability of the Baltic Sea: 2. Role of freshwater inflow and large-scale atmospheric circulation for salinity. *Journal of Geophysical Research: Oceans*, 108(C11), 2003. ISSN 2156-2202. doi: 10.1029/2003JC001799. URL http://dx.doi.org/10.1029/2003JC001799. 3368.

E. Zorita and A. Laine. Dependence of salinity and oxygen concentrations in the Baltic Sea on large-scale atmospheric circulation. *Climate Research*, 14:25–41, January 2000. doi: 10.3354/cr014025.

H. E. Markus Meier. Baltic Sea climate in the late twenty-first century: a dynamical downscaling approach using two global models and two emission scenarios. *Climate Dynamics*, 27(1):39–68, Jul 2006. ISSN 1432-0894. doi: 10.1007/s00382-006-0124-x. URL https://doi.org/10.1007/s00382-006-0124-x.

Madline Kniebusch, H.E. Markus Meier, and Hagen Radtke. Changing Salinity Gradients in the Baltic Sea As a Consequence of Altered Freshwater Budgets. *Geophysical Research Letters*, 46(16):9739–9747, 2019b. doi: 10.1029/2019GL083902. URL https://agupubs.onlinelibrary.wiley.com/doi/abs/10.1029/2019GL083902.

M. Placke, H. E. M. Meier, U. Gräwe, T. Neumann, and Y. Liu. Long-term mean circulation of the Baltic Sea as represented by various ocean circulation models. *Frontiers in Marine Science*, 2018. doi: 10.3389/fmars.2018.00287.

A. Lehmann, K. Getzlaff, and J. Harlaß. Detailed assessment of climate variability in the Baltic Sea area for the period 1958 to 2009. *Climate Research*, 46:185–196, March 2011. doi: 10.3354/cr00876.

Volker Mohrholz, Jörg Dutz, and Gerd Kraus. The impact of exceptionally warm summer inflow events on the environmental conditions in the Bornholm Basin. *Journal of Marine Systems*, 60(3):285 – 301, 2006. ISSN 0924-7963. doi: https://doi.org/10.1016/j.jmarsys.2005.10.002. URL http://www.sciencedirect.com/science/article/pii/S0924796305001715.

Malgorzata Stramska and Jagoda Białogrodzka. Spatial and temporal variability of sea surface temperature in the Baltic Sea based on 32-years (1982–2013) of satellite data. *Oceanologia*, 57(3):223 – 235, 2015. ISSN 0078-3234. doi: https://doi.org/10.1016/j.oceano.2015.04.004. URL http://www.sciencedirect.com/science/article/pii/S0078323415000718.

BACC II Author Team. *Second Assessment of Climate Change for the Baltic Sea Basin*, volume 1. 2015. ISBN 978-3-319-16006-1.

H. E. Markus Meier, Germo Väli, Michael Naumann, Kari Eilola, and Claudia Frauen. Recently Accelerated Oxygen Consumption Rates Amplify Deoxygenation in the Baltic Sea. *Journal of Geophysical Research: Oceans*, 123(5):3227–3240, 2018b. doi: 10.1029/2017JC013686. URL https://agupubs.onlinelibrary.wiley.com/doi/abs/10.1029/2017JC013686.

H. E. M. Meier, A. Höglund, K. Eilola, and E. Almroth-Rosell. Impact of accelerated future global mean sea level rise on hypoxia in the Baltic Sea. *Climate Dynamics*, 49(1-2):163–172, July 2017. doi: 10.1007/s00382-016-3333-y.

Thomas Neumann, Hagen Radtke, and Torsten Seifert. On the importance of Major Baltic Inflows for oxygenation of the central Baltic Sea. *Journal of Geophysical Research: Oceans*, 122(2):1090–1101, 2017. doi: 10.1002/2016JC012525. URL https://agupubs.onlinelibrary.wiley.com/doi/abs/10.1002/2016JC012525.

Emil Vahtera, Daniel J. Conley, Bo G. Gustafsson, Harri Kuosa, Heikki Pitkänen, Oleg P. Savchuk, Timo Tamminen, Markku Viitasalo, Maren Voss, Norbert Wasmund, and Fredrik Wulff. Internal Ecosystem Feedbacks Enhance Nitrogen-fixing Cyanobacteria Blooms and Complicate Management in the Baltic Sea. *AMBIO: A Journal of the Human Environment*, 36(2):186 – 194, 2007. doi: 10.1579/0044-7447(2007)36[186:IEFENC]2.0.CO;2. URL https://doi.org/10.1579/0044-7447(2007)36[186:IEFENC]2.0.CO;2.

Daniel J. Conley. Terrestrial ecosystems and the global biogeochemical silica cycle. *Global Biogeochemical Cycles*, 16(4):68–1–68–8, 2002. doi: 10.1029/2002GB001894. URL https://agupubs.onlinelibrary.wiley.com/doi/abs/10.1029/2002GB001894.

Patrick Samuelsson, Colin G. Jones, Ulrika Willen, Anders Ullerstig, Stefan Ollvik, Ulf Hanson, Christer Jansson, Erik Kjellström, Grigory Nikullin, and Klaus Wyser. The Rossby Centre Regional Climate model RCA3: model description and performance. *Tellus A*, 63(1):4–23, 2011. ISSN 1600-0870. doi: 10.1111/j.1600-0870.2010.00478.x. URL http://dx.doi.org/10.1111/j.1600-0870.2010.00478.x.

H. E. Markus Meier, Ralf Döscher, and Torgny Faxén. A multiprocessor coupled ice-ocean model for the baltic sea: Application to salt inflow. *Journal of Geophysical Research: Oceans*, 108(C8), 2003. doi: 10.1029/2000JC000521. URL https://agupubs.onlinelibrary.wiley.com/doi/abs/10.1029/2000JC000521.

Christopher Torrence and Gilbert P. Compo. A Practical Guide to Wavelet Analysis. *Bulletin of the American Meteorological Society*, 79(1):61–78, 1998. doi: 10.1175/1520-0477(1998)079<0061:APGTWA>2.0.CO;2. URL https://doi.org/10.1175/1520-0477(1998)079<0061:APGTWA>2.0.CO;2.

A Dawson. eofs: A library for eof analysis of meteorological, oceanographic, and climate data. *Journal of Open Research Software*, 4(1):e14, 2016.

A. Hannachi, I. T. Jolliffe, and D. B. Stephenson. Empirical orthogonal functions and related techniques in atmospheric science: A review. *International Journal of Climatology*, 27

(9):1119–1152, 2007. doi: 10.1002/joc.1499. URL https://rmets.onlinelibrary.wiley.com/doi/abs/10.1002/joc.1499.

Laura Landrum, Bette L. Otto-Bliesner, Eugene R. Wahl, Andrew Conley, Peter J. Lawrence, Nan Rosenbloom, and Haiyan Teng. Last Millennium Climate and its variability in CCSM4. *Journal of Climate*, 26(4):1085–1111, 2013. doi: 10.1175/JCLI-D-11-00326.1. URL https://doi.org/10.1175/JCLI-D-11-00326.1.

Leela M. Frankcombe, Anna von der Heydt, and Henk A. Dijkstra. North Atlantic Multidecadal Climate Variability: An Investigation of Dominant Time Scales and Processes. *Journal of Climate*, 23(13):3626–3638, 2010b. doi: 10.1175/2010JCLI3471.1. URL https://doi.org/10.1175/2010JCLI3471.1.

Wei Wei, Gerrit Lohmann, and Mihai Dima. Distinct Modes of Internal Variability in the Global Meridional Overturning Circulation Associated with the Southern Hemisphere Westerly Winds. *Journal of Physical Oceanography*, 42(5):785–801, 2012. doi: 10.1175/JPO-D-11-038.1. URL https://doi.org/10.1175/JPO-D-11-038.1.

Timo Vihma and Jari Haapala. Geophysics of sea ice in the Baltic Sea: A review. *Progress in Oceanography*, 80(3):129 – 148, 2009. ISSN 0079-6611. doi: https://doi.org/10.1016/j.pocean.2009.02.002. URL http://www.sciencedirect.com/science/article/pii/S0079661109000123.

Anders Omstedt and Deliang Chen. Influence of atmospheric circulation on the maximum ice extent in the Baltic Sea. *Journal of Geophysical Research: Oceans*, 106(C3):4493–4500, 2001. doi: 10.1029/1999JC000173. URL https://agupubs.onlinelibrary.wiley.com/doi/abs/10.1029/1999JC000173.

Birgit Hünicke and Eduardo Zorita. Influence of temperature and precipitation on decadal Baltic Sea level variations in the 20th century. *Tellus A*, 58(1):141–153, 2006. doi: 10.1111/j.1600-0870.2006.00157.x. URL https://onlinelibrary.wiley.com/doi/abs/10.1111/j.1600-0870.2006.00157.x.

Deliang Chen and Cecilia Hellström. The influence of the North Atlantic Oscillation on the regional temperature variability in Sweden: spatial and temporal variations. *Tellus A: Dynamic Meteorology and Oceanography*, 51(4):505–516, 1999. doi: 10.3402/tellusa.v51i4.14086. URL https://doi.org/10.3402/tellusa.v51i4.14086.

H.E.M Meier and F Kauker. Simulating Baltic Sea climate for the period 1902-1998 with the Rossby Centre coupled ice-ocean model. *Reports Oceanography*, 30:111 pp., 2002.

Romana Beranová and Radan Huth. Time variations of the effects of circulation variability modes on European temperature and precipitation in winter. *International Journal of Climatology*, 28(2):139–158, 2008. doi: 10.1002/joc.1516. URL https://rmets.onlinelibrary.wiley.com/doi/abs/10.1002/joc.1516.

Dehai Luo, Zhihui Zhu, Rongcai Ren, Linhao Zhong, and Chunzai Wang. Spatial Pattern and Zonal Shift of the North Atlantic Oscillation. Part I: A Dynamical Interpretation. *Journal of the Atmospheric Sciences*, 67(9):2805–2826, 2010. doi: 10.1175/2010JAS3345.1. URL https://doi.org/10.1175/2010JAS3345.1.

S. Schimanke, H. E. M. Meier, E. Kjellström, G. Strandberg, and R. Hordoir. The climate in the Baltic Sea region during the last millennium. *Climate of the Past Discussions*, 8:1369–1407, April 2012. doi: 10.5194/cpd-8-1369-2012.

Karoline Kabel, Matthias Moros, Christian Porsche, Thomas Neumann, Florian Adolphi, Thorbjørn Joest Andersen, Herbert Siegel, Monika Gert, Thomas Leipe, Eystein Janssen, and Jaap Damste. Impact of climate change on the Baltic Sea ecosystem over the past 1000 years. *Nature Climate Change*, 2:871–874, 2012. ISSN 1758-678X.

Ilppo Vuorinen, Jari Haenninen, Marjut Rajasilta, Paeivi Laine, Jan Eklund, Federico Montesino-Pouzols, Francesco Corona, Karin Junker, H.E.Markus Meier, and Joachim W. Dippner. Scenario simulations of future salinity and ecological consequences in the Baltic Sea and adjacent North Sea areas–implications for environmental monitoring. *Ecological Indicators*, 50:196 – 205, 2015. ISSN 1470-160X. doi: https://doi.org/10.1016/j.ecolind.2014.10.019. URL http://www.sciencedirect.com/science/article/pii/S1470160X14005123.

A

Curriculum Vitae

homepage: florianboergel.github.io
florianboergel

Florian Börgel

Education

09/2017 - 10/2020 **Dr. rer. nat.** *Physical (computational) Oceanography*, Leibniz Institute for Baltic Sea Research, Warnemünde, Thesis: Long-term climate variability of the Baltic Sea.

10/2014 - 09/2017 **Master of Science (1.2)**, *Engineering Physics*, University of Oldenburg, Master thesis: The influence of sea ice on Baltic inflows (1.3)
Relevant course work: Computational fluid dynamics, computational intelligence, computational physics.

09/2010 - 02/2014 **Bachelor of Engineering (2.0)**, *Energy, building and environmental engineering*, Münster University of Applied Sciences,
Bachelor thesis: Planning of a local area heating system in the historic city of Warendorf (1,3).

Experience

Professional

since 09/2017 **Research scientist**, *Physical Oceanography*, Leibniz Institute for Baltic Sea Research, Warnemünde.

- numerical climate modeling of the Baltic Sea using a coupled ice-ocean model (MOM, NEMO, ERGOM)
- statistical analysis of long-term climate variability on regional and global scales
- analysis of ensemble simulations (past and future)
- regional climate reconstructions of the last millenium
- sea level prediction based on atmospheric data
- visualization and scientific evaluation of large amounts of data: data pre- and post-processing of large model output (>TB)
- parallel computation on super computers (HLRN)
- successful application for computational time at the North-German Supercomputing Alliance (HLRN) for the project 'Baltic Model Intercomparsion Project'

08/2019 - 08/2020 **Parental leave, my son Leo Heidenreich was born**.

04/2016 - 09/2017 **Research assistant**, *Physical Oceanography*, Leibniz Institute for Baltic Sea Research, Warnemünde.

- application and development of a sea-ice model
- numerical modeling of the Baltic Sea
- statistical analysis of big data sets
- model validation with measurement data

01/2014 - 10/2015 **Research assistant**, *Energy Systems Analysis*, Fraunhofer Institute for Manufacturing Technology and Applied Materials Research, Bremen.
- co-development of a tool to estimate the energy usage of a smart home system
- work within the project HeiCePeCe

Further

11/2014 - 11/2015 **Technical assistant**, *EWE Baskets Oldenburg*, Oldenburg.
- camera work
- control of the advertising boards

04/2013 - 03/2014 **Student assistant**, *energielenker GmbH (formerly infas enermetric)*, Greven.
- planning of environment and climate concepts for cities
- organization of events that deal with CO_2-reduction, energy management and the future use of renewable energies
- planning of a local area heating system in the historic city of Warendorf

07/2010 - 09/2010 **Internship**, *ExKern GmbH*, Münster.
- gutting and reconstruction of buildings

Honors & Scholarships

11/2014 **Fulbright Scholarship**, *Full scholarship to study in the United States for one year (declined).*

Teaching

03/2019 **Baltic Earth Winter School (BEWS)**, *Interactive lecture about wavelet analysis (master level)*, University of Rostock.

WS 2018/19 **Climate of the ocean**, *Introduction to Atmospheric Physics (master level)*, University of Rostock.

WS 2018/19 **Climate of the ocean**, *Teaching assistant for exercises*, University of Rostock.

Training courses

09/2016 **Marine biology course**, *Alfred-Wegener-Institute*, Helgoland.

08/2016 - 09/2016 **International Summer School on Climate of the Baltic Sea Region**, *Baltic Earth*, Askö.

Publications in peer-reviewed journals

2020 **Börgel, F., C. Frauen, T. Neumann, and H. E. M. Meier.**, *The Atlantic Multidecadal Oscillation controls the impact of the North Atlantic Oscillation on North European climate*, Environmental Research Letters, https://doi.org/10.1088/1748-9326/aba925.
2020

2020 **Meier H. E. M., Börgel F., Frauen C., Radtke H.**, *Commentary: Lake or Sea? The Unknown Future of Central Baltic Sea Herring* , Frontiers in Ecology and Evolution, https://doi.org/10.3389/fevo.2020.00055.
2020

2019 **Kniebusch, M., Meier, H. E. M., Neumann, T., and Börgel, F.**, *Temperature variability of the Baltic Sea since 1850 and attribution to atmospheric forcing variables*, Journal of Geophysical Research: Oceans, https://doi.org/10.1029/2018JC013948.
2019

2019 **Radtke, H, Börgel, F, Brunnabend, S-E, Eggert, A, Kniebusch, M, Meier, H E M, Neumann, D, Neumann, T and Placke, M**, *Validator a Web-Based Interactive Tool for Validation of Ocean Models at Oceanographic Stations.*, Journal of Open Research Software, https://doi.org/10.5334/jors.259.
2019

2018 **Börgel, F., C. Frauen, T. Neumann, S. Schimanke, and H. E. M. Meier.**, *Impact of the Atlantic Multidecadal Oscillation on Baltic Sea variability*, Geophysical Research Letters, 45., https://doi.org/10.1029/2018GL078943.
2018

Publications in preparation

2020 **Börgel, F., Kaiser J. M. and Meier, H. E. M**, *The impact of the Atlantic Multidecadal Oscillation on North European Climate - A review.*

2020 **Meier, H. E. M., Börgel. F., Radtke, H., Frauen, C., Kaiser, J. M**, *Low-frequency variability of Baltic Sea salinity.*

2020 **Placke M., Meier, H. E. M., Radtke, H., Gräwe, U., Börgel F., Neumann, T., Gröger, M., Väli, G**, *The idea and benefit of the Baltic Sea Model Intercomparison Project (BMIP).*

2020 **Meier, H. E. M., Bŕgel, F., Bossing-Christensen, O. , Dieterich, C., Dutheil, C., Edman, M., Gröger, M., Kjellström, E.**, *Baltic Sea Scenario Simulations - a review.*

2020 **Meier, H. E. M. et al.**, *BACC III: Current knowledge about past and future climate changes for the Baltic Sea region.*

Referee for international scientific journals

11/2018 **IPCC special report**, *Reviewer for the Intergovernmental Panel on Climate Change's (IPCC) special report on the Ocean and Cryosphere in a Changing Climate.*

Scientific presentations

04/2019 **The impact of the Atlantic Multidecadal Oscillation on Baltic Sea variability**, *Poster session at EGU*, Vienna.

06/2018 **The impact of the Atlantic Multidecadal Oscillation on Baltic Sea variability**, *Speaker at Baltic Earth Conference*, Helsingor.

06/2017 **The influence of sea ice on Baltic Inflows**, *Poster session at Baltic Sea Science Congress*, Rostock.

Outreach

07/2019 **Coastal Research on Tour**, *Presenting my research to a broad audience, organized by Helmholtz-Zentrum Geesthacht*, Rostock.

07/2019 **Warnemünder Abende**, *Presenting my research to a broad audience, organized by Leibniz-Institute for Baltic Sea Research*, Warnemünde.

06/2019 **Rostock's Eleven, science communication challenge**, *Nominee for the Leibniz Institute of Baltic Sea Research*, Rostock.

11/2018 **Create your own #Scicomm bot**, *Host of an interactive session at Forum Wissenschaftskommunikation (German forum science communication)*, Bonn.

Computer skills

Expert **Python, Matlab, Linux/Unix**.

Advanced **R, Fortran, C, parallel computing on super computers**, docker, Twitter API, climate data operators (cdo).

Basic Django framework for Python, HTML, Java, Content Management Systems

Languages

English fluent (TOEFL: 95 - C1)

French Basic knowledge

Volunteer work

since 02/2020 **Deputy speaker of the state working group Energy and Climate**, *Bündnis 90/Die Grünen*, Schwerin.

04/2019 **Candidate for the local election**, *Bündnis 90/Die Grünen*, Rostock.

since 06/2018 **Member of Radentscheid Rostock**, *Citizen-initiated cycling referendum for the City of Rostock*, Rostock.

06/2018 - 02/2020 **Vice chairman of the bicycle forum representing Bündnis 90/Die Grünen**, *Fahrradforum*, Rostock.

06/2018 **Co-organization of the young scientists event at Baltic Earth conference**, *Baltic Earth Conference*, Helsingor.

06/2014 - 07/2014 **Co-organization of the art exhibition 'Ferdast - A journey through Iceland' in the Geological Museum in Münster**, *Art Exhibition 'Ferdast - A journey through Iceland'*, Münster, http://fotoausstellungisland.wordpress.com/.

Additional

since 01/2016 **Member of the German Physical Society**, *DPG*.

11/2010 - 01/2016 **Member of the Association of German Engineers**, *VDI*.

Hobbys **Cyber security, basketball, badminton**

.

Berlin, October 14, 2020

B

Declaration of my contributions to the publications

B.1 Impact of the Atlantic Multidecadal Oscillation on Baltic Sea Variability

This paper was created during my first year as a PhD student at the Institute for Baltic Sea Research, Warnemünde. In the beginning of my PhD, my supervisor recommended to analyze the data of the Schimanke and Meier (2016). Everything after this recommendation - the concept and the writing for this paper - was mainly performed by me. All the figures were created by me. As most of this work relies of the interpretation of a continuous wavelet transformation, I studied wavelet analysis in depth. The manuscript has been reviewed by all co-authors. They provided helpful notes and comments. However, in the end all revisions were implemented by me.

B.2 Influence of the Atlantic Multidecadal Oscillation on the spatial pattern of the North Atlantic Oscillation during the last millennium

The second paper is the result of my second year as PhD student. Again, the data of Schimanke and Meier (2016) was used. The concept and the writing for this paper - was mainly

performed by me. All the figures were created by me. This study uses a method of overlapping EOFs which was implemented by myself, based on the idea of Lehmann et al. (2012). The manuscript has been reviewed by all co-authors. They provided helpful notes and comments. However, in the end all revisions were implemented by me.

B.3 Temperature Variability of the Baltic Sea Since 1850 and Attribution to Atmospheric Forcing Variables

For this paper I set up a 1D box model of the ocean circulation model MOM to answer the concerns of the reviewer whether the SAT is truly the main driver of the SST. The box model had to be set up from scratch. I was also involved and helped writing and editing the part of the box model in the revised manuscript. Further, I helped with the physical interpretation of the results of the box model.

C
Publications

The following publications are included in the appendix in the order of appearance:

A Börgel, F., *Frauen, C., Neumann, T., Schimanke, S., and Meier, H. E. M.* (2018). Impact of the Atlantic Multidecadal Oscillation on Baltic Sea variability. Geophysical Research Letters, 45, 9880– 9888. https://doi.org/10.1029/2018GL078943

B Börgel, F., *Frauen, C., Neumann, T and Meier, H. E. M.* (2020). The Atlantic Multidecadal Oscillation controls the impact of the North Atlantic Oscillation on North European climate. Environmental Research Letters, (under review)

C *Kniebusch, M., Meier, H. E. M., Neumann, T.,* and Börgel, F. (2019). Temperature variability of the Baltic Sea since 1850 and attribution to atmospheric forcing variables. Journal of Geophysical Research: Oceans, 124, 4168– 4187. https://doi.org/10.1029/2018JC013948

AGU100 ADVANCING EARTH AND SPACE SCIENCE

Geophysical Research Letters

RESEARCH LETTER
10.1029/2018GL078943

Key Points:
- Downscaling of global climate simulation shows the impact of the Atlantic Multidecadal Oscillation (AMO) on coastal seas like the Baltic Sea
- AMO-induced changes in the atmospheric circulation impact the precipitation over the Baltic Sea catchment area
- Precipitation affects river runoff which in turn affects the salinity of the Baltic Sea

Supporting Information:
- Supporting Information S1

Correspondence to:
F. Börgel,
florian.boergel@io-warnemuende.de

Citation:
Börgel, F., Frauen, C., Neumann, T., Schimanke, S., & Meier, H. E. M. (2018). Impact of the Atlantic Multidecadal Oscillation on Baltic Sea variability. *Geophysical Research Letters, 45*. https://doi.org/10.1029/2018GL078943

Received 28 MAY 2018
Accepted 11 SEP 2018
Accepted article online 17 SEP 2018

Impact of the Atlantic Multidecadal Oscillation on Baltic Sea Variability

Florian Börgel[1], Claudia Frauen[1], Thomas Neumann[1], Semjon Schimanke[2], and H. E. Markus Meier[1,2]

[1]Leibniz Institute for Baltic Sea Research Warnemünde, Rostock, Germany, [2]Swedish Meteorological and Hydrological Institute, Norrköping, Sweden

Abstract The Atlantic Multidecadal Oscillation (AMO) is a natural mode of variability of the North Atlantic sea surface temperature. The AMO can be used to describe the complex interaction of the coupled atmosphere-ocean system of the North Atlantic. By analyzing a preindustrial period of 850 years with a regional climate model, we show that the AMO influences the Baltic Sea. AMO-related changes of the atmospheric circulation affect precipitation over the Baltic Sea region, which leads to altered river runoff influencing the salinity of the Baltic Sea. A wavelet coherence analysis reveals a persistent coherence between AMO and salinity for the whole period of 850 years. This suggests that the Baltic Sea is under the constant influence of the AMO. Our results provide strong evidence for long-term changes in the Baltic Sea as a result of changing AMO phases.

Plain Language Summary Coastal seas are of great importance to society. A prominent example of such a coastal sea is the Baltic Sea, since it is strongly impacted by human activities. However, besides the human footprint there are also natural phenomena, that influence the Baltic Sea. Especially climate phenomena over the North Atlantic can have a strong impact on the Baltic Sea. One such phenomenon is the so-called Atlantic Multidecadal Oscillation (AMO), a seesaw between warm and cold sea surface temperatures in the North Atlantic with a period of 60-90 years. Reliable observations only exist for a period of about 150 years, which is too short to study multidecadal time scales. Therefore, we use an 850 years long model simulation. Our results show that changes in North Atlantic sea surface temperature associated with the AMO influence the atmospheric circulation, which impacts the rain and snowfall over the Baltic Sea region. This in turn enhances or decreases the river runoff into the Baltic Sea and thus impacts the Baltic Sea salinity. Thus, the AMO has a strong influence on the Baltic Sea.

1. Introduction

Coastal marine environments are among the most socioeconomically used areas on the planet (Harley et al., 2006). They are under the influence of both human activities and natural climate variability. However, the effect of climate variability is often neglected when the state of the marine environment is discussed, since dynamics are very complex and vary on different time scales. There are interannual patterns like El Nino–Southern Oscillation (Wang et al., 1999), decadal modes such as the North Atlantic Oscillation (NAO; Hurrell, 1995) and the Pacific Decadal Oscillation (Krishnan & Sugi, 2003), multidecadal patterns like the Atlantic Multidecadal Oscillation (AMO; Knight et al., 2005) and even millennial-scale climate oscillations such as the Medieval Climate Anomaly (MCA) and the Little Ice Age (LIA; Mann et al., 2009). Several studies have shown that coastal oceans such as the Baltic Sea or the Mediterranean Sea are affected by decadal oscillations (NAO; Lehmann et al., 2002) or even multidecadal oscillations like the AMO (Zampieri et al., 2017).

The semienclosed Baltic Sea is a prominent example for coastal oceans, since it responds very sensitive and fast to atmospheric changes (e.g., Belkin, 2009) and its state is a result of external forcing (Conley et al., 2009; Stigebrandt & Gustafsson, 2003).

The salinity of the Baltic Sea is mainly driven by external forcing: freshwater supply and saltwater inflows from the North Sea. The freshwater input into the Baltic Sea comes either as river runoff or as positive net precipitation (precipitation minus evaporation) over the sea surface. The latter amounts to about 11% of the total freshwater supply (Meier & Döscher, 2002). The river runoff is controlled by precipitation and evaporation over

the drainage basin. More than 50% of the variability in salinity of the Baltic Sea is explained by the river runoff (Meier & Kauker, 2003). Saltwater inflows can be divided into barotropic and baroclinic inflows (Meier et al., 2006). Barotropic inflows are large perturbations that occur irregularly during winter. They are governed by large-scale atmospheric circulations and are initiated by periods of strong easterly winds followed by strong westerly winds on time scales of about 40 days (Schinke & Matthäus, 1998). Baroclinic inflows are driven by salinity gradients and occur mostly during summer (Mohrholz et al., 2006).

The dominant mode of climate variability affecting Europe is the NAO (Hurrell, 1995). However, studies have shown that the AMO is affecting Europe's climate, for example, variability of extreme precipitation (Casanueva et al., 2014) or European summer climate (Enfield et al., 2001). In addition, there are several studies relating AMO states to large-scale circulation patterns over Europe (Landrum et al., 2013; Peings & Magnusdottir, 2014).

The AMO is defined as a mode of climate variability of sea surface temperature (SST) in the North Atlantic with alternating warm and cold phases with a period of about 60–90 years (Knight et al., 2006). It is closely related to the Atlantic Meridional Overturning Circulation (AMOC), which is responsible for the poleward transport of heat toward higher latitudes (Smeed et al., 2018).

Recently, ecological studies started to incorporate the effect of the AMO. Nye et al. (2014) summarized possible impacts of AMO-associated changes to coastal and marine populations. Similar results for the Baltic Sea are discussed by Alheit et al. (2014). However, both studies argue that the lack of observational data limits predictions about the possible impact of the AMO.

The goal of this study is to investigate a possible impact of the AMO on the Baltic Sea. With a frequency of 60–90 years, effects of the AMO are difficult to evaluate, since observations are limited to about 150 years. Tracking records of marine species are even shorter, making statistically significant analyses impossible. One way to avoid this lack of data is to use numerical models.

Although Zhang and Wang (2013) found a large intermodel spread in their analysis of 27 general circulation models (GCMs) regarding the AMO, numerical models are necessary to make statistically significant statements about the impact of the AMO. In our simulation we used the GCM ECHO-G. Medhaug and Furevik (2011) analyzed 24 GCMs and found that ECHO-G's representation of the AMO variability performs reasonably well within the model spread. ECHO-G was one of 10 GCMs that matched the mean observed overturning circulation with a significant correlation between AMO and AMOC.

To exclude anthropogenic influences in our analysis, we have chosen a 850-year preindustrial period. A wavelet coherence analysis has been performed to find different modes of variability and to compare time-localized oscillations between AMO and the mean salinity of the Baltic Sea. Further, atmospheric patterns during AMO+ and AMO− phases are evaluated.

2. Methods and Data

The model results in this study are based on simulations of Schimanke and Meier (2016). They used the regional Rossby Centre Ocean model (RCO) to simulate the Baltic Sea from 950 to 1800. RCO is a primitive equation circulation model with a horizontal resolution of 3.7 km and 83 vertical layers, each with a thickness of 3 m and a maximum depth of 250 m (Meier et al., 2003).

For the time period from 950 to 1800, no observational data for a model validation are available. However, several studies have shown that RCO is capable of modeling observed characteristics of the Baltic Sea on long time scales, for example, Meier and Kauker (2003, their Figures 5 and 7), Schimanke and Meier (2016, Figure 2), Meier et al. (2003, their Figures 6 to 8), Placke et al. (2018), Meier (2007, his Figures 3 to 6), or Eilola et al. (2011, their Figures 5 and 6). Meier et al. (2018) analyzed the time period from 1850 to 2008. In their study they compared RCO model results with long-term monitoring data of temperature, salinity and oxygen, hydrogen sulfide, and nutrient concentrations as well as lightship measurements of temperature and salinity. RCO was able to reproduce the data to a satisfactory degree. Especially, no artificial drift of the model results was observed and RCO showed a good performance for the period after 1960, when better observational data are available. Therefore, it is assumed that RCO is able to reproduce the correct characteristics of the Baltic Sea. RCO is forced by the Rossby Centre Atmosphere model (RCA3; Samuelsson et al., 2011) with a horizontal resolution of 0.44° covering nearly the whole area of Europe. RCA3 is driven by ECHO-G at the lateral boundaries (Legutke & Voss, 1999). This dynamical downscaling approach of ECHO-G allows to include

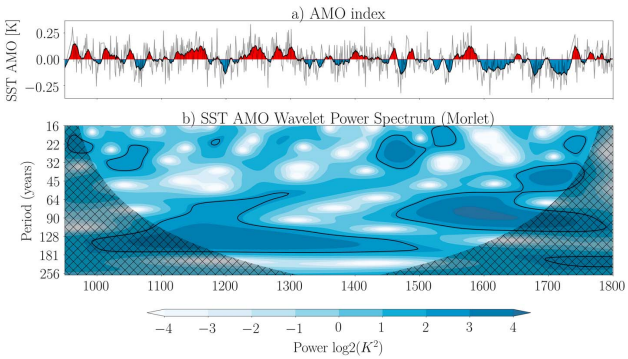

Figure 1. Calculated AMO index (a) and corresponding continuous wavelet transform of the AMO index (b). The black contour lines show statistical significance according to Grinsted et al. (2004). The cone of influence where edge effects might influence the results is hatched (Grinsted et al., 2004). AMO = Atlantic Multidecadal Oscillation; SST = sea surface temperature.

regional effects, for example, a better captured geographical distribution of precipitation (Schimanke et al., 2012). RCA3 provides 10-m wind, 2-m air temperature, 2-m specific humidity, precipitation, total cloudiness, and sea level pressure fields as atmospheric forcing for RCO. For a more detailed description of the atmospheric model and its validation, see Samuelsson et al. (2011). The added value of the dynamical downscaling approach is discussed in Schimanke et al. (2012). The river runoff is estimated from the freshwater budget (precipitation minus evaporation) over the Baltic Sea catchment area using a statistical model presented in Meier et al. (2012).

For our study, we define the AMO as the area-weighted average SST (0–70°N, 90°W to 0°E), following the approach of Landrum et al. (2013). To isolate the Atlantic variability, the global signal is removed by subtracting the global mean SST at each time step (Trenberth & Shea, 2006). To depict low-frequency variations, a 10-year running mean is applied (see Figure 1a). The SST fields of the North Atlantic are taken from ECHO-G.

In our analysis we apply a continuous wavelet transform (CWT) following Grinsted et al. (2004). CWT expands a time series into a time frequency space, which reveals localized oscillations and areas with high power. Since we are interested in the relationship between two parameters, the AMO and the mean salinity of the Baltic Sea, we use wavelet coherence (WTC), which can be understood as a local coherence between two continuous wavelet transforms. This allows to find locally phase-locked behavior (Torrence & Compo, 1998). To reveal areas with high common power, we use the cross-wavelet transform.

3. Results

To analyze the AMO in ECHO-G we use CWT (see Figure 1). The AMO index alternates between warm and cold phases. During the MCA from 950 to 1300 it has the tendency to remain in a warm state. During the transition period and the LIA from 1400 to 1700 cold phases appear more frequently. The AMO signal in ECHO-G has two persistent low-frequency signals during 950–1800. The CWT reveals that from 1150 to 1400, the AMO has significant power in the periodicity band of 120–180 years. During the LIA the energy shifts into the 60- to 90-year periodicity band (see Figure 1).

Meier and Kauker (2003) showed that the relationship between the mean salinity of the Baltic Sea and forcing parameters (e.g., wind and freshwater input) was not necessarily steady in time. Therefore, we use WTC to find nonstationary, low-frequency coherence between the quasi-global signal of the AMO and the mean salinity of the Baltic Sea (Figure 2a). The relation between river runoff into the Baltic Sea and the AMO is shown in Figure 2b. The domain of the Baltic Sea catchment area is shown in Figure 3.

The WTC reveals a significant coherence between AMO and mean salinity for the period from 1150 to 1400 in the 120- to 180-year band. This is followed by a significant coherence from 1450 to 1650 in the 60- to 90-year

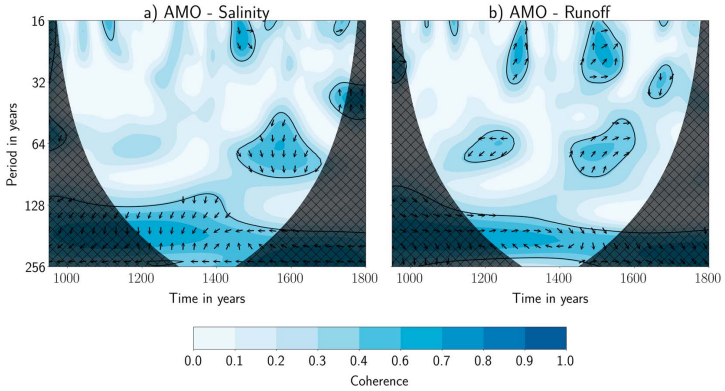

Figure 2. Wavelet coherence of the Atlantic Multidecadal Oscillation (AMO) index and the mean salinity of the Baltic Sea (a) and AMO index and river runoff into the Baltic Sea (b). The black contour lines show the 95% significance level (Grinsted et al., 2004). The arrows in the significant regions indicate the phase relationship between the signals: pointing right (left) in phase (antiphase), and AMO leading (lagging) straight up (down).

band. The phase relationship reveals that the salinity leads the AMO signal. This corresponds to a negative correlation between AMO and salinity. Therefore, we find that the AMO leads the salinity signal by 35 years during 1150–1400 and by 20 years during 1450–1650. This means that AMO+ (AMO−) leads to a decrease (increase) of the mean salinity. A cross-wavelet transform analysis confirms that areas with a high coherence also share high common power (see supporting information Figure S1).

Similar to the coherence between AMO and mean salinity, we find a significant coherence between river runoff and AMO in the 120- to 180-year band from 1150 to 1400. From 1400 to 1650 we find a strong coherence in the 60- to 90-year periodicity band. The phase relationship between AMO and runoff reveals that between 1150 and 1400 the AMO leads the river runoff by 10–15 years, while from 1450 to 1650 both signals are nearly in phase with the AMO leading by 5 years. This is in good agreement with the previously found relationship between AMO and salinity, since higher river runoff causes lower salinities. Following the results of the wavelet analysis, we investigate the atmospheric response to AMO+ and AMO− phases by computing seasonal differences of AMO+ and AMO− phases. Precipitation represents a good estimate of the river runoff, since it is directly related to the freshwater budget over the Baltic Sea catchment area (Kauker & Meier, 2003, their Figure 14).

Figure 3a shows the differences in precipitation associated with AMO shifts in winter (see Figure 1a). Local differences reach up to 10% of the seasonal mean precipitation. Nearly the whole Baltic Sea catchment area shows positive deviations in AMO+ phases, which account for up to 3.5% of the seasonal mean precipitation in winter. In spring (Figure 3b) we find a similar pattern: The whole Baltic Sea region shows positive deviations, that correspond to 4.4% of the seasonal mean. In summer (Figure 3c) the precipitation pattern becomes very noisy with drier conditions in the southern region of the Baltic Sea and wetter conditions in the north. Averaging over the whole Baltic Sea catchment area does not reveal a significant increase of precipitation during summer. In autumn (Figure 3d), we find wetter conditions for almost the entire Baltic Sea region. However, we are not able to find a statistically significant increase in precipitation for the Baltic Sea catchment area in autumn. The coherent change of seasonal precipitation suggests that the AMO influences the atmospheric circulation, which can be partly explained by sea level pressure (SLP) anomalies and the corresponding wind anomalies.

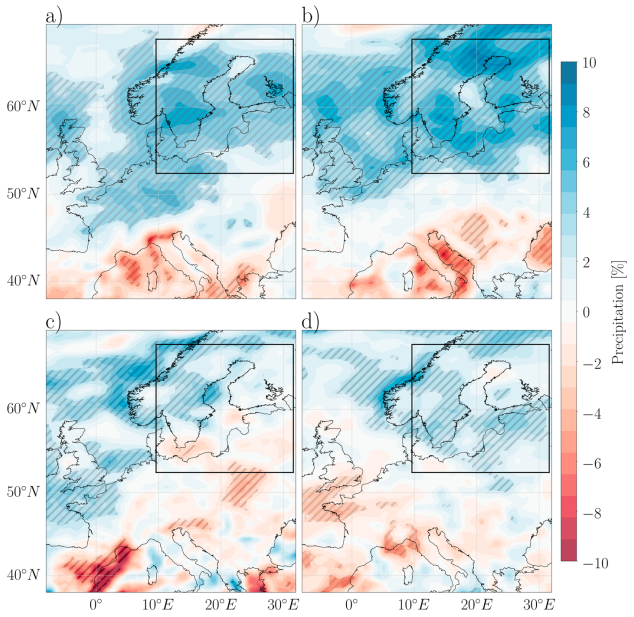

Figure 3. Difference in precipitation between AMO+ and AMO−. (a) Winter (December, January, February), (b) Spring (March, April, May), (c) Summer (June, July, August), (d) Autumn (September, October, November). The scale shows the relative difference to the local seasonal mean. Statistical significance is hatched and calculated with a two-tailed Student's *t* test ($\alpha = 0.05$), where the calculated differences are compared against seasonal fluctuations. The rectangular indicates the defined Baltic Sea catchment area (9.6°E to 32°E and 52.4°N to 67.4°N), which accumulates all of the freshwater input into the Baltic Sea.

Since only winter and spring show a statistically significant increase of precipitation over the Baltic Sea catchment area, only SLP fields of winter and spring are analyzed (Figure 4).

The mean state of winter SLP (Figure 4a) shows a low-pressure regime over Iceland and a high-pressure system over southern Europe. During winter, the dominating direction of winds entering the Baltic Sea region is southwest. Figure 4b shows the differences in SLP between AMO+ and AMO− phases in winter. We find significant negative anomalies (low SLP) over the northern part of Europe. The negative anomaly covers the Baltic Sea region, reaching up to −80 Pa. A high SLP anomaly can be found over southwestern Europe, resembling a dipole-like pattern. The corresponding wind differences between AMO+ and AMO− states show increasing southwesterly anomalies. The mean state in spring shows a similar pattern with a low-pressure field over the northern part of Europe and a high-pressure field located over southern Europe (Figure 4c). However, the horizontal SLP gradients are much smaller than during winter. The mean wind directions during spring differ from those during winter in a more complex pattern. In spring (Figure 4d), the negative pressure anomaly is located over northern Europe, similar to winter. However, the center of the low-pressure anomaly is shifted and is now located directly over the Baltic Sea. Regarding the mean state of spring, we find that the gradient between low- and high-pressure fields is increased. In addition, we find a similar wind pattern to Figure 4b with increased southwesterlies but with smaller wind speed anomalies over the Baltic Sea than during winter.

Both seasons can be associated with a north-south dipole of SLP differences with a similar pattern as the NAO+ phase and are dominated by low-pressure anomalies located over the Baltic Sea.

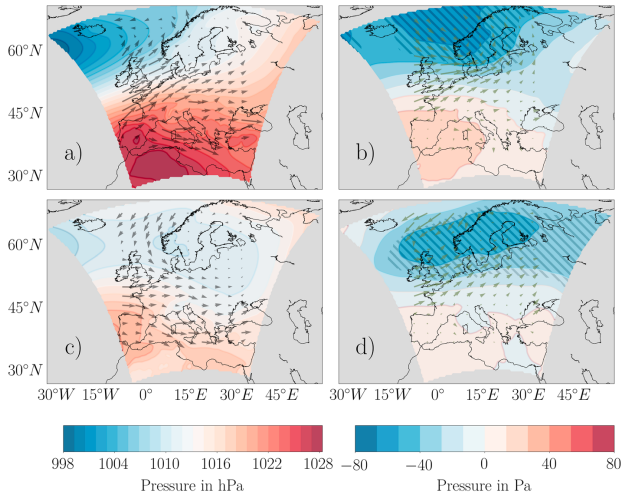

Figure 4. Mean sea level pressure (SLP) during winter in hPa (a), SLP difference between AMO+ and AMO− during winter in Pa (b), mean SLP during spring in hPa (c), SLP difference between AMO+ and AMO− during spring in Pa (d). The arrows indicate the wind direction. Statistical significance is hatched and calculated with a two-tailed Student's *t* test ($\alpha = 0.05$) where the calculated differences are compared with seasonal fluctuations.

4. Discussion and Conclusion

The wavelet coherence revealed that the Baltic Sea is affected by the quasi-global climate mode AMO (Figure 2). To track the AMO signal in the Baltic Sea we investigated its impact on the mean salinity.

We found a strong coherence between the Baltic Sea salinity and the North Atlantic SST variability in a frequency range that can be related to the AMO. The frequency varies between 120 and 180 years during the MCA and 60–90 years during the LIA. The AMO in our model simulation tends to stay in a warm state (AMO+) during the MCA, which is confirmed by Landrum et al. (2013) and Mann et al. (2009). Wei and Lohmann (2012) proposed that background climate conditions can modulate the periodicity and magnitude of the AMO. By analyzing the whole ECHO-G simulation which covers 7000 years, we find that frequency shifts of the AMO appear throughout the simulation (see supporting information Figure S3). Centennial frequency shifts of the AMO have been linked to AMOC variations induced by Southern Hemisphere westerly winds (Wei et al., 2012). Frankcombe et al. (2010) suggested that the AMO is a damped oscillatory internal ocean mode that is excited by atmospheric noise, modulating the dominant frequency. This explanation is confirmed by Chylek et al. (2012), who found shifts of AMO periodicities in a Greenland ice core record. Certainly, it is difficult to compare our results to these studies. However, they could be an explanation for the observed frequency shift between MCA and LIA in our simulation. A similar coherence as for salinity was found between AMO and river runoff into the Baltic Sea. This indicates that the low-frequency variability of the river runoff driven by the AMO influences the low-frequency variability of the mean salinity of the Baltic Sea. This linkage between AMO, river runoff, and salinity can also be confirmed by the phase relationship of both wavelets (Figures 2b and 2c) in accordance with Schimanke and Meier (2016). While the phase relationship between AMO and both salinity and river runoff changes between MCA and LIA, the phase difference between salinity and river runoff remains constant with the runoff leading by approximately 20 years. This agrees with studies by Schimanke and Meier (2016), who found a 15-year lagged response of river runoff and mean salinity of the Baltic Sea. In addition, findings of Meier (2006) also agree with the observed phase relationship. He found an *e*-folding time scale of about 20 years for the response of salinity to atmospheric and hydrological changes in the Baltic Sea. The river runoff responds to the AMO with a lag in the order of 5–15 years. This time scale suggests an underlying

ocean process in the North Atlantic due to the ocean's high inertia. Concluding, we find that the AMO significantly impacts the freshwater balance into the Baltic Sea which then influences, with a lagged response, the salinity of the Baltic Sea.

By applying a bandwidth filter for the dominant frequency of the AMO during MCA (120–180 years) and LIA (60–90 years) we find that the AMO explains 80% of the low-frequency runoff variability into the Baltic Sea during winter and spring. The results of the wavelet analysis are confirmed by Figure 3, where we found that the AMO causes significant changes in precipitation over the Baltic Sea catchment area, especially during winter and spring. This accounts for 3.5% and 4.4% of the mean precipitation during winter and spring, respectively, and 2.5% annually. The increase in precipitation over the Baltic Sea catchment area during AMO+ phases then leads to the observed higher river runoff.

Since these changes occur not on decadal but on multidecadal time scales, we attribute significant salinity changes to the AMO: A low-pass filtered salinity record with a cutoff period of 50 years reveals multidecadal salinity changes of about 0.7 g/kg. As the mean salinity of the Baltic Sea amounts to 7.4 g/kg (Meier & Kauker, 2003), the magnitude of these multidecadal changes is of the order of decadal salinity changes which add up to about 1 g/kg (Meier & Kauker, 2003). In addition, most rivers are located in the northern part of the Baltic Sea. Therefore, higher river runoff will cause increased horizontal surface salinity gradients within the Baltic Sea.

The observed changes in precipitation driving runoff changes are linked to changes in the atmospheric circulation. SLP differences between AMO+ and AMO− (Figures 4b and 4d) of both winter and spring affect the wind over the Baltic Sea region. During AMO+ a low-pressure anomaly in the north and a high-pressure anomaly in the south increases the gradient between the Azores high- and Iceland low-pressure system (Figures 4a and 4c), enhancing the strength of the prevailing westerlies (Hurrell, 1995). Westerly winds transport moist air masses from the North Atlantic to Europe, which results in higher precipitation over the Baltic Sea region (Jaagus, 2009). This is in good agreement with our model results, since we observe increased westerlies during AMO+ phases in winter and spring (Figures 4b and 4d). AMO− phases are characterized by a more continental climate with less westerly winds over this region.

While our results are in agreement with the model simulation (GFDL CM2.1) evaluated by Ruprich-Robert et al. (2017) or Landrum et al. (2013), they partly contradict Sutton and Dong (2012), since they attributed drier conditions in spring and autumn to AMO+ phases. However, we analyzed a longer time period, making direct comparisons difficult. In addition, differences between these studies could also be related to different atmospheric responses to AMO states in climate models. Nevertheless, our results clearly show a persistent low-frequency signal in the Baltic Sea, originating from the North Atlantic.

Summing up, we find that the Baltic Sea region is influenced by low-frequency variability in the North Atlantic, defined as the AMO. Our results show that besides anthropogenic influences, the Baltic Sea is affected by multidecadal natural variability. In our study we focus on the mean salinity; however, similar relationships can be found for more parameters, for example, SST (see supporting information Figure S2). Nearly closed systems like the Baltic Sea vary much faster than open systems like the North Sea. A better understanding of the AMO helps to put the response of these different systems into perspective. Our findings for the Baltic Sea suggest that the state of the AMO should be considered when discussing the state of a coastal ocean.

Acknowledgments
The research presented in this study is part of the Baltic Earth program (Earth System Science for the Baltic Sea region, see http://www.baltic.earth) and was funded partly by the Swedish Research Council for Environment, Agricultural Sciences and Spatial Planning (FORMAS) within the project "Cyanobacteria life cycles and nitrogen fixation in historical reconstructions and future climate scenarios (1850–2100) of the Baltic Sea" (grant 214-2013-1449). Eduardo Zorita is acknowledged for providing ECHO-G data. We thank two anonymous reviewers whose constructive comments greatly improved earlier drafts of the manuscript. All data for this paper are properly cited and referred to in the reference list. The python code used for the analysis is attached as supporting information.

References

Alheit, J., Licandro, P., Coombs, S., Garcia, A., Giráldez, A., Santamaría, M. T. G., et al. (2014). Reprint of Atlantic Multidecadal Oscillation (AMO) modulates dynamics of small pelagic fishes and ecosystem regime shifts in the eastern North and Central Atlantic. *Journal of Marine Systems*, *133*, 88–102. https://doi.org/10.1016/j.jmarsys.2014.02.005

Belkin, I. M. (2009). Rapid warming of large marine ecosystems. *Progress in Oceanography*, *81*(1), 207–213. https://doi.org/10.1016/j.pocean.2009.04.011

Casanueva, A., Rodríguez-Puebla, C., Frías, M. D., & González-Reviriego, N. (2014). Variability of extreme precipitation over Europe and its relationships with teleconnection patterns. *Hydrology and Earth System Sciences*, *18*(2), 709–725. https://doi.org/10.5194/hess-18-709-2014

Chylek, P., Folland, C., Frankcombe, L., Dijkstra, H., Lesins, G., & Dubey, M. (2012). Greenland ice core evidence for spatial and temporal variability of the Atlantic Multidecadal Oscillation. *Geophysical Research Letters*, *39*, L09705. https://doi.org/10.1029/2012GL051241

Conley, D. J., Björck, S., Bonsdorff, E., Carstensen, J., Destouni, G., Gustafsson, B. G., et al. (2009). Hypoxia-related processes in the Baltic Sea. *Environmental Science & Technology*, *43*, 3412–3420. https://doi.org/10.1021/es802762a

Eilola, K., Gustafsson, B., Kuznetsov, I., Meier, H., Neumann, T., & Savchuk, O. (2011). Evaluation of biogeochemical cycles in an ensemble of three state-of-the-art numerical models of the Baltic Sea. *Journal of Marine Systems*, *88*(2), 267–284. https://doi.org/10.1016/j.jmarsys.2011.05.004

Enfield, D. B., Mestas-NuÃ±ez, A. M., & Trimble, P. J. (2001). The Atlantic Multidecadal Oscillation and its relation to rainfall and river flows in the continental U.S. *Geophysical Research Letters*, *28*(10), 2077–2080. https://doi.org/10.1029/2000GL012745

Frankcombe, L. M., von der Heydt, A., & Dijkstra, H. A. (2010). North Atlantic multidecadal climate variability: An investigation of dominant time scales and processes. *Journal of Climate*, *23*(13), 3626–3638. https://doi.org/10.1175/2010JCLI3471.1
Grinsted, A., Moore, J. C., & Jevrejeva, S. (2004). Application of the cross wavelet transform and wavelet coherence to geophysical time series. *Nonlinear Processes in Geophysics*, *11*(5/6), 561–566. https://doi.org/10.5194/npg-11-561-2004
Harley, C. D. G., Randall Hughes, A., Hultgren, K. M., Miner, B. G., Sorte, C. J. B., Thornber, C. S., et al. (2006). The impacts of climate change in coastal marine systems. *Ecology Letters*, *9*(2), 228–241. https://doi.org/10.1111/j.1461-0248.2005.00871.x
Hurrell, J. W. (1995). Decadal trends in the North Atlantic Oscillation: Regional temperatures and precipitation. *Science*, *269*(5224), 676–679. https://doi.org/10.1126/science.269.5224.676
Jaagus, J. (2009). Regionalisation of the precipitation pattern in the Baltic Sea drainage basin and its dependence on large-scale atmospheric circulation. *Boreal Environment Research*, *14*(1), 31–44.
Kauker, F., & Meier, H. E. M. (2003). Modeling decadal variability of the Baltic Sea: 1. Reconstructing atmospheric surface data for the period 1902–1998. *Journal of Geophysical Research*, *108*(C8), 3267. https://doi.org/10.1029/2003JC001797
Knight, J. R., Allan, R. J., Folland, C. K., Vellinga, M., & Mann, M. E. (2005). A signature of persistent natural thermohaline circulation cycles in observed climate. *Geophysical Research Letters*, *32*, L20708. https://doi.org/10.1029/2005GL024233
Knight, J. R., Folland, C. K., & Scaife, A. A. (2006). Climate impacts of the Atlantic Multidecadal Oscillation. *Geophysical Research Letters*, *33*, L17706. https://doi.org/10.1029/2006GL026242
Krishnan, R., & Sugi, M. (2003). Pacific Decadal Oscillation and variability of the Indian summer monsoon rainfall. *Climate Dynamics*, *21*(3), 233–242. https://doi.org/10.1007/s00382-003-0330-8
Landrum, L., Otto-Bliesner, B. L., Wahl, E. R., Conley, A., Lawrence, P. J., Rosenbloom, N., et al. (2013). Last millennium climate and its variability in CCSM4. *Journal of Climate*, *26*(4), 1085–1111. https://doi.org/10.1175/JCLI-D-11-00326.1
Legutke, S., & Voss, R. (1999). The Hamburg atmosphere-ocean coupled circulation model ECHO-G. https://doi.org/10.2312/WDCC/DKRZ_Report_No18
Lehmann, A., Krauss, W., & Hinrichsen, H.-H. (2002). Effects of remote and local atmospheric forcing on circulation and upwelling in the Baltic Sea. *Tellus A: Dynamic Meteorology and Oceanography*, *54*(3), 299–316. https://doi.org/10.3402/tellusa.v54i3.12138
Mann, M. E., Zhang, Z., Rutherford, S., Bradley, R. S., Hughes, M. K., Shindell, D., et al. (2009). Global signatures and dynamical origins of the little ice age and medieval climate anomaly. *Science*, *326*(5957), 1256–1260. https://doi.org/10.1126/science.1177303
Medhaug, I., & Furevik, T. (2011). North Atlantic 20th century multidecadal variability in coupled climate models: Sea surface temperature and ocean overturning circulation. *Ocean Science*, *7*(3), 389–404. https://doi.org/10.5194/os-7-389-2011
Meier, H. E. M. (2006). Baltic Sea climate in the late twenty-first century: A dynamical downscaling approach using two global models and two emission scenarios. *Climate Dynamics*, *27*(1), 39–68. https://doi.org/10.1007/s00382-006-0124-x
Meier, H. E. M. (2007). Modeling the pathways and ages of inflowing salt- and freshwater in the Baltic Sea. *Estuarine Coastal and Shelf Science*, *74*(4), 610–627. https://doi.org/10.1016/j.ecss.2007.05.019
Meier, H. E. M., & Döscher, R. (2002). Simulated water and heat cycles of the Baltic Sea using a 3D coupled atmosphere-ice-ocean model. *Boreal Environment Research*, *7*(4), 327–334.
Meier, H. E. M., Döscher, R., & Torgny, F. (2003). A multiprocessor coupled ice-ocean model for the Baltic Sea: Application to salt inflow. *Journal of Geophysical Research: Oceans*, *108*(C8), 3273. https://doi.org/10.1029/2000JC000521
Meier, H. E. M., Eilola, K., Almroth-Rosell, E., Schimanke, S., Kniebusch, M., Höglund, A., et al. (2018). Disentangling the impact of nutrient load and climate changes on Baltic Sea hypoxia and eutrophication since 1850. *Climate Dynamics*. https://doi.org/10.1007/s00382-018-4296-y
Meier, H. E. M., Feistel, R., Piechura, J., Arneborg, L., Burchard, H., Fiekas, V., et al. (2006). Ventilation of the Baltic Sea deep water: A brief review of present knowledge from observations and models. *Oceanologia*, *48*, 133–164.
Meier, H. E. M., Hordoir, R., Andersson, H. C., Dieterich, C., Eilola, K., Gustafsson, B. G., et al. (2012). Modeling the combined impact of changing climate and changing nutrient loads on the Baltic Sea environment in an ensemble of transient simulations for 1961–2099. *Climate Dynamics*, *39*(9), 2421–2441. https://doi.org/10.1007/s00382-012-1339-7
Meier, H. E. M., & Kauker, F. (2003). Modeling decadal variability of the Baltic Sea: 2. Role of freshwater inflow and large-scale atmospheric circulation for salinity. *Journal of Geophysical Research*, *108*(C11), 3368. https://doi.org/10.1029/2003JC001799
Mohrholz, V., Dutz, J., & Kraus, G. (2006). The impact of exceptionally warm summer inflow events on the environmental conditions in the Bornholm basin. *Journal of Marine Systems*, *60*(3-4), 285–301. https://doi.org/10.1016/j.jmarsys.2005.10.002
Nye, J. A., Baker, M. R., Bell, R., Kenny, A., Kilbourne, K. H., Friedland, K. D., et al. (2014). Ecosystem effects of the Atlantic Multidecadal Oscillation. *Journal of Marine Systems*, *133*, 103–116. https://doi.org/10.1016/j.jmarsys.2013.02.006
Peings, Y., & Magnusdottir, G. (2014). Forcing of the wintertime atmospheric circulation by the multidecadal fluctuations of the North Atlantic Ocean. *Environmental Research Letters*, *9*(3), 034018.
Placke, M., Meier, H. E. M., Gräwe, U., Neumann, T., & Liu, Y. (2018). Long-term mean circulation of the Baltic Sea as represented by various ocean circulation models. *Frontiers in Marine Science*, *5*, 287. https://doi.org/10.3389/fmars.2018.00287
Ruprich-Robert, Y., Msadek, R., Castruccio, F., Yeager, S., Delworth, T., & Danabasoglu, G. (2017). Assessing the climate impacts of the observed Atlantic Multidecadal variability using the GFDL CM2.1 and NCAR CESM1 global coupled models. *Journal of Climate*, *30*(8), 2785–2810. https://doi.org/10.1175/JCLI-D-16-0127.1
Samuelsson, P., Jones, C. G., Willen, U., Ullerstig, A., Ollvik, S., Hanson, U., et al. (2011). The Rossby Centre Regional Climate model RCA3: Model description and performance. *Tellus A*, *63*(1), 4–23. https://doi.org/10.1111/j.1600-0870.2010.00478.x
Schimanke, S., & Meier, H. E. M. (2016). Decadal-to-centennial variability of salinity in the Baltic Sea. *Journal of Climate*, *29*(20), 7173–7188. https://doi.org/10.1175/JCLI-D-15-0443.1
Schimanke, S., Meier, H. E. M., Kjellström, E., Strandberg, G., & Hordoir, R. (2012). The climate in the Baltic Sea region during the last millennium. *Climate of the Past Discussions*, *8*, 1369–1407. https://doi.org/10.5194/cpd-8-1369-2012
Schimanke, S., Meier, H. E. M., Kjellström, E., Strandberg, G., & Hordoir, R. (2012). The climate in the Baltic Sea region during the last millennium simulated with a regional climate model. *Climate of the Past*, *8*(5), 1419–1433. https://doi.org/10.5194/cp-8-1419-2012
Schinke, H., & Matthäus, W. (1998). On the causes of major Baltic inflows—An analysis of long time series. *Continental Shelf Research*, *18*(1), 67–97. https://doi.org/10.1016/S0278-4343(97)00071-X
Smeed, D. A., Josey, S. A., Beaulieu, C., Johns, W. E., Moat, B. I., Frajka-Williams, E., et al. (2018). The North Atlantic Ocean is in a state of reduced overturning. *Geophysical Research Letters*, *45*, 1527–1533. https://doi.org/10.1002/2017GL076350
Stigebrandt, A., & Gustafsson, B. G. (2003). Response of the Baltic Sea to climate change—Theory and observations. *Journal of Sea Research*, *49*(4), 243–256. https://doi.org/10.1016/S1385-1101(03)00021-2
Sutton, R. T., & Dong, B. (2012). Atlantic Ocean influence on a shift in European climate in the 1990s. *Nature Geoscience*, *5*, 788–792. https://doi.org/10.1038/ngeo1595

Torrence, C., & Compo, G. P. (1998). A practical guide to wavelet analysis. *Bulletin of the American Meteorological Society*, *79*(1), 61–78. https://doi.org/10.1175/1520-0477(1998)079<0061:APGTWA>2.0.CO;2

Trenberth, K. E., & Shea, D. J. (2006). Atlantic hurricanes and natural variability in 2005. *Geophysical Research Letters*, *33*, L12704. https://doi.org/10.1029/2006GL026894

Wang, H.-J., Zhang, R.-H., Cole, J., & Chavez, F. (1999). El Niño and the related phenomenon southern oscillation (ENSO): The largest signal in interannual climate variation. *Proceedings of the National Academy of Sciences*, *96*(20), 11,071–11,072. https://doi.org/10.1073/pnas.96.20.11071

Wei, W., & Lohmann, G. (2012). Simulated Atlantic Multidecadal Oscillation during the Holocene. *Journal of Climate*, *25*(20), 6989–7002. https://doi.org/10.1175/JCLI-D-11-00667.1

Wei, W., Lohmann, G., & Dima, M. (2012). Distinct modes of internal variability in the global meridional overturning circulation associated with the Southern Hemisphere westerly winds. *Journal of Physical Oceanography*, *42*(5), 785–801. https://doi.org/10.1175/JPO-D-11-038.1

Zampieri, M., Toreti, A., Schindler, A., Scoccimarro, E., & Gualdi, S. (2017). Atlantic Multi-Decadal Oscillation influence on weather regimes over Europe and the Mediterranean in spring and summer. *Global and Planetary Change*, *151*, 92–100. https://doi.org/10.1016/j.gloplacha.2016.08.014

Zhang, L., & Wang, C. (2013). Multidecadal North Atlantic sea surface temperature and Atlantic meridional overturning circulation variability in CMIP5 historical simulations. *Journal of Geophysical Research: Oceans*, *118*, 5772–5791. https://doi.org/10.1002/jgrc.20390

Supporting Information for

"Impact of the Atlantic Multidecadal Oscillation on Baltic Sea variability"

Florian Börgel[1], Claudia Frauen[1], Thomas Neumann[1], S. Schimanke[2], H. E. Markus Meier[1,2]

[1]Leibniz Institute for Baltic Sea Research Warnemünde, Rostock, Germany

[2]Swedish Meteorological and Hydrological Institute, Norrköping, Sweden

Contents

Corresponding author: Florian Börgel, florian.boergel@io-warnemuende.de

1 Figures

1.1 Figure S1

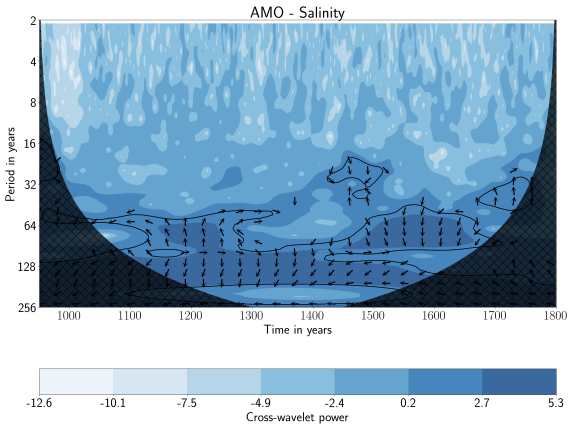

Figure 1. Cross-wavelet of AMO index and mean salinity of the Baltic Sea. The black contour lines show the 95% significance level. The arrows in the significant regions indicate the phase relationship between the signals: pointing right (left) in phase (anti-phase), and AMO leading (lagging) straight up (down).

1.2 Figure S2

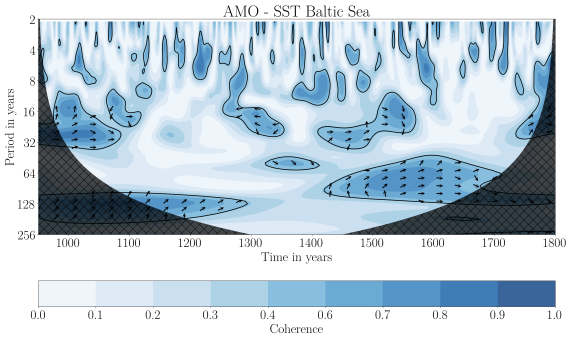

Figure 2. Wavelet coherence of AMO index and mean surface temperature of the Baltic Sea. The black contour lines show the 95% significance level. The arrows in the significant regions indicate the phase relationship between the signals: pointing right (left) in phase (anti-phase), and AMO leading (lagging) straight up (down).

1.3 Figure S3

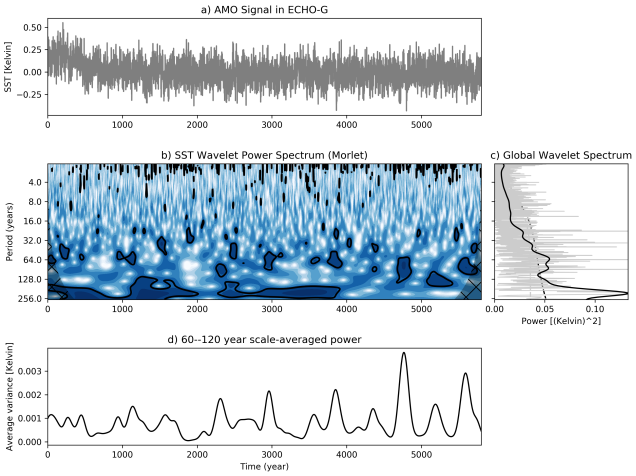

Figure 3. Calculated AMO index of ECHO-G for 7000 year (a). Year 0 corresponds to 5000 BC. CWT of the AMO index (b). The black contour lines show statistical significance. The cone of influence (COI) where edge effects might influence the results is hatched. The global wavelet spectrum (c) and the scale-averaged power in (d).

The Atlantic Multidecadal Oscillation controls the impact of the North Atlantic Oscillation on North European climate

Florian Börgel [1], **Claudia Frauen** [2], **Thomas Neumann** [1] **and H.E. Markus Meier** [1,3]

[1] Institute for Baltic Sea Research, Warnemünde, Rostock
[2] German Climate Computing Centre, Hamburg
[3] Swedish Meteorological and Hydrological Institute, Norrköping

E-mail: florian.boergel@io-warnemuende.de

21 May 2020

Abstract. European climate is heavily influenced by the North Atlantic Oscillation (NAO). However, the spatial structure of the NAO is varying with time, affecting its regional importance. By analyzing an 850-year global climate model simulation of the last millennium it is shown that the variations in the spatial structure of the NAO can be linked to the Atlantic Multidecadal Oscillation (AMO). The AMO changes the zonal position of the NAO centers of action, moving them closer to Europe or North America. During AMO+ states, the Icelandic Low moves further towards North America while the Azores High moves further towards Europe and vice versa for AMO- states. The results of a regional downscaling for the east Atlantic/European domain show that AMO-induced changes in the spatial structure of the NAO reduce or enhance its influence on regional climate variables of the Baltic Sea such as sea surface temperature, ice extent or river runoff.

Keywords: Atlantic Multidecadal Oscillation, North Atlantic Oscillation, regional climate Submitted to: *Environ. Res. Lett.*

1. Introduction

The North Atlantic Oscillation (NAO) and the Atlantic Multidecadal Oscillation (AMO) are two of the most prominent low-frequency modes of climate variability in the Northern Hemisphere (NH). European climate is heavily affected by these two modes. The NAO describes a sea level pressure (SLP) difference between the subpolar Icelandic Low (IL) and the subtropical Azores High (AH) (Hurrell et al. 2003). It affects regional climate and weather patterns in the NH and is responsible for more than 80% of the SLP variability over the North Atlantic and Europe and explains about 40% of the SLP variability for the whole Northern Hemisphere during winter (Kauker & Meier 2003).

As a result the NAO is the most important pattern of atmospheric variability in the NH (Hurrell 1995). Typical time scales cover intra-seasonal to decadal variability (Visbeck et al. 2001).

Often, the NAO is discussed under the assumption that the spatial structure of both centers of action - IL and AH - does not change. However, several studies found that both the IL and the AH exhibit a change in its spatial structure over time (Hilmer & Jung 2000, Jung & Hilmer 2001, Jung et al. 2003, Johnson et al. 2008). Hilmer & Jung (2000) found that the zonal position of both pressure centers influences regional climate conditions in the Arctic region. Further, Lehmann et al. (2011) showed that an eastward shift of the NAO changes the number and pathways of deep cyclones influencing the wind patterns over the Baltic Sea. Beranová & Huth (2008) summarized that the correlation between the NAO index and surface air temperature and precipitation changes across Europe. They concluded that the changes in correlation are linked to the longitudinal position of the IL and the AH. When the NAO centers of action are located further east, the correlation between the NAO and European climate increases. Different physical causes have been identified to influence zonal shifts of the NAO pattern: increasing greenhouse gas concentrations (Ulbrich & Christoph 1999) or an increase of mean westerlies in the Atlantic Basin (Peterson et al. 2002). Further, Peterson et al. (2003) argued that the spatial pattern of the NAO exhibits an eastward shift during the transition from a negative to a positive NAO phase. Luo et al. (2010) proposed that an eastward shift of the Atlantic storm track activity, associated with an increase of the mean westerly flow, is likely causing an eastward shift of the whole NAO pattern. In addition to the impact of the NAO on the climate of the NH, several studies have shown that the AMO impacts the climate of the NH as well. It influences regional climate such as European summer climate, precipitation over Europe, Africa, and North America and cold weather episodes in Europe during winter (Enfield et al. 2001, Knight et al. 2006, Börgel et al. 2018, Sutton & Hodson 2005, Ting et al. 2011, Casanueva et al. 2014, Ruprich-Robert et al. 2017, Peings & Magnusdottir 2014). The AMO describes an alternation between warm and cold sea surface temperature (SST) anomalies in the North Atlantic (Knight et al. 2006), with a periodicity of about 50 to 90 years (e.g. Knight et al. 2006, Knudsen et al. 2011).

In the past, the AMO and the NAO have mostly been discussed separately. More recently, studies started to investigate how these climate modes interact with each other. By analyzing observational data Li et al. (2013) showed that multidecadal fluctuations of the NAO lead the AMO signal by approximately 15 to 20 years. Peings & Magnusdottir (2014) found that multidecadal fluctuations of the wintertime NAO and the AMO are positively correlated when the NAO is leading the AMO by 10 to 20 years. Further, positive NAO anomalies lead to a strengthening of the Atlantic Meridional Overturning Circulation (AMOC) (e.g. Sun et al. 2015). Wills et al. (2019) discussed these interactions between the NAO, the AMO, and the AMOC by applying a low-frequency component analysis (LFCA). They showed that the interaction between the NAO and the AMOC plays a key role in the AMO variability, which confirms studies

of Sun et al. (2015), Delworth & Zeng (2016), Delworth et al. (2017). In contrast Clement et al. (2015) found that the AMO is the response to stochastic forcing from the mid-latitude atmospheric circulation, i.e. NAO. By analyzing a suite of slab ocean models they showed that the ocean does not play an important role for AMO variability. However, Wills et al. (2019) presented evidence that the mechanism of the AMO in a slab ocean model does not agree with observational data.

It is evident that a better understanding of the complex relationship between the AMO and the NAO is necessary to understand the climate of the Northern Hemisphere. Therefore, this study aims to assess the impact of the AMO on the spatial structure of the NAO. Using the example of the Baltic Sea region, we show the importance of this spatial change for the North European climate.

In the following, first the relationship between the AMO and the NAO is analyzed based on a pre-industrial period of the last millennium using a global circulation model. Then the shift of the NAO pattern is identified and linked to the AMO. Further, the impact of the AMO on the mean position of the storm tracks over Northern Europe is evaluated. Lastly, the influence of the spatial position of the NAO on regional climate patterns in the Baltic Sea region is discussed.

2. Material and Methods

2.1. Model description

This study is based on the model results as described in Schimanke & Meier (2016). In their study they used a multi-centennial paleoclimate simulation based on the global circulation model (GCM) ECHO-G, focusing on the last millennium. ECHO-G consists of an atmospheric component with a horizontal resolution of approximately 3.75° x 3.75° and 19 vertical levels and an ocean component with a horizontal resolution of about 2.8° x 2.8° and 20 vertical levels. The ECHO-G Holocene simulation is forced with variations in orbital parameters, solar irradiance, and greenhouse gases and covers 7000 years BP (Hünicke et al. 2010).

The spatial resolution of ECHO-G is too coarse to analyze regional impacts such as local wind patterns. To overcome this problem a dynamical downscaling was performed for the European region with the regional circulation model Rossby Centre regional climate model (RCA3). The downscaling covers the period 950 to 1800 and was forced with the ECHO-G Holocene simulation at the lateral boundaries. RCA3 has a horizontal resolution of 0.44° x 0.44° with 24 vertical levels and a 30 minute time step. It covers nearly the whole area of Europe, ranging from northern Africa to northern Scandinavia (33.0°W to 58.52°E; 26.0°N to 71.76°N). A detailed model description of RCA3 is given by Samuelsson et al. (2011). The resulting atmospheric fields were used to force the regional ocean model Rossby Centre Ocean Model (RCO), simulating the Baltic Sea from 950 to 1800. RCO is a Bryan-Cox-Semtner primitive equation circulation model

and has a resolution of 3.7km x 3.7km. It consists of 83 vertical layers, each with a thickness of 3m. A detailed description of RCO is given by Meier et al. (2003). This simulation has also been analyzed by Börgel et al. (2018) to study the impact of the AMO on Baltic Sea variability and has proven to be suitable to analyze the role of the AMO for Northern European climate. Studies by Zhang & Wang (2013) showed that the spatial and temporal representation of the AMO varies among every GCM. Medhaug & Furevik (2011) analyzed the representation of the AMO in 24 different GCMs. They showed that ECHO-G, which is used in this study, performs reasonably well within the model spread and captures the AMO variability to a satisfying degree. Further, ECHO-G was one out of ten GCMs that matched the mean observed overturning circulation and showed a significant correlation between the AMO and the AMOC. The representation of the NAO generated by ECHO-G is sufficient. Its variability matches the variability of observations and captures regional correlations with precipitation and surface air temperature (Min et al. 2005).

2.2. Modes of variability

In this study the AMO is defined as area-weighted average SST across the North Atlantic domain (0°W to 80°W;0°N to 60°N). Further, the global signal is removed by subtracting the global mean SST (Trenberth & Shea 2006). Zanchettin et al. (2013) showed that it is difficult to separate between low-frequency variability and forced global changes when discussing the AMO. They showed that the AMO is strongly influenced by volcanic eruptions, which are not included in this simulation. In addition, they stressed that the AMO definition of Trenberth & Shea (2006) may cause some variability loss in the North Atlantic, but it removes the impact of external forcing, too. Hence, we argue that the impact of forced global changes on the AMO as discussed in this study is rather small. The NAO is defined as the first empirical orthogonal function (EOF) of the monthly sea-level pressure anomalies (20°N to 70°N; 90°W to 40°E) of the winter season (DJFM). The NAO pattern is mainly associated with a north-south dipole, and the centers of action are referred to as IL and AH in this study. Since RCA3 covers only the European domain, the SLP and SST fields are taken from ECHO-G.

2.3. EOF analysis with overlapping time windows

A reference NAO pattern is defined by calculating the first EOF of the period from 950 to 1800 simulated by ECHO-G. To analyze the change of the spatial position of the NAO an EOF analysis with overlapping time windows is performed. The idea of this concept is similar to a centered moving average. For each time step t an EOF is calculated considering [t-n,t+n] time steps of the SLP anomalies. It should be noted that the anomalies are calculated relative to the mean of that segment, without any detrending. The next EOF is calculated with the same window length [t-n,t+n] but t is now shifted by the time increment dt. This creates a series of EOFs, one for each time step. For every time step the first four EOFs are calculated to ensure that the NAO

pattern is captured. To identify the NAO pattern, they are compared to the reference NAO pattern by applying a spatial correlation.

Based on this series of NAO patterns the movement of the NAO centers of action (IL and AH) is tracked by applying a k-means cluster algorithm which is related to the algorithm proposed by Lloyd (1982). The cluster algorithm (CA) finds k cluster centroids that minimize the distance between data points and the nearest centroid. The CA is a robust way to identify the minimum and maximum of the NAO pattern. The center of each cluster is obtained by calculating the mean position of the cluster.

The idea of an EOF analysis with overlapping time windows has also been applied by Lehmann et al. (2011) to track the spatial shift of the NAO centers of action. They performed an EOF analysis for the time period 1958 to 1997 with time windows of 20 years with each period overlapping by 10 years. However, in the present study the overlapping EOF is constructed separately for each time step.

2.4. Wavelet transformation

A continuous wavelet transform (CWT) is used to analyze the power spectrum of the AMO signal. Similar to a common power spectrum, CWT expands a time series into frequency space, but without losing the time information. This allows analyzing time-localized oscillations in the signal (Torrence & Compo 1998). To find a relationship between the AMO and the NAO, wavelet coherence (WTC) is used. WTC compares two CWTs and finds locally phase-locked behavior of two signals. By using Monte Carlo simulations, the statistical significance level of the WTC is tested. A large ensemble of n=300 surrogate dataset pairs with the same AR1 coefficients as the input datasets is created. For each scale of the CWT the significance level is estimated by calculating the wavelet coherence with each pair of datasets. (Grinsted et al. 2004).

2.5. Storm tracks

To evaluate the impact of the AMO on the storm tracks a calculus-based cyclone identification (CCI) method is used. CCI uses multiple least squares regression to a truncated series of sinusoids to estimate the coefficients of the Fourier approximation. Solving the first and second derivative along the north-south and east-west profiles of the SLP searching for zero crossings and positive values respectively, results in the local minima. A detailed description is given by Benestad & Chen (2006).

3. Results

To analyze the relationship between the AMO and the NAO in ECHO-G we use CWT and WTC (see Figure 1). The AMO and the NAO alternate between positive and negative states. During the Medieval Climate Anomaly (MCA) from 950 to 1300, the AMO and the NAO are predominantly positive. During the transition to the Little Ice Age (LIA; 1400 to 1700), AMO- and NAO- states appear more frequently and the

number of positive and negative states is more balanced (Figure 1 (a)). The CWT reveals that the AMO has two persistent low-frequency components (Figure 1 (b)). From 1150 to 1400 the AMO has significant power in the frequency band from 90 to 180 years. During the LIA the power distribution changes and significant power is found in the frequency band from 60 to 90 years. As the power of the AMO signal is not stationary in time and changes between the MCA and the LIA, we use WTC to reveal a non-stationary, low-frequency coherence between the AMO and the NAO (Figure 1 (c)). The WTC shows that the AMO and the NAO have a significant coherence in the time span from 1150 to 1450 in the frequency range from 90 to 180 years. During the LIA from approximately 1450 to 1700, a significant coherence is found in the frequency range from 60 to 90 years. For the phase relationship we find that the AMO is leading the NAO by roughly 12 years during the MCA. As the dominant frequency shifts from 90 to 180 years to 60 to 90 years during the LIA, the phase relationship changes with the NAO leading the AMO by 6 years on average.

To capture the spatial variability of the NAO, we perform an EOF analysis with overlapping time windows of 30 years (see Figure 2). As the wavelet analysis revealed that the dominant frequency of the AMO changes between the MCA and the LIA, we analyze both climate states separately, to see if the frequency of the AMO impacts the spatial shift of the NAO.

Figure 2 (a) shows the spatial variability of the IL and AH during the MCA. We find that the mean position of the IL is shifted westwards (eastwards) during AMO+ (AMO-) phases. In contrast, the mean position of the AH is shifted eastwards (westwards) during AMO+ (AMO-) phases. The wind fields are extracted from RCA3 and therefore do not cover the whole domain. However, matching the observed shift of the IL and AH, we find increased westerlies at the location of the Azores High and increased easterlies at the location of the IL. The distance between the mean position during AMO+ and AMO- phases is greater for the AH than for the IL.

Figure 2 (b) shows the spatial variability of the IL and AH during the LIA. Again, we find that the mean position of the IL is shifted westwards (eastwards) during AMO+ (AMO-) phases. The AH is shifted in the opposite direction as during AMO+ (AMO-) phases the AH is located further east (west). The wind difference between AMO+ and AMO- phases shows stronger westerlies at the location of the AH and stronger easterlies at the location of the IL. The distance between the mean position during AMO+ and AMO- phases is slightly greater for the AH than for the IL.

Comparing the MCA and the LIA we find that both time periods show similar results. The IL is located further west during AMO+ phases and further east during AMO- phases. The opposite relationship is found for the AH. While the impact on the AH remains similar during the MCA and the LIA, the distance between the mean position of the IL during AMO+ and AMO- increases during the LIA. Since both centers are moving away from each other, we observe a tilting of the axis between the IL and the AH. It should be noted that the results are independent of the selected time window for the EOF analysis (see Figure 5).

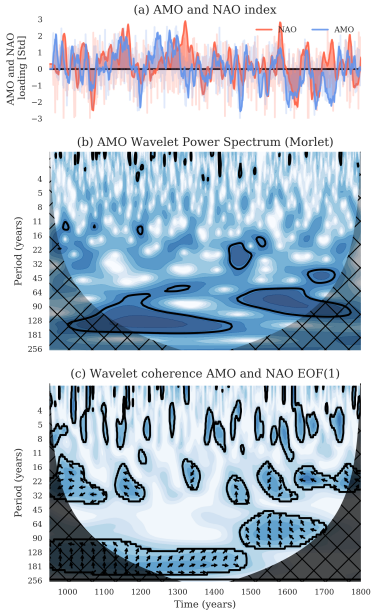

Figure 1. Calculated AMO and NAO index (a), wavelet power spectrum of the AMO (b) and the wavelet coherence of the AMO and the NAO (c). The black contour lines show statistical significance according to Grinsted et al. (2004). The cone of influence where edge effects might influence the results is hatched (Grinsted et al. 2004) The arrows in the significant regions indicate the phase relationship between the signals: pointing right (left) in phase (antiphase), and AMO leading (lagging) straight up (down). AMO = Atlantic Multidecadal Oscillation; NAO = North Atlantic Oscillation.

During AMO+ phases the IL and the AH are located further west and east respectively (Figure 2). The position of the of both NAO centers of action is likely related to the position of the storm tracks (Luo et al. 2010). Therefore, we analyze the impact of the shift on the storm track density,.

Figure 3 (a) shows the mean storm track activity over Northern Europe for the period 950 to 1800. The center of the mean storm track density is located at approximately 22°W and ranges from 54°N to 66°N. Further, we find that the storm track density stretches east across northern Scandinavia. Figure 3 (b) shows the storm

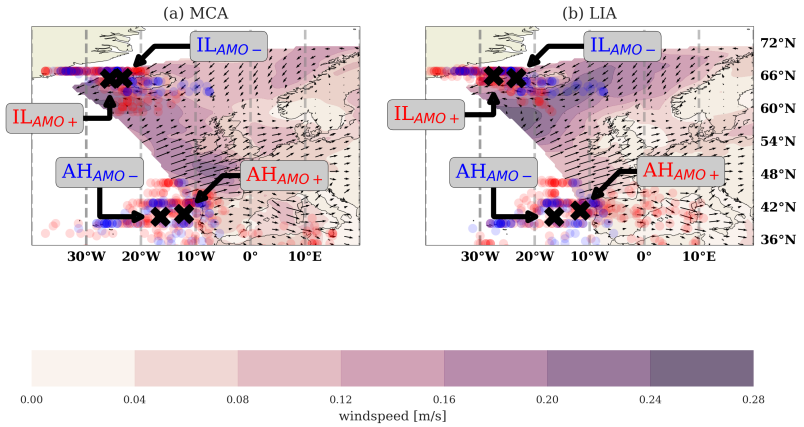

Figure 2. Spatial shift of the Icelandic Low and the Azores High sorted by AMO+ and AMO- phases during MCA (a) and LIA (b). Each marker corresponds to the center position obtained by the EOF analysis with overlapping time windows. Red (blue) markers indicate AMO+ (AMO-) phases. The black markers show the mean position of both NAO centers of action (AH and IL) during AMO+ and AMO- phases. The arrows show the mean wind field and are scaled to [m/s]. The contour shows the wind speed difference between AMO+ and AMO- phases. MCA = Medieval Climate Anomaly; LIA = Little Ice Age.; IL = Icelandic Low; AH = Azores High

track density difference associated with zonal shifts of the IL for the period 950 to 1800. The shifts of the IL are defined as the deviation from its mean position. We find that the storm track density decreases in the northern part of the model domain, starting west of Iceland and stretching east across northern Scandinavia. Further, we find a slight decrease at 20°W and 54°N west of Great Britain. A slight increase is found east of Great Britain at 0°E and 60°N. However, only the decrease near Iceland stretching east is statistically significant.

Next, the regional importance of the NAO for Northern Europe is analyzed using the example of the Baltic Sea (Figure 3 at 9°E to 30°E; 54°N to 66°N). Figure 4 (a) shows the 30-year running correlation between the NAO and regional climate variables - mean SST, sea ice extent and runoff of the Baltic Sea, respectively - and the longitudinal position of the Icelandic Low.

The SST shows a positive correlation with the NAO of up to 0.8 from 960 to 1090 but decreases to 0.0 at around 1750. The correlation between the NAO and the sea ice extent is negative and varies between -0.2 to -0.8. Lastly, the correlation between the NAO and runoff amounts to 0.5 from 1000 to 1100 but then changes sign with about -0.2 during 1120. All variables exhibit strong multidecadal variability.

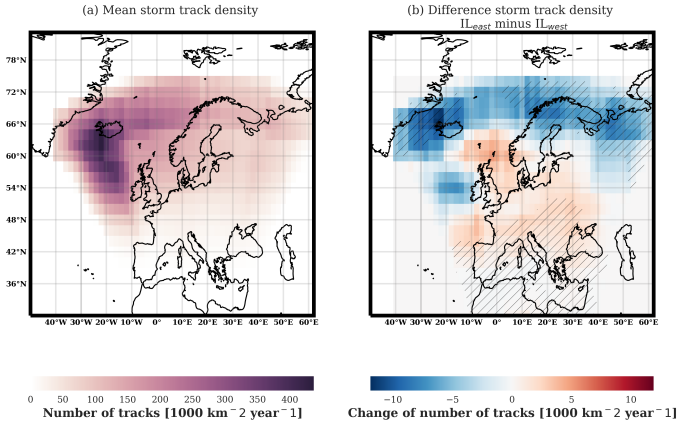

Figure 3. Mean storm track density for the period 950 to 1800 (a). Storm track density difference between IL_{east} - IL_{west} (b). Statistical significance is hatched and calculated with a two-tailed Student's t test ($\alpha = 0.05$), where the calculated differences are compared to yearly storm track fluctuations. IL = Icelandic Low

The longitudinal position of the IL varies between 12°W and 20°E. Similar to the three regional variables it also exhibits multidecadal fluctuations. To analyze the importance of the IL for the regional climate of the Baltic Sea, the correlation between the position of the IL and all three running correlations is computed. Considering the time lag due to the inertia of the ocean, we find a correlation of 0.5 for the SST, a correlation of 0.42 for the sea ice extent, and a correlation of 0.35 for the runoff.

The same analysis is repeated for the AH (see Figure 4 (b)). Just like the IL, the AH exhibits multidecadal variability. Its position varies between 20°W and 22°E. Again, we compute the correlation between the running correlations of the regional climate variables with the NAO and the longitudinal position of the Azores High. For SST, sea ice extent and runoff we find correlations of up to -0.1, 0.05, and -0.14 respectively. Comparing the position of the IL and the AH, the position of the IL plays an important role for the climate of the Baltic Sea, while the position of the AH does not have a significant impact on the climate of the Baltic Sea.

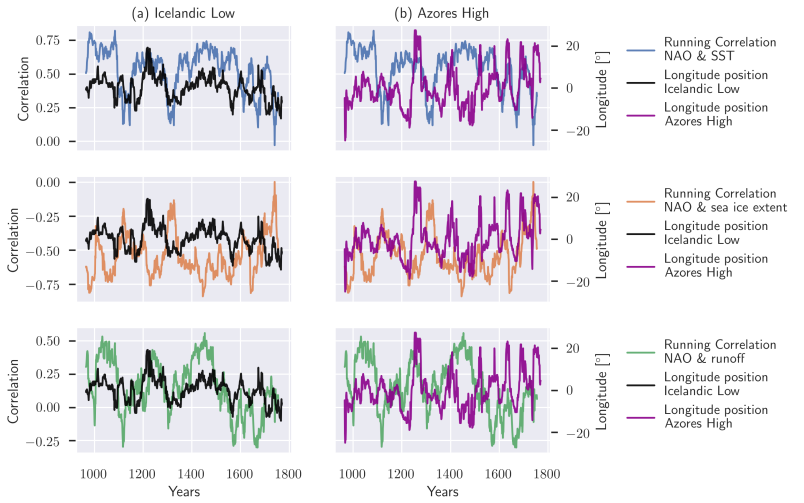

Figure 4. Comparison of the longitudinal position of the IL (a) and the AH (b) with the 30-year running correlation between the NAO and regional climate variables of the Baltic Sea, namely, sea ice extent, runoff and SST. NAO = North Atlantic Oscillation; SST = sea surface temperature; IL = Icelandic Low; AH = Azores High

4. Discussion

The climate mode AMO influences the spatial pattern of the NAO. This connection is revealed by the EOF analysis with overlapping time windows (Figure 2). We find that the state of the AMO influences the zonal position of the IL and the AH. AMO+ states cause a westward shift of the IL which in turn reduces the regional importance of the NAO for the North European climate.

To analyze the characteristics of the AMO in ECHO-G and its relationship with the NAO we use CWT and WTC (Figure 1). The frequency of the AMO varies from 90 to 180 years during the MCA and from 60 to 90 years during the LIA. The simulated AMO tends to stay in a positive phase during the MCA, which is in agreement with studies by Mann et al. (2009), Landrum et al. (2013). Frequency shifts of the AMO appear throughout the entire 7000 years of the ECHO-G Holocene simulation. There are several studies discussing possible reasons for these shifts of the AMO on centennial time scales: By analyzing seven Holocene climate proxies Knudsen et al. (2011) revealed changes in the dominant frequency and regional importance of the AMO over a period of 8000 years. Further, Frankcombe et al. (2010) proposed that the AMO can be viewed as a damped oscillatory internal ocean mode that is excited by atmospheric noise, modulating its dominant frequency. In addition, changes of the dominant frequency of the AMO were

also found in a Greenland ice core record (Chylek et al. 2012). The simulated NAO in ECHO-G tends to stay in a positive state during the MCA as well, which is also found by Trouet et al. (2009). They argued that the climate transition between MCA and LIA was coupled to prevailing La Niña– like conditions which were amplified by an intensified AMOC during the MCA. These studies are in good agreement with the dynamical interpretation of the AMOC and the NAO interplay proposed by Wills et al. (2019) or Delworth & Zeng (2016) as they described the frequency of the AMO as a result of the interaction between atmosphere, i.e. NAO, and the ocean.

The WTC between the AMO and the NAO reveals a significant coherence in a frequency range that can be attributed to the AMO. We find that the phase relationship between the AMO and the NAO changes between the MCA and the LIA. However, with a frequency of 50 to 90 years during the LIA the AMO lags the NAO as discussed by Delworth & Zeng (e.g. 2016), Sun et al. (e.g. 2015), Wills et al. (e.g. 2019). We argue that the changing phase relationship is also caused by the previously described climate transition between the MCA and the LIA.

The impact of the AMO on the spatial position of the NAO is analyzed in Figure 2 and distinguishes between MCA (a) and LIA (b). However, independent of both climate states we find similar results for both periods as the AMO causes a westward shift of the IL and an eastward shift of the AH during AMO+ phases. Previous studies argued that the change of the mean flow causes a zonal shift of the IL and AH (Jung et al. 2003, Luo & Gong 2006, Luo et al. 2010). Hence, the observed shift of both pressure centers is likely related to the difference in the wind fields between AMO+ and AMO-. Further, Luo et al. (2010) found that the position the Atlantic storm track likely influences the position of both NAO centers of action. However, we find that the position of the IL and the AH as influenced by the AMO is not affecting the position of the mean storm track density. Instead of an increasing storm track densities during an eastward shift of the IL, we find a lower numbers of storms (Figure 3 (b)). By analyzing the SLP fields we find that the state of the AMO is influencing the number of storm tracks instead of the position of both centers. A westward or eastward shift of the IL corresponds to AMO+ and AMO- states respectively (Figure 2). The SLP difference between westward and eastward shifts of the IL shows negative values at the location of the IL and positive values at the position of the AH, resembling an NAO+ pattern (Figure 6). This results in a higher SLP gradient and a higher number of storms (not shown). Further, the difference between eastward shifts of the AH and westwards shifts of the AH, corresponding to AMO+ and AMO- states, results in the same SLP pattern as for the IL. We find a higher SLP gradient, increasing the number of storms.

Nevertheless, the shift of the IL and the AH is of particular importance when studying the impact of the NAO on, e.g., local precipitation patterns. Studies discussing global climate such as Landrum et al. (2013) neglected that the correlations of the NAO and regional climate variables change over time. However, a few regional climate studies considered that the influence of the NAO on regional climate variables in Europe changes over time (Vihma & Haapala 2009, Omstedt & Chen 2001, Hünicke & Zorita

2006, Chen & Hellström 1999, Meier & Kauker 2002, Beranová & Huth 2008). The Baltic Sea has been shown to respond very sensitively to external forcing (Belkin 2009). It is exposed to a variety of anthropogenic pressures such as agricultural, industrial, and urban activities. In this study we are investigating the impact of natural variability on the environmental state of the Baltic Sea because this impact may be even more important than anthropogenic climate change in the near future, as 58% of the decadal variability in the Baltic Sea mean SST can be explained by the AMO (Kniebusch et al. 2019).

Using the Baltic Sea as an example for the impact of the NAO on regional climate (Figure 4), we find that the correlation between regional climate variables and the NAO varies on multidecadal time scales. The correlation between the NAO and SST varies immensely with correlations ranging from 0.0 to 0.8. Beranová & Huth (2008) found a higher correlation between the NAO and the European climate when the NAO centers of action are located farther east. While our findings support their claims, we find that only the position of the IL is relevant for the regional correlation with the NAO in Northern Europe.

Previous studies have focused on the stationary relationship between the AMO and the NAO. The present study is the first showing an influence of the multidecadal variability of the AMO on the spatial structure of the NAO over longer periods of time. As presented in this study, the AMO influences the east-west position of the IL and the AH, with a NW-SE shift during AMO+ phases. We find that it is important to consider the respective state of the AMO since it indicates whether the correlation between the NAO and regional climate will increase or decrease.

Appendix

The first row of Figure 6 shows the sea level pressure anomaly for an eastward shift of the IL and a westward shift of the AH. The observed shift corresponds to an AMO+ state. The second row shows the sea level pressure anomaly for the IL located west and the AH located east, which corresponds to an AMO- state. The last row shows the sea level pressure difference between a westward (eastward) shift and eastward (westward) shift of the IL (AH). It is found that during AMO+ phases the sea level pressure gradient between the IL and the AH is higher compared to AMO- phases.

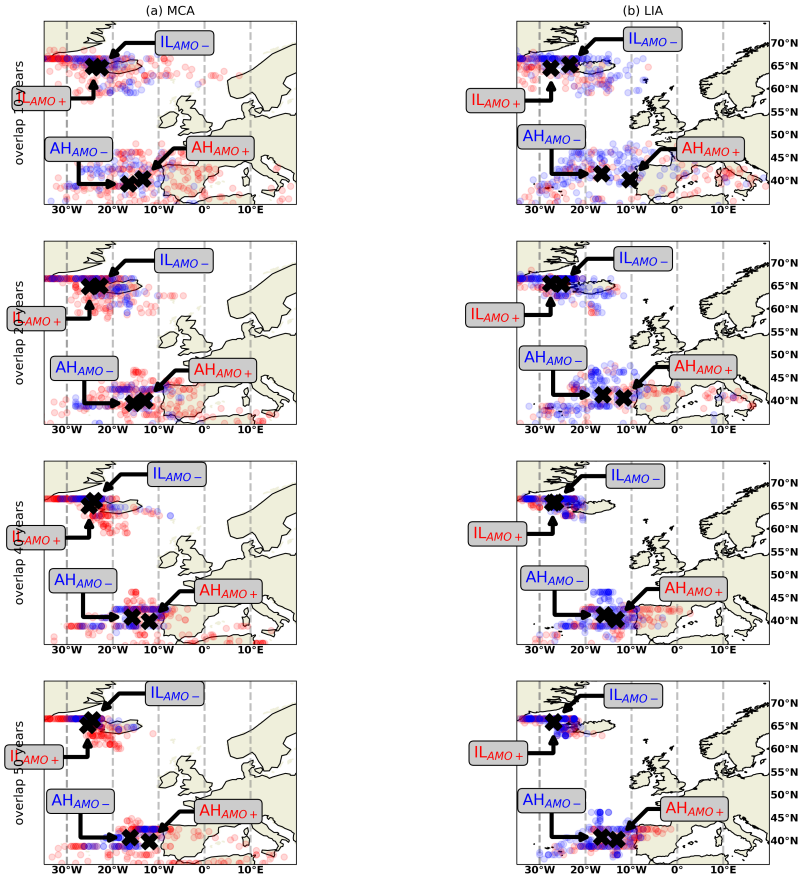

Figure 5. Center position of the Icelandic Low and Azores High for different EOF overlap time windows. Each marker represents one period, with blue (red) markers indicating AMO- (AMO+) phases. On the left (right) side the relationship during the Medieval Climate Anomaly (Little Ice Age) is shown. The rows represent EOF overlapping time windows of 20, 30, 40, and 50 years. The black marker shows the mean position of NAO centers of action during AMO+ and AMO- phases.

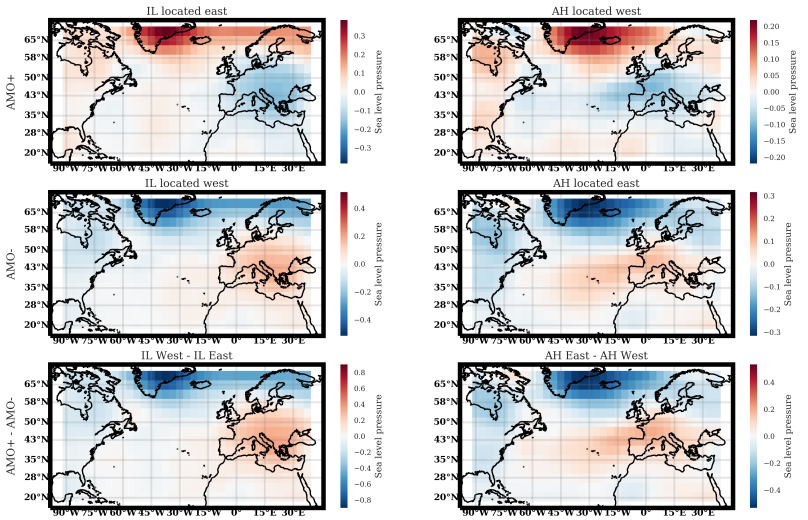

Figure 6. Sea level pressure anomaly associated with the zonal position of the IL and the AH. IL = Icelandic Low; AH = Azores High

References

References

Belkin, I. M. (2009), 'Rapid warming of Large Marine Ecosystems', *Progress in Oceanography* **81**(1), 207 – 213.
URL: *http://www.sciencedirect.com/science/article/pii/S0079661109000317*

Benestad, R. E. & Chen, D. (2006), 'The use of a calculus-based cyclone identification method for generating storm statistics', *Tellus A* **58**(4), 473–486.
URL: *https://onlinelibrary.wiley.com/doi/abs/10.1111/j.1600-0870.2006.00191.x*

Beranová, R. & Huth, R. (2008), 'Time variations of the effects of circulation variability modes on European temperature and precipitation in winter', *International Journal of Climatology* **28**(2), 139–158.
URL: *https://rmets.onlinelibrary.wiley.com/doi/abs/10.1002/joc.1516*

Börgel, F., Frauen, C., Neumann, T., Schimanke, S. & Meier, H. E. M. (2018), 'Impact of the Atlantic Multidecadal Oscillation on Baltic Sea Variability', *Geophysical Research Letters* **45**(18), 9880–9888.
URL: *https://agupubs.onlinelibrary.wiley.com/doi/abs/10.1029/2018GL078943*

Casanueva, A., Rodríguez-Puebla, C., Frías, M. D. & González-Reviriego, N. (2014), 'Variability of extreme precipitation over Europe and its relationships with

teleconnection patterns', *Hydrology and Earth System Sciences* **18**(2), 709–725.
URL: *https://www.hydrol-earth-syst-sci.net/18/709/2014/*

Chen, D. & Hellström, C. (1999), 'The influence of the North Atlantic Oscillation on the regional temperature variability in Sweden: spatial and temporal variations', *Tellus A: Dynamic Meteorology and Oceanography* **51**(4), 505–516.
URL: *https://doi.org/10.3402/tellusa.v51i4.14086*

Chylek, P., Folland, C., Frankcombe, L., Dijkstra, H., Lesins, G. & Dubey, M. (2012), 'Greenland ice core evidence for spatial and temporal variability of the Atlantic Multidecadal Oscillation', *Geophysical Research Letters* **39**(9).

Clement, A., Bellomo, K., Murphy, L. N., Cane, M. A., Mauritsen, T., Rädel, G. & Stevens, B. (2015), 'The atlantic multidecadal oscillation without a role for ocean circulation', *Science* **350**(6258), 320–324.
URL: *https://science.sciencemag.org/content/350/6258/320*

Delworth, T. L. & Zeng, F. (2016), 'The Impact of the North Atlantic Oscillation on Climate through Its Influence on the Atlantic Meridional Overturning Circulation', *Journal of Climate* **29**(3), 941–962.
URL: *https://doi.org/10.1175/JCLI-D-15-0396.1*

Delworth, T. L., Zeng, F., Zhang, L., Zhang, R., Vecchi, G. A. & Yang, X. (2017), 'The Central Role of Ocean Dynamics in Connecting the North Atlantic Oscillation to the Extratropical Component of the Atlantic Multidecadal Oscillation', *Journal of Climate* **30**(10), 3789–3805.
URL: *https://doi.org/10.1175/JCLI-D-16-0358.1*

Enfield, D. B., Mestas-Nuñez, A. M. & Trimble, P. J. (2001), 'The Atlantic Multidecadal Oscillation and its relation to rainfall and river flows in the continental U.S.', *Geophysical Research Letters* **28**(10), 2077–2080.
URL: *http://dx.doi.org/10.1029/2000GL012745*

Frankcombe, L. M., von der Heydt, A. & Dijkstra, H. A. (2010), 'North Atlantic Multidecadal Climate Variability: An Investigation of Dominant Time Scales and Processes', *Journal of Climate* **23**(13), 3626–3638.
URL: *https://doi.org/10.1175/2010JCLI3471.1*

Grinsted, A., Moore, J. C. & Jevrejeva, S. (2004), 'Application of the cross wavelet transform and wavelet coherence to geophysical time series', *Nonlinear Processes in Geophysics* **11**(5/6), 561–566.
URL: *https://www.nonlin-processes-geophys.net/11/561/2004/*

Hilmer, M. & Jung, T. (2000), 'Evidence for a recent change in the link between the North Atlantic Oscillation and Arctic Sea ice export', *Geophysical Research Letters* **27**(7), 989–992.
URL: *https://agupubs.onlinelibrary.wiley.com/doi/abs/10.1029/1999GL010944*

Hünicke, B. & Zorita, E. (2006), 'Influence of temperature and precipitation on decadal Baltic Sea level variations in the 20th century', *Tellus A* **58**(1), 141–153.
URL: *https://onlinelibrary.wiley.com/doi/abs/10.1111/j.1600-0870.2006.00157.x*

Hünicke, B., Zorita, E. & Haeseler, S. (2010), 'Baltic holocene climate and regional sea-level change: A statistical analysis of observations, reconstructions and simulations within present and past as analogues for future changes', *GKSS Reports* .

Hurrell, J. W. (1995), 'Decadal Trends in the North Atlantic Oscillation: Regional Temperatures and Precipitation', *Science* **269**(5224), 676–679.
URL: *http://science.sciencemag.org/content/269/5224/676*

Hurrell, J. W., Kushnir, Y., Ottersen, G. & Visbeck, M. (2003), 'The North Atlantic Oscillation: Climatic Significance and Environmental Impact', *GEOPHYSICAL MONOGRAPH SERIES* **134**, 279 pp.

Johnson, N. C., Feldstein, S. B. & Tremblay, B. (2008), 'The Continuum of Northern Hemisphere Teleconnection Patterns and a Description of the NAO Shift with the Use of Self-Organizing Maps', *Journal of Climate* **21**(23), 6354–6371.
URL: *https://doi.org/10.1175/2008JCLI2380.1*

Jung, T. & Hilmer, M. (2001), 'The Link between the North Atlantic Oscillation and Arctic Sea Ice Export through Fram Strait', *Journal of Climate* **14**(19), 3932–3943.
URL: *https://doi.org/10.1175/1520-0442(2001)014<3932:TLBTNA>2.0.CO;2*

Jung, T., Hilmer, M., Ruprecht, E., Kleppek, S., Gulev, S. K. & Zolina, O. (2003), 'Characteristics of the Recent Eastward Shift of Interannual NAO Variability', *Journal of Climate* **16**(20), 3371–3382.
URL: *https://doi.org/10.1175/1520-0442(2003)016<3371:COTRES>2.0.CO;2*

Kauker, F. & Meier, H. E. M. (2003), 'Modeling decadal variability of the Baltic Sea: 1. Reconstructing atmospheric surface data for the period 1902–1998', *Journal of Geophysical Research: Oceans (1978–2012)* **108**(C8).
URL: *https://doi.org/10.1029/2003JC001797*

Kniebusch, M., Meier, H. M., Neumann, T. & Börgel, F. (2019), 'Temperature variability of the baltic sea since 1850 and attribution to atmospheric forcing variables', *Journal of Geophysical Research: Oceans* **124**(6), 4168–4187.
URL: *https://agupubs.onlinelibrary.wiley.com/doi/abs/10.1029/2018JC013948*

Knight, J. R., Folland, C. K. & Scaife, A. A. (2006), 'Climate impacts of the Atlantic Multidecadal Oscillation', *Geophysical Research Letters* **33**(17).
URL: *http://dx.doi.org/10.1029/2006GL026242*

Knudsen, M., Seidenkrantz, M.-S., Jacobsen, B. & Kuijpers, A. (2011), 'Tracking the atlantic multidecadal oscillation through the last 8,000 years', *Nature communications* **2**, 178.

Landrum, L., Otto-Bliesner, B. L., Wahl, E. R., Conley, A., Lawrence, P. J., Rosenbloom, N. & Teng, H. (2013), 'Last Millennium Climate and its variability in CCSM4', *Journal of Climate* **26**(4), 1085–1111.
URL: *https://doi.org/10.1175/JCLI-D-11-00326.1*

Lehmann, A., Getzlaff, K. & Harlaß, J. (2011), 'Detailed assessment of climate

variability in the Baltic Sea area for the period 1958 to 2009', *Climate Research* **46**, 185–196.

Li, J., Sun, C. & Jin, F.-F. (2013), 'NAO implicated as a predictor of Northern Hemisphere mean temperature multidecadal variability', *Geophysical Research Letters* **40**(20), 5497–5502.
URL: *https://agupubs.onlinelibrary.wiley.com/doi/abs/10.1002/2013GL057877*

Lloyd, S. (1982), 'Least squares quantization in PCM', *IEEE Transactions on Information Theory* **28**(2), 129–137.

Luo, D. & Gong, T. (2006), 'A possible mechanism for the eastward shift of interannual NAO action centers in last three decades', *Geophysical Research Letters* **33**(24).
URL: *https://agupubs.onlinelibrary.wiley.com/doi/abs/10.1029/2006GL027860*

Luo, D., Zhu, Z., Ren, R., Zhong, L. & Wang, C. (2010), 'Spatial Pattern and Zonal Shift of the North Atlantic Oscillation. Part I: A Dynamical Interpretation', *Journal of the Atmospheric Sciences* **67**(9), 2805–2826.
URL: *https://doi.org/10.1175/2010JAS3345.1*

Mann, M. E., Zhang, Z., Rutherford, S., Bradley, R. S., Hughes, M. K., Shindell, D., Ammann, C., Faluvegi, G. & Ni, F. (2009), 'Global Signatures and Dynamical Origins of the Little Ice Age and Medieval Climate Anomaly', *Science* **326**(5957), 1256–1260.
URL: *http://science.sciencemag.org/content/326/5957/1256*

Medhaug, I. & Furevik, T. (2011), 'North Atlantic 20th century multidecadal variability in coupled climate models: sea surface temperature and ocean overturning circulation', *Ocean Science* **7**(3), 389–404.
URL: *https://www.ocean-sci.net/7/389/2011/*

Meier, H. E. M., Döscher, R. & Faxén, T. (2003), 'A multiprocessor coupled ice-ocean model for the baltic sea: Application to salt inflow', *Journal of Geophysical Research: Oceans* **108**(C8).
URL: *https://agupubs.onlinelibrary.wiley.com/doi/abs/10.1029/2000JC000521*

Meier, H. & Kauker, F. (2002), 'Simulating Baltic Sea climate for the period 1902-1998 with the Rossby Centre coupled ice-ocean model', *Reports Oceanography* **30**, 111 pp.

Min, S.-K., Legutke, S., Hense, A. & Kwon, W.-T. (2005), 'Internal variability in a 1000-yr control simulation with the coupled climate model echo-g — i. near-surface temperature, precipitation and mean sea level pressure', *Tellus A: Dynamic Meteorology and Oceanography* **57**(4), 605–621.
URL: *https://doi.org/10.3402/tellusa.v57i4.14712*

Omstedt, A. & Chen, D. (2001), 'Influence of atmospheric circulation on the maximum ice extent in the Baltic Sea', *Journal of Geophysical Research: Oceans* **106**(C3), 4493–4500.
URL: *https://agupubs.onlinelibrary.wiley.com/doi/abs/10.1029/1999JC000173*

Peings, Y. & Magnusdottir, G. (2014), 'Forcing of the wintertime atmospheric circulation by the multidecadal fluctuations of the North Atlantic ocean',

Environmental Research Letters **9**(3), 034018.
URL: *http://stacks.iop.org/1748-9326/9/i=3/a=034018*

Peterson, K. A., Greatbatch, R. J., Lu, J., Lin, H. & Derome, J. (2002), 'Hindcasting the NAO using diabatic forcing of a simple AGCM', *Geophysical Research Letters* **29**(9), 50–1–50–4.
URL: *https://agupubs.onlinelibrary.wiley.com/doi/abs/10.1029/2001GL014502*

Peterson, K. A., Lu, J. & Greatbatch, R. J. (2003), 'Evidence of nonlinear dynamics in the eastward shift of the NAO', *Geophysical Research Letters* **30**(2).
URL: *https://agupubs.onlinelibrary.wiley.com/doi/abs/10.1029/2002GL015585*

Ruprich-Robert, Y., Msadek, R., Castruccio, F., Yeager, S., Delworth, T. & Danabasoglu, G. (2017), 'Assessing the Climate Impacts of the Observed Atlantic Multidecadal Variability Using the GFDL CM2.1 and NCAR CESM1 Global Coupled Models', *Journal of Climate* **30**(8), 2785–2810.
URL: *https://doi.org/10.1175/JCLI-D-16-0127.1*

Samuelsson, P., Jones, C. G., WillEn, U., Ullerstig, A., Gollvik, S., Hansson, U., Jansson, E., Kjellstro¨M, C., Nikulin, G. & Wyser, K. (2011), 'The rossby centre regional climate model rca3: model description and performance', *Tellus A: Dynamic Meteorology and Oceanography* **63**(1), 4–23.
URL: *https://doi.org/10.1111/j.1600-0870.2010.00478.x*

Schimanke, S. & Meier, H. E. M. (2016), 'Decadal-to-Centennial Variability of Salinity in the Baltic Sea', *Journal of Climate* **29**(20), 7173–7188.
URL: *https://doi.org/10.1175/JCLI-D-15-0443.1*

Sun, C., Li, J. & Jin, F.-F. (2015), 'A delayed oscillator model for the quasi-periodic multidecadal variability of the NAO', *Climate Dynamics* **45**(7), 2083–2099.
URL: *https://doi.org/10.1007/s00382-014-2459-z*

Sutton, R. T. & Hodson, D. L. R. (2005), 'Atlantic ocean forcing of north american and european summer climate', *Science* **309**(5731), 115–118.
URL: *https://science.sciencemag.org/content/309/5731/115*

Ting, M., Kushnir, Y., Seager, R. & Li, C. (2011), 'Robust features of atlantic multi-decadal variability and its climate impacts', *Geophysical Research Letters* **38**(17).

Torrence, C. & Compo, G. P. (1998), 'A Practical Guide to Wavelet Analysis', *Bulletin of the American Meteorological Society* **79**(1), 61–78.
URL: *https://doi.org/10.1175/1520-0477(1998)079<0061:APGTWA>2.0.CO;2*

Trenberth, K. E. & Shea, D. J. (2006), 'Atlantic hurricanes and natural variability in 2005', *Geophysical Research Letters* **33**(12). L12704.
URL: *http://dx.doi.org/10.1029/2006GL026894*

Trouet, V., Esper, J., Graham, N. E., Baker, A., Scourse, J. D. & Frank, D. C. (2009), 'Persistent positive north atlantic oscillation mode dominated the medieval climate

anomaly', *Science* **324**(5923), 78–80.
URL: *https://science.sciencemag.org/content/324/5923/78*

Ulbrich, U. & Christoph, M. (1999), 'A shift of the NAO and increasing storm track activity over Europe due to anthropogenic greenhouse gas forcing', *Climate Dynamics* **15**(7), 551–559.
URL: *https://doi.org/10.1007/s003820050299*

Vihma, T. & Haapala, J. (2009), 'Geophysics of sea ice in the baltic sea: A review', *Progress in Oceanography* **80**(3), 129 – 148.
URL: *http://www.sciencedirect.com/science/article/pii/S0079661109000123*

Visbeck, M. H., Hurrell, J. W., Polvani, L. & Cullen, H. M. (2001), 'The North Atlantic Oscillation: Past, present, and future', *Proceedings of the National Academy of Sciences* **98**(23), 12876–12877.
URL: *https://www.pnas.org/content/98/23/12876*

Wills, R. C. J., Armour, K. C., Battisti, D. S. & Hartmann, D. L. (2019), 'Ocean–Atmosphere Dynamical Coupling Fundamental to the Atlantic Multidecadal Oscillation', *Journal of Climate* **32**(1), 251–272.
URL: *https://doi.org/10.1175/JCLI-D-18-0269.1*

Zanchettin, D., Bothe, O., Graf, H. F., Lorenz, S. J., Luterbacher, J., Timmreck, C. & Jungclaus, J. H. (2013), 'Background conditions influence the decadal climate response to strong volcanic eruptions', *Journal of Geophysical Research: Atmospheres* **118**(10), 4090–4106.
URL: *https://agupubs.onlinelibrary.wiley.com/doi/abs/10.1002/jgrd.50229*

Zhang, L. & Wang, C. (2013), 'Multidecadal North Atlantic sea surface temperature and Atlantic meridional overturning circulation variability in CMIP5 historical simulations', **118**, 5772–5791.

JGR Oceans

RESEARCH ARTICLE
10.1029/2018JC013948

Temperature Variability of the Baltic Sea Since 1850 and Attribution to Atmospheric Forcing Variables

Madline Kniebusch[1], **H.E. Markus Meier**[1,2], **Thomas Neumann**[1], **and Florian Börgel**[1]

[1]Leibniz Institute for Baltic Sea Research Warnemünde, Rostock, Germany, [2]Swedish Meteorological and Hydrological Institute, Norrköping, Sweden

Abstract The Baltic Sea is highly impacted by global warming and other anthropogenic changes and is one of the fastest-warming marginal seas in the world. To detect trends in water temperature and to attribute them to atmospheric parameters, the results of two different ocean circulation models driven by reconstructed atmospheric forcing fields for the period 1850–2008 were analyzed. The model simulations were analyzed at temporal and spatial scales from seasonal to centennial and from intrabasin to basin, respectively. The strongest 150-year trends were found in the annual mean bottom temperature of the Bornholm Deep (0.15 K/decade) and in summer mean sea surface temperature (SST) in Bothnian Bay (0.09–0.12 K/decade). A comparison of the time periods 1856–2005 and 1978–2007 revealed that the SST trends strengthened tenfold. An attribution analysis showed that most of the SST variability could be explained by the surface air temperature (i.e., sensible heat flux) and the latent heat flux. Wind parallel to the coast and cloudiness additionally explained SST variability in the coastal zone affected by the variations in upwelling and in offshore areas affected by the variations in solar radiation, respectively. In contrast, the high variability in stratification caused by freshwater and saltwater inflows does not impact the long-term variability in the SST averaged over the Baltic Sea. The strongest SST trends since the 1980s can be explained by the superposition of global warming and a shift from the cold to the warm phase of the Atlantic Multidecadal Oscillation.

Key Points:
- The Baltic Sea SST trend is mainly driven by SAT, which has been reinforced by the positive phase of the AMO since 1980
- Wind parallel to the coast and cloudiness are important for the SST in upwelling and offshore areas, respectively
- Changing stratification due to inflows from the North Sea do not affect long-term variability in the SST

Supporting Information:
- Supporting Information S1

Correspondence to:
M. Kniebusch,
madline.kniebusch@io-warnemuende.de

Citation:
Kniebusch, M., Meier, H. E. M., Neumann, T., & Börgel, F. (2019). Temperature variability of the Baltic Sea since 1850 and attribution to atmospheric forcing variables. *Journal of Geophysical Research: Oceans*, *124*, 4168–4187. https://doi.org/10.1029/2018JC013948

Received 28 FEB 2018
Accepted 23 APR 2019
Accepted article online 10 MAY 2019
Published online 24 JUN 2019

1. Introduction

With a volume of 21,700 km^3, including the Kattegat (BACC Author Team, 2008), and a salinity range from 3 to 12 g/kg (Fonselius & Valderrama, 2003), the Baltic Sea is one of the largest brackish seas in the world. Its physical characteristics such as salinity and temperature and also oxygen concentration are dominated by changes in the atmosphere, particularly temperature, sea level pressure, precipitation and river runoff, the cloudiness/radiation budget, wind, and nutrient inputs from rivers and the atmosphere. The Baltic Sea is connected to the open sea only by the narrow Danish straits. Moreover, its strong stratification prohibits vertical mixing due to a permanent halocline (Matthäus & Franck, 1992).

As climate change results in an increase in temperature as well as changes in circulation patterns, the Baltic Sea is also affected by increasing air and water temperatures (BACC II Author Team, 2015). Belkin (2009) analyzed reconstructed sea surface temperature (SST) trends of all large marine ecosystems between 1982 and 2006, collocating them by their trends. The Baltic Sea showed the largest temperature change of 1.35 K since 1982, followed by the North Sea, with a change of 1.31 K. Both changes were more than 7 times larger than the global rate. Coastal seas are known to be more sensitive to global climate change, as the absorption of sunlight at the surface of shallow and turbid waters is higher (Belkin, 2009), but also among coastal seas, the temperature rise in the Baltic Sea region is extreme. Considering a longer time period (1957–2006) produces different results because the local minimum in the 1980s was lower in the Baltic Sea than in other large marine ecosystems. Thus, the total temperature increase during the last 50 years was smaller than that during the last 30 years.

Hence, it is of special interest to investigate why the temperature change in the Baltic Sea was so strong during the last 30 years. The air temperature in the Baltic Sea catchment area rose by 0.4 K/decade during 1970–2008 (BACC II Author Team, 2015; Lehmann et al., 2011), while the values for the northern Baltic Sea were even larger. The global change amounts to 0.177 K/decade (IPCC AR4, 2007a).

Several publications have dealt with satellite-derived SST trends, considering different periods and spatial means of the Baltic Sea (Belkin, 2009; Gustafsson et al., 2012; Lehmann et al., 2011; Siegel et al., 2006). In addition, many publications reported the strongest SST trends during the summer months (Lehmann et al., 2011; Siegel et al., 2006; Stramska & Białogrodzka, 2015). With monitoring data from the southern Baltic Sea, MacKenzie and Schiedek (2007a) showed that the summer SST increased 2–5 times faster between 1985 and the early 2000s than the global rate over the same period of time. Belkin (2009), Siegel et al. (2006), Lehmann et al. (2011), and Stramska and Białogrodzka (2015) calculated similar annual Baltic Sea mean SST changes of approximately 0.56–0.57 K/decade during 1982–2006 and 1990–2004 and 0.5 K/decade during 1990–2008 and 1982–2013.

Although many publications (e.g., Lehmann et al., 2011; MacKenzie & Schiedek, 2007a; Stramska & Białogrodzka, 2015) have analyzed the general evolution of the hydrographic state of the Baltic Sea, particularly the SST, and reported exceptionally strong temperature trends in that region, very few studies have dealt with the temperature variability and its atmospheric drivers in detail. Lehmann et al. (2011) examined a large increase in air temperature but also a decrease in cloud cover, which could be an important factor warming the Baltic Sea surface water. There is also evidence for increasing warm summer inflow events during the last decades bringing warm surface water from the North Sea to deeper areas of the Baltic Sea (BACC II Author Team, 2015; Leppäranta & Myrberg, 2009; Meier et al., 2006; Mohrholz et al., 2006). Thus, in 100 years, the bottom temperature at Bornholm Deep increased exceptionally fast (Fonselius & Valderrama, 2003). A sensitivity test showed that higher absorption rates due to increased turbidity led to higher temperatures at the surface (Löptien & Meier, 2011). Eutrophication led to increased algal blooms and a remarkable decrease in Secchi depth during the last 100 years (Laamanen et al., 2004). However, the strong trends in summer SST since 1880 cannot be explained by increased algal blooms alone (Löptien & Meier, 2011). Stramska and Białogrodzka (2015) found higher annual variability in shallow coastal areas with large riverine nutrient inputs.

Many publications have also looked at the connection between the North Atlantic Oscillation (NAO; e.g., Hurrell, 1995; Visbeck et al., 2001) and SST changes, which is strongest in winter (Lehmann et al., 2011; Stramska & Białogrodzka, 2015). The NAO describes the strength of the dipole between the Icelandic low and Azores high pressure systems and plays an important role in the large-scale circulation pattern over Northern Europe. However, the NAO is not always the dominant pattern representing the atmospheric variability of the Baltic Sea region (Kauker & Meier, 2003; Meier & Kauker, 2003). The Atlantic Multidecadal Oscillation (AMO; Knight et al., 2006) is another important index of large-scale internal climate variability and is represented by the mean SST averaged over the North Atlantic (Knight et al., 2006). The associated atmospheric and oceanic circulation has an impact on the climate in the Northern Hemisphere, including Europe and the Baltic Sea. The AMO is related to variations in the transport of warm water toward Europe (Pohlmann et al., 2006; Sutton & Hodson, 2005) via the Gulf Stream and North Atlantic Current. This effect is more pronounced during the summer season. The northward heat transport in the Atlantic is the reason that Europe is warmer than North America, although they are located at the same latitudes (Pohlmann et al., 2006). Hence, in phases with a high AMO (anomalous high SST over the North Atlantic), there is increased heat transport toward Europe. Börgel et al. (2018) showed that the AMO also has an effect on the Baltic Sea salinity.

Temperature variability, especially at the surface, affects the ecosystems of the Baltic Sea. For instance, SST is an important factor for the onset and spatial distribution of cyanobacterial blooms (Kanoshina et al., 2003; Neumann et al., 2012) and for the populations of some fish species (MacKenzie & Köster, 2004). The complex system of the Baltic Sea has changed in different ways during the last 160 years since the first observations of temperature, salinity, and Secchi depth were recorded. Numerous studies concerning the long-term changes in the Baltic Sea using observations (Fonselius & Valderrama, 2003; Winsor et al., 2001) as well as simulations (Meier & Kauker, 2003; Schimanke et al., 2014) were performed during the last two decades. This study uses simulations of two models of the physical and biogeochemical evolution of the Baltic Sea from 1850 to 2008 with the same atmospheric forcing variables to understand the changes in temperature variability of the Baltic Sea. The advantage of model simulations over observational data sets is that the former are dynamically consistent and provide better spatial and temporal resolution. This study is, to the best of our knowledge, the first attempt to analyze temperature trends of the Baltic Sea with respect to seasonal and spatial differences with model simulations as well as several observational data sets and

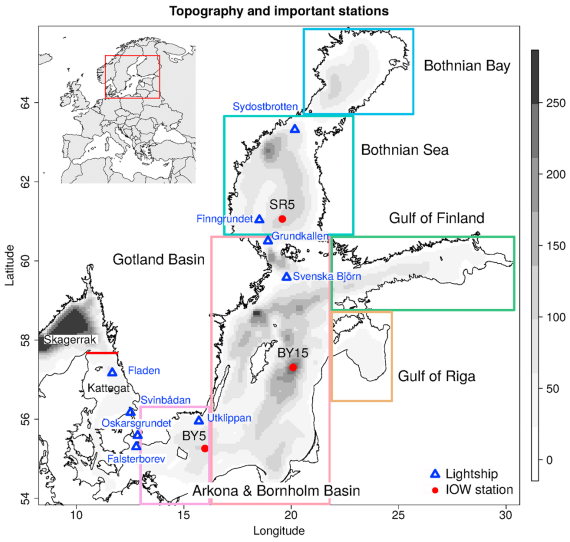

Figure 1. Bathymetry of the MOM setup with basins and stations (from the database of the Leibniz Institute for Baltic Sea Research IOW and lightships) used in this study. The red line between Kattegat and Skagerrak represents the boundary of the RCO model.

attribute the changes to variability in the atmosphere. We also provide a possible explanation of why the Baltic Sea warmed so quickly during 1982–2006.

In section 2, the model simulations, observations, and reconstructions used for the evaluation as well as the statistical methods are introduced. Section 3 presents simulated temperature trends and their evaluation relative to observations. Our results are also compared with the results from previous publications, and the trends are attributed to atmospheric forcing parameters. In sections 4 and 5, the results are discussed, and the conclusions of this study are drawn, respectively.

2. Data and Methods

2.1. Models

Two models were used. The Modular Ocean Model coupled with the Ecological ReGional Ocean Model (MOM-ERGOM; Neumann, 2000) and the Rossby Centre Ocean circulation model coupled with the Swedish Coastal and Ocean Biogeochemical Model (RCO-SCOBI; Eilola et al., 2009; Meier et al., 2003) were both forced with the same reconstructed High-Resolution Atmospheric Forcing Fields (HiResAFF) by Schenk and Zorita (2012). The model domains and bathymetry are shown in Figure 1. Both models use the same atmospheric forcing, river runoff, and bathymetry data. However, the latter data were interpolated to different grids with a different spatial resolution.

2.1.1. RCO-SCOBI

The RCO model is a Bryan-Cox-Semnter-type ocean circulation model coupled to a Hibler-type sea ice model (Meier et al., 1999, 2003). The horizontal and vertical resolutions are 3.7 km and 3 m, respectively. The subgrid-scale mixing in the ocean is parameterized using a k-ϵ turbulence closure scheme with flux boundary conditions (Meier, 2001). A flux-corrected, monotonicity-preserving transport scheme is embedded without explicit horizontal diffusion (Meier, 2007). The model domain comprises the Baltic Sea and Kattegat with lateral open boundaries in the northern Kattegat. In the case of inflow temperature, salinity, nutrients (phosphate, nitrate, and ammonium), and detritus, the values are nudged toward observed

climatological profiles, and in the case of outflow, a modified Orlanski radiation condition is used (Meier et al., 2003). Daily sea level variations in the Kattegat at the open boundary of the model domain were calculated from the meridional sea level pressure gradient across the North Sea using a statistical model (Gustafsson et al., 2012). The SCOBI model comprises the dynamics of nitrate, ammonium, phosphate, oxygen, hydrogen sulfide, three phytoplankton species (including nitrogen-fixing cyanobacteria), zooplankton, and detritus (Eilola et al., 2009). The sediment contains nutrients in the form of benthic nitrogen and benthic phosphorus. Processes including assimilation, remineralization, nitrogen fixation, nitrification, denitrification, grazing, mortality, excretion, sedimentation, resuspension, and burial are considered. With a simplified wave model, resuspension of organic matter is calculated (Almroth-Rosell et al., 2011). Fluxes of heat, incoming longwave and shortwave radiation, momentum, and matter between the atmosphere, ocean, and sea ice are parameterized using bulk formulae adapted to the Baltic Sea region (Meier, 2002). Inputs to the bulk formulae are state variables of the atmospheric planetary boundary layer, including 2-m air temperature, 2-m specific humidity, 10-m wind, cloudiness, and mean sea level pressure, and ocean variables such as SST, sea surface salinity (SSS), sea ice concentration, albedo, and water and sea ice velocities. A detailed description of the model setup can be found in Meier et al. (2018).

2.1.2. MOM-ERGOM

"The physical part of the model is based on the circulation model MOM (version 5.1) (Griffies, 2004) and has been adapted to the Baltic Sea with an open boundary condition to the North Sea and riverine freshwater input. The MOM is complemented with a sea ice model to estimate ice cover thickness and extent. The horizontal resolution of the model grid is approximately 5 km, while vertically, the model is resolved into 134 layers, with a layer thickness of 2 m" (Neumann et al., 2017).

Since the MOM is operated in an uncoupled manner (without an atmospheric model) in this application, the downward heat fluxes have to be prescribed. The longwave radiation is calculated according to Berliand and Berliand (1952) with an adjustment of the cloud coverage (Kondratyev, 1969). For shortwave radiation, we used the model by Bodin (1979).

Essentially, the ERGOM simulates the marine nitrogen and phosphorus cycles. Three functional phytoplankton groups are involved in primary production (large cells, small cells, and cyanobacteria). A dynamically developing bulk zooplankton variable provides grazing pressure on the phytoplankton. Dead particles accumulate in the detritus state variable. In the sedimentation process, a portion of the detritus is mineralized into dissolved ammonium and phosphate. Another portion reaches the sea bottom, where it accumulates as sedimentary detritus and is subsequently buried, mineralized, or resuspended into the water column, depending on the velocity of near-bottom currents. Under oxic conditions, some of the mineralized phosphate is bound by iron oxides and is thus retained in the sediment, becoming liberated when conditions become anoxic. Oxygen development in the model is coupled to biogeochemical processes via stoichiometric ratios, with oxygen levels in turn controlling processes such as denitrification and nitrification.

Additionally, we created a box model in the MOM (hereafter called MOMbox) by constructing a rectangular basin with 3×3 grid points and a flat bottom with a depth of 100 m. We positioned the box model in the Gotland Basin from 19.5°E to 20.5°E longitude and 57.0°N to 57.5°N latitude. To omit advectional processes, the horizontal ocean currents were set to 0. Since neither sporadic inflows through the Danish straits nor freshwater input from the rivers was considered in the 1-D model, the salinity profile had to be predescribed, while precipitation was maintained. In this manner, the box model was initialized each year with a new salinity profile to maintain the vertical stratification. We followed two approaches: One simulation used the same vertical salinity profile for each year, and the second used the salinity profile from the original simulation to meet the temporal variability in the salinity. The time series of SST, SSS, and bottom salinity of the box models are shown in the supporting information. The box model was driven by the same atmospheric forcing as in the previous simulations.

2.2. Forcing Data

The HiResAFF data set developed by Schenk and Zorita (2012) were used in this study. This data set was already used and evaluated in Gustafsson et al. (2012) and Meier et al. (2012). Schenk and Zorita (2012) applied the analogue method to assign regionalized reanalysis data to the few available observational stations in the early periods. In this manner, the authors obtained consistent multivariate forcing fields without artificial interpolation. Simulations of the Rossby Centre regional Atmosphere-Ocean (RCAO; Döscher et al., 2002) model with a $0.25° \times 0.25°$ spatial resolution and daily model output were performed, using

ERA40 reanalysis data (Uppala et al., 2005) during 1958–2007 as forcing variables. The fields for 2-m air temperature were taken from an atmosphere-only simulation with RCA3, which was driven by observed SSTs (Samuelsson et al., 2011). The generated pool of daily atmospheric forcing fields (analogue pool, 1958–2008) including air temperature, wind, relative humidity, total cloud cover, precipitation, and mean sea level pressure was assigned to available observations during 1850–1957 (reconstructed period) using the analogue method (Schenk & Zorita, 2012). This method has been tested using various settings of the analogue method and by comparing the results with reanalyzed data and observations, which indicated that the data set is reliable and robust. River runoff and riverine nutrient loads were reconstructed following Meier et al. (2012) and Gustafsson et al. (2012), respectively.

2.3. Observations

For model evaluation, long-term observations from various observational data sets were used. The in situ temperature and salinity observations from the Leibniz Institute for Baltic Sea Research Warnemünde (IOW) database (https://www.io-warnemuende.de/en_iowdb.html) provide profiles at the most important stations, while reconstructions such as the U.K. Meteorological Office Hadley Centre data set HadISST1 (Rayner et al., 2003; https://www.metoffice.gov.uk/hadobs/hadisst/data/HadISST_sst.nc.gz) and the Optimum Interpolation SST (OISST) Version 2 satellite data from the National Oceanic and Atmospheric Administration (NOAA; Reynolds et al., 2007,http://monitor.cicsnc.org/obs4MIPs/data/OISST/Monthly/) provided spatial information for the SST. The daily OISST (Reynolds et al., 2007; Stramska & Białogrodzka, 2015) data have a spatial resolution of 0.25° × 0.25° but are only available since 1982. Many satellite data provide only sea skin temperature, but with the so-called optimum interpolation method (Reynolds et al., 2007) the data can be interpolated to real sea surface water temperatures; thus, the data can be compared directly with model results. The HadISST1 data set is a reconstruction of merchant ship measurements, in situ observations, and values from other sources (MacKenzie & Schiedek, 2007b; Rayner et al., 2003) and provides only monthly data with a resolution of 1° × 1° but includes data collected since the 1870s. This data set has already been used for analyses in the Intergovernmental Panel on Climate Change (IPCC) report (IPCC AR5, 2013). Additionally, temperature measurements from Swedish lightships (Lindkvist & Lindow, 2006; http://smhi.diva-portal.org/smash/record.jsf?pid=diva2%3A947588&dswid=-8586) were used to verify simulations back to the 1860s. Sea ice data of the Baltic Sea were provided by the European Environment Agency (EEA; Baltic Sea ice data (FMI), 2017, https://www.eea.europa.eu/data-and-maps/daviz/maximum-extent-of-ice-cover).

To quantify the variability in surface air temperature (SAT), a long record of air temperature measurements in Stockholm collected at the old astronomical observatory since the 1750s was considered (Moberg et al., 2002; https://bolin.su.se/data/stockholm/homogenized_monthly_mean_temperatures.php).

In addition, time series of the large-scale NAO and AMO climate indices were used to attribute the Baltic Sea mean SST variability to external drivers. Long-term observations of the sea level pressure differences between Reykjavik, Iceland, and Gibraltar, Spain, constitute the NAO index, which is available from the Climatic Research Unit, University of East Anglia (Jones et al., 1997; https://crudata.uea.ac.uk/cru/data/nao/nao.dat). The AMO index is defined as the mean SST over −80°E to 0°E and 0°N to 60°N detrended by the global mean SST change and shows a periodicity of approximately 60 years, oscillating between high and low mean SST values. A time series of the AMO index based on the HadISST1 data set is available from the Royal Netherlands Meteorological Institute (KNMI) Climate Explorer (Kennedy et al., 2011; Trenberth & Shea, 2005, https://climexp.knmi.nl/data/iamo_hadsst_ts.dat).

2.4. Statistical Methods

The analysis of the data mentioned above was performed using either the Climate Data Operators (CDO, 2015) or the statistical program R (R Core Team, 2015), while many figures were created using the package "ggplot2" (Wickham, 2009).

In this paper, anomalies were calculated relative to the period 1981–2008 because of the shortest observational data set (OISST). Baltic Sea mean temperatures refer to areas east of 13°E longitude (Figure 1). In the figures, time series of temperature are low-pass filtered with a cutoff frequency of 10 years to visualize the long-term variability. However, the linear and multilinear regression analyses were performed using the unfiltered annual or seasonal (winter, December to February [DJF]; spring, March to May [MAM]; summer, June to August [JJA]; and autumn, September to November [SON]) mean. The linear regression analysis was performed using the general least square fit method by maximum likelihood, taking the autocorrela-

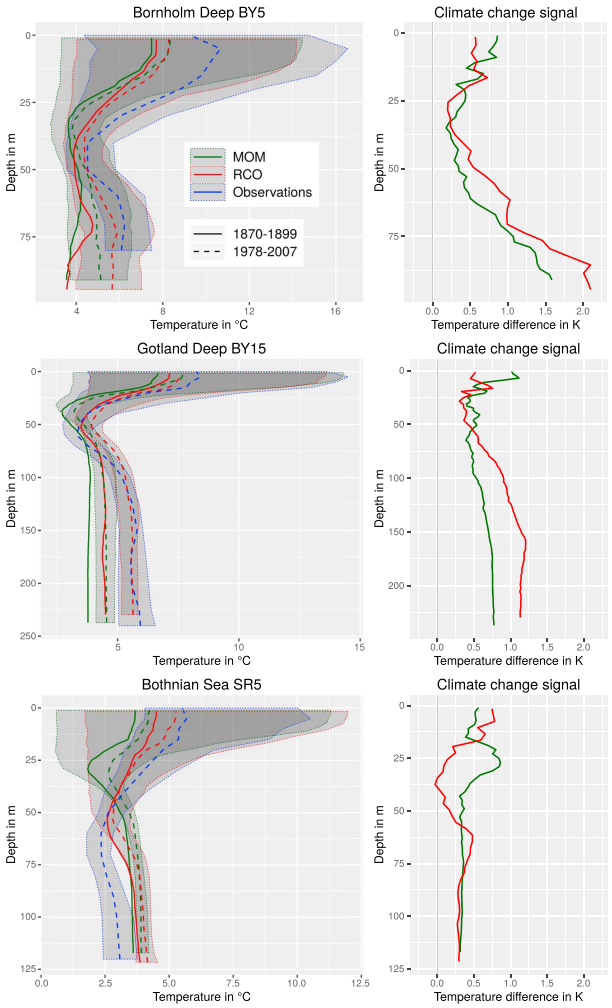

Figure 2. Profiles of simulated and observed temperatures in the Bornholm Deep (BY5), Gotland Deep (BY15), and Bothnian Sea (SR5). In the left column, for both simulations and observations, dashed and dotted lines show the median and the 25th and 75th percentiles during 1978–2007, respectively. In addition, the solid lines show median temperatures in the simulations during 1870–1899. In the right column, the simulated climate change signal in temperatures for the periods 1870–1899 and 1978–2007 is shown.

Table 1
Mean Annual Maximum Ice Extent in Observations and Simulations (in 10^6 m^2), Root-Mean-Square Error (RMSE), and Correlation (Cor) of Simulations Compared to Observations for the Whole Simulated Period (1850–2008), the Reconstructed Period (1850–1957), and the Period of the Analogue Pool (1958–2008)

	Mean			RMSE		Cor	
Time	Obs	RCO	MOM	RCO	MOM	RCO	MOM
1850–2008	198.5	165.8	293.9	74.8	117.1	0.79	0.79
1850–1957	205.4	172.5	301.8	83.5	123.3	0.76	0.76
1958–2008	183.8	151.7	277.0	52.0	102.9	0.88	0.89

tion at a time lag of 1 (alpha) into account, which is a measure of the internal variability and important for calculating realistic confidence intervals (Ribes et al., 2016). To determine alpha, the first 50 years of each time series were used, while for shorter time series such as the OISST or lightship data, the value for alpha of the corresponding time series in the model simulations was used. For the regression analysis, the R package "Linear and nonlinear effect models" (Pinheiro et al., 2016) was applied. The interpretation of significance levels based on the *p* value and the corresponding thresholds was carried out according to Box 1.1 ("Treatment of Uncertainties in the Working Group I") in the IPCC AR4 (2007a), while the null hypothesis was that no trend existed. Furthermore, the considered period for long-term trends (1856–2005) was chosen according to IPCC AR4 (2007a), while the short-term trends were calculated for the last 30 years in the simulation (1978–2007) without the record year 2008 (cf. Figure 12).

The correlation coefficient was calculated using Pearson's correlation, while its squared value was used to indicate the explained variance (Wilks, 2011).

Lastly, a ranking analysis was performed to determine which atmospheric drivers are most important for the variability in the Baltic Sea SST. Since air temperature explains most of the variability in the SST and is not stationary, the SST was subtracted by the residuals from a linear model fitting the SST to the SAT. The trend in air temperature dominated the time series of SST and thus masked other effects, which is why it was removed. To identify the second and third most important drivers of the SST, a cross-correlation analysis was applied because the effects of wind on the SST in upwelling areas is delayed by several days. For each grid point and variable (cloudiness, latent heat flux, and both wind components), the explained variance with a maximum time lag of 30 days was calculated. Finally, the variable explaining the most and second most variance was identified for each grid point.

3. Results

3.1. Evaluation of the Model Results

In situ observations from the IOW database were used to validate the temperature profiles at three exemplary stations from south to north (Bornholm Deep [BY5], Gotland Deep [BY15], and Bothnian Sea [SR5]; cf. Figure 1).

In Figure 2, the vertical mean temperature profiles for the period 1978–2007 show good agreement at the selected stations, which represent different vertical temperature gradients. The SST is underestimated in both models but is still within the standard deviation of the observations, except for the MOM in the Bothnian Sea. Simulated profiles are also shown for the period 1870–1899. The difference between the two periods in the model results represents the climate change signal and is shown in the right column. The change in temperature at every station and depth is positive. The largest changes occurred at Bornholm Deep with differences between 1.7 and 2 K. Toward the north, the changes become smaller for both the surface and deeper layers. In general, the changes at and below the thermocline are the smallest. In the deeper layers of the Gotland and Bornholm basins, saltwater inflows dominate the variability in water masses, with higher temperature changes than in the surface layer.

Since sea ice is a very important factor for the temperature variability in the Baltic Sea, in Table 1, the simulated maximum ice extent is compared with observations (Baltic Sea ice data (FMI), 2017). In this study, the total area of all grid points with a monthly mean sea ice concentration larger than 10% was summarized (Meier & Kauker, 2003). According to the observations, this was performed for the whole simulation area, while the RCO was corrected by 6.4% due to the data missing from the Skagerrak. The observed mean annual maximum ice extent during 1850–2008 amounts to 198.5×10^6 m^2, while the MOM produces a mean of

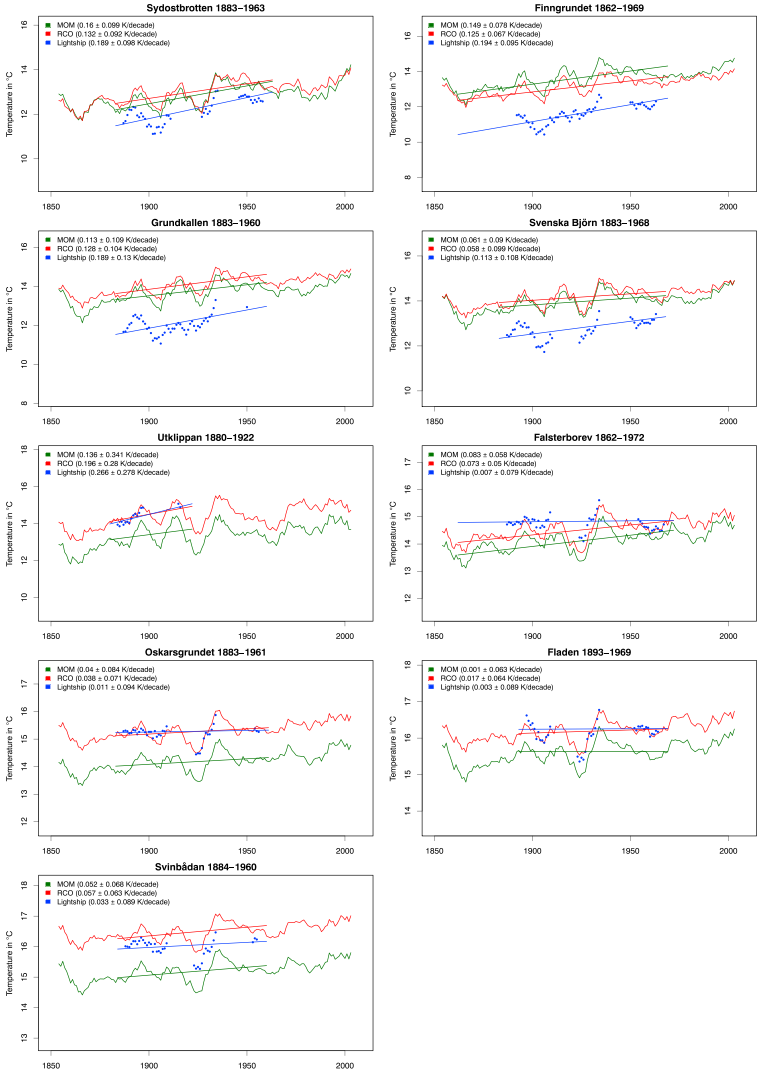

Figure 3. Simulated and observed 10-year running mean summer sea surface temperatures at lightship sites (cf. Figure 1) and corresponding linear trends during time periods with lightship observations.

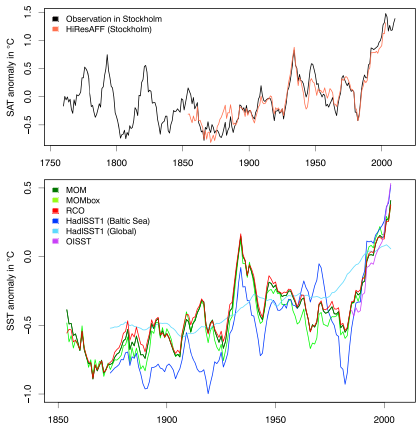

Figure 4. Ten-year running mean of simulated and observed time series. (top) SAT anomalies in Stockholm. (bottom) Baltic Sea mean and Gotland Deep SST anomaly. SAT = surface air temperature; SST = sea surface temperature.

293.9 × 10^6 m^2 and the RCO produces a mean of 165.8 × 10^6 m^2, with root-mean-square errors of 117.1 × 10^6 and 74.8 × 10^6 m^2, respectively. In addition, the variability in the annual maximum ice extent is underestimated in both models, while the MOM reproduces years with a completely ice-covered sea surface but overestimates the absolute mean, whereas the RCO result is closer to the observations but underestimates the mean sea ice extent.

Hereafter, mainly SST will be considered because the effects of the atmospheric forcing are most obvious for this variable. If measurements are available, these data sets (HadISST1 and OISST) will be included in the graphs to verify the detected long-term trends and variability.

To evaluate the long-term SST variability back to the 1860s, Figure 3 compares the 10-year running mean lightship measurements (Lindkvist & Lindow, 2006) with the corresponding simulated temperature at the closest model grid points. Since winter measurements during that time are very sparse, especially in the northern Baltic Sea, only the summer months (JJA) are considered.

The temperature variability is well reproduced by both models at all stations, while the mean error differs spatially. At the most northern station, Sydostbrotten, and in the southern areas (Utklippan and Falsterborev), the time series show good agreement, especially for the RCO in southern areas. However, in areas around the Archipelago Sea (Finngrundet, Grundkallen and Svenska Björn), the models show a large positive bias of 2–3 K. Nevertheless, at all stations, the variability in the measurements and simulations shows very good agreement. The estimated trends for periods when observations are available show qualitative agreement. All time series exhibit the highest trends at Utklippan and the lowest at Fladen. Due to the different time periods of measurements at each lightship, conclusions about the spatial distribution of trends cannot be made. With respect to missing values and long periods with gaps in the measurements, we conclude that the variability in summer SST is well reproduced by both simulations. Figure 3 emphasizes the differences between the models. In northern areas, the MOM simulates slightly higher (or almost identical) temperatures than the RCO model. However, the more south the station is, the less the simulated SST of the MOM follows the observations and the lower it is below the observations, while the RCO values and observations are very close.

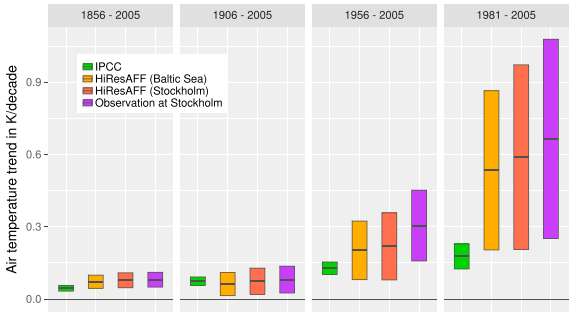

Figure 5. Trends in global (IPCC AR4, 2007a) and Baltic Sea annual mean surface air temperature in different periods. The global trends are taken from Table TS.6 of IPCC AR4 (2007b).

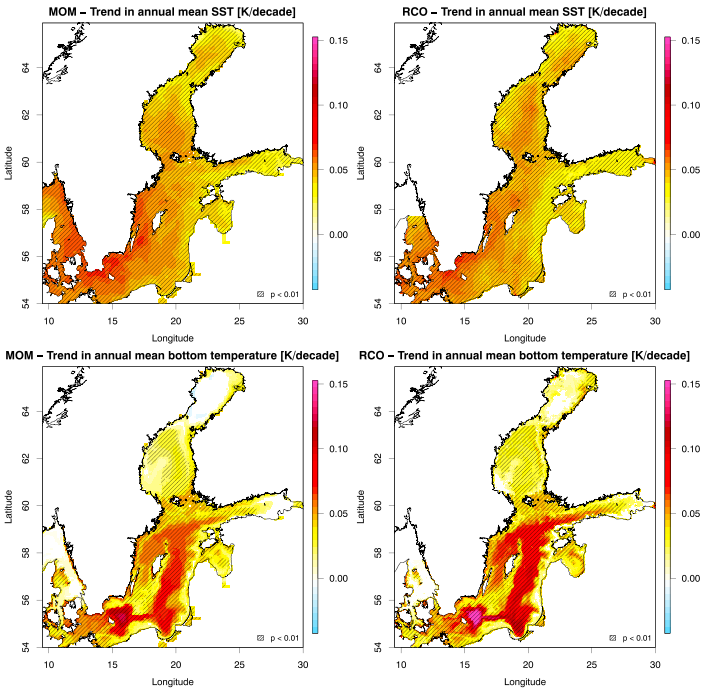

Figure 6. Maps of simulated 150-year linear SST (top row) and bottom temperature (bottom row) trends in Kelvin per decade for the MOM (left column) and RCO model (right column) during 1856–2005. Areas with a high significance level are hatched (p values lower than 0.01), and areas with no significance (p values larger than 0.33) are excluded (white). SST = sea surface temperature.

3.2. Detection of SST and Bottom Temperature Trends

Figure 4 shows the temperature development of both SAT (top panel) and SST (bottom panel) anomalies in the Baltic Sea region. The temperature variability in the forcing fits well with the long-term temperature measurement in Stockholm (Moberg et al., 2002). The correlation on a monthly scale amounts to 0.9. Additionally, the warm periods in the 1930s and 1990/2000s, which were repeatedly reported in recent studies (BACC II Author Team, 2015; IPCC AR4, 2007a), are clearly visible. The temperature after 2000 exceeded the highest values ever measured since 1756.

In the bottom panel of Figure 4, the results of both model simulations and observations from the Baltic Sea mean SST show good agreement, with correlations between 0.8 for the HadISST1 data set and 0.85 for the OISST data set. The mean error of the simulated SST amounts to −0.4 K for the MOM and +0.1 K for the RCO model, while the errors differ spatially, as seen in Figures 2 and 3. Nevertheless, the correlations between measurements and simulations are very high, which allows us to assess the temperature variability from continuous simulations since 1850.

Figure 5 summarizes Baltic Sea mean air temperature trends in different periods and data sets as well as the global trend reported in Table TS.6 by the IPCC AR4 (2007b). The temperature trends are consistently higher in the Baltic Sea than at the global scale. Especially during the last 25 years, the trends in the Baltic Sea were 3 times higher. The observations in Stockholm show even higher values. The error bars of the Baltic Sea air

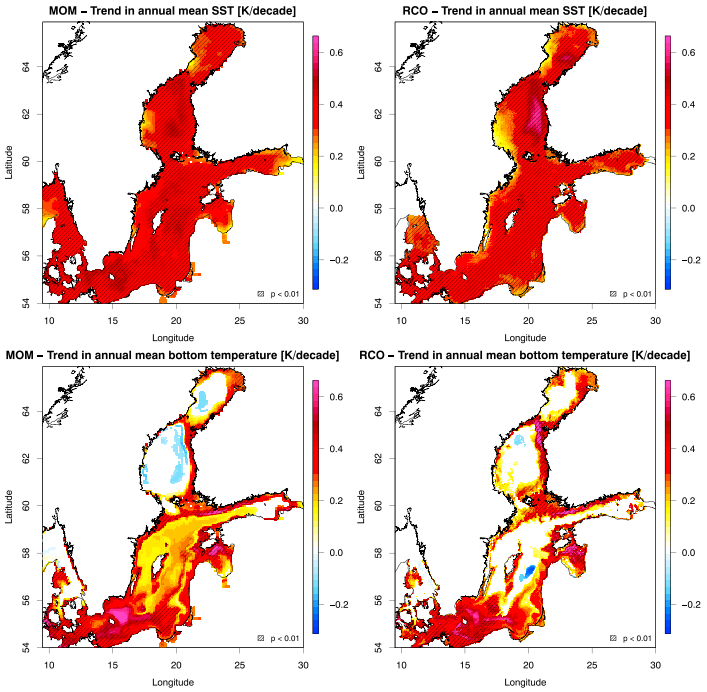

Figure 7. Maps of simulated 30-year linear SST (top row) and bottom temperature (bottom row) trends in Kelvin per decade for the MOM (left column) and RCO model (right column) during 1978–2007, as in Figure 6. SST = sea surface temperature.

temperature trends are much taller than those for the global trends due to the higher variability in the former (Figure 4). However, the overlap of the confidence intervals of global and Baltic Sea trends during the last period is very small or lacking (Stockholm observations), which shows that the increase in temperature in the Baltic Sea region during recent decades has been significantly larger than the global rate. However, the trends are underestimated in the forcing data.

The spatial distributions of the sea surface and bottom temperature trends during 1856–2005 with a significance level higher than 66% are shown in Figure 6. The models show comparable results regarding the spatial distribution, although the MOM simulated slightly stronger SST trends, especially in western areas, and the RCO model simulated stronger bottom temperature trends in the deeper parts of the Baltic Sea. The increase in the bottom temperature during 1856–2005 generally followed the bathymetry of the Baltic Sea. Most striking is the strong trend at Bornholm Deep, which amounts to almost 0.15 K/decade in the RCO model and 0.13 K/decade in the MOM and is comparable to the results in Figure 2.

Because the rate of global warming has increased in recent decades (cf. Figure 5), it is interesting to examine whether the spatial distribution changed. Figure 7 shows the same results as Figure 6 but for the period 1978–2007. Regions with relatively strong SST trends expanded to northern areas, while the RCO model simulates higher values than the MOM. In contrast, the SST trends at the Swedish coastline are weaker than those throughout the whole Baltic Sea, especially in the RCO simulation. The bottom temperature trends in deeper parts of the Baltic Sea are different from those shown in Figure 6. In deeper parts below 60 m, the

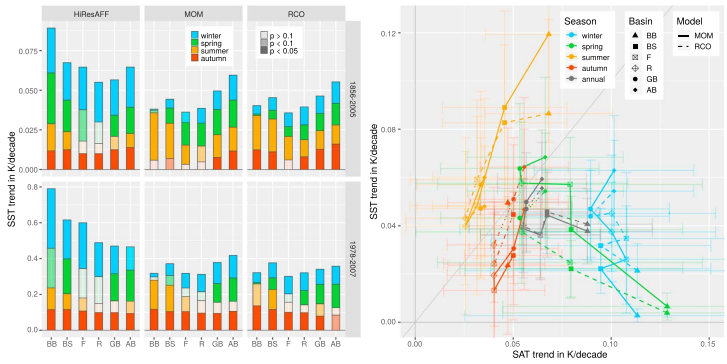

Figure 8. Seasonal and regional (basins, cf. Figure 1) trends in simulated SST and reconstructed air temperature. (left) The height of the bars represents the trend in the annual mean SST for two time periods (1856–2005 and 1978–2007). The height of the colored bars shows one quarter of the seasonal trends, representing the proportion of the seasons. (right) Scatter plot of SST over SAT trends with 90% confidence intervals; the gray line represents the direct relation between SAT and SST. Basins: BB = Bothnian Bay; BS = Bothnian Sea; F = Gulf of Finland; R = Gulf of Riga; GB = Gotland Basin; AB = Arkona Basin and Bornholm Basin. Seasons: DJF = winter; MAM = spring; JJA = summer; SON = autumn. SST = sea surface temperature; SAT = surface air temperature.

differences between the models are quite large, and most of the trends are not significant; in fact, even the signs of the trends differ. In shallow areas (up to a 50 m depth), the surface layer is well mixed, and the SST trends of this layer are homogeneous with depth, which can be seen for both models.

3.3. Seasonal Variability in SST and SAT

For a closer look at the seasonal and spatial variations of the SST and SAT trends, Figure 8 shows simulated and reconstructed trends in different seasons and subbasins (cf. Figure 1) of two different periods (150 and 30 years, cf. Figures 6 and 7). The significance levels are represented by the transparency of the colors, but strong trends mainly have a significance level higher than 90%. The bar plot (left column) shows both periods in direct comparison, while the height and the color of the bars represent the annual trend and the proportion of the seasonal trend (since all trends are positive), respectively. The trends during the last three decades are approximately 10 times stronger than those since 1856, which can also be seen in Figures 6 and 7.

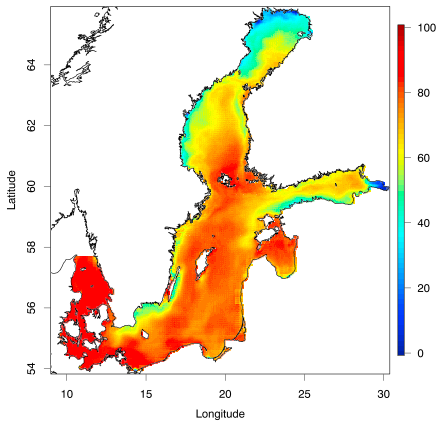

Figure 9. Explained variance (in percent) between the simulated annual mean sea surface temperature (RCO) and the forcing air temperature (HiResAFF) over the whole simulated period.

In addition, the scatter plot on the right-hand side of Figure 8 compares the trends in SST and air temperature during 1856–2005 directly, while the gray line represents the direct relation between them. Points above this line mean that the water temperature rises faster than the air temperature, and vice versa. The simulations show similar results, with small differences in the magnitude of the temperature increase between subbasins and seasons. The temperature trends show very high seasonal and regional variability. The strongest seasonal SST trends can be found in Bothnian Bay during summer, which are stronger than equivalent trends in the forcing air temperature (Figure 8), while the strongest SAT trends occur during winter and spring. The increase in air temperature is larger in northern than in southern areas in all seasons except autumn, especially in Bothnian Bay during winter and spring. Except in summer, the trends in SST are weaker than those in the SAT. The differences between SST and SAT are not significant, except in the northern basins (Bothnian Sea and Bothnian Bay) during summer (at least in the MOM), winter, and spring, with 90% confidence.

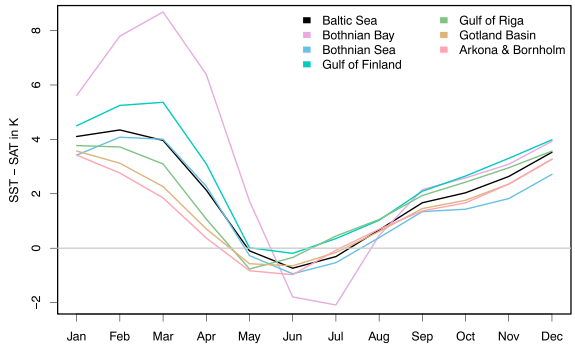

Figure 10. Annual cycle of the mean difference during 1850–2008 between SAT and SST in Kelvin for all basins and the whole Baltic Sea. The temperature difference between water and air is a measure of the sensible heat flux. SST = sea surface temperature; SAT = surface air temperature.

3.4. Attributing the SST Trends to the Atmospheric Forcing and Oceanographic Variables

The main driver of SST is the variability in the air temperature, with the highest explained variances on an annual scale of between 80% and 93% in the RCO model in the central areas of the Baltic Sea (Figure 9). The 1-D simulation of the MOMbox confirms this result (cf. bottom panel of Figure 4) because the long-term temporal variability does not change considerably when advectional processes are omitted. Furthermore, a sensitivity analysis by Meier et al. (2018) showed that the long-term trends in SST vanish if the interannual variability in the forcing SAT is removed. Already shown by Omstedt and Rutgersson (2000), the Baltic Sea thermodynamically behaves like a closed ocean basin, and heat fluxes through the Danish straits are small. Hence, the attribution is confirmed, and we can apply the statistical approach of removing the induced variability in the air temperature to identify other important atmospheric variables, which was not previously possible because the variability in the air temperature was too dominant.

However, the link between SST and SAT is not always apparent. As shown in Figures 8 and 9, SST trends show different behaviors among seasons and regions. Indeed, Figure 9 shows lower explained variances in coastal areas, river mouths, the Bothnian Sea, Bothnian Bay, and the Gulf of Finland. To explain the discrepancies between SAT and SST during the different seasons, Figure 10 shows the mean difference between air and water temperature, which is a measure of the sensible heat flux according to the applied bulk formula (Meier, 2002; Meier et al., 1999). In most of the seasons, the difference is positive, which means that the water is warmer than the air. Only at the end of spring and in early summer is the heat flux directed toward the water, while the difference is largest in Bothnian Bay, where the strongest SST trends can be found.

The other atmospheric variables affecting the SST are both wind components, the latent heat flux and cloudiness (representative of the radiation budget). Precipitation and air pressure are highly correlated with cloudiness and have no direct impact on the SST.

The results of the ranking analysis are presented in Figure 11. The 2-day simulation output of the RCO model is used because the effects of wind cannot be detected on a monthly scale as provided by the MOM since upwelling only occurs over time periods from several days to weeks (Lehmann & Myrberg, 2008). All results show high significance with p values less than 0.01.

The latent heat flux is the second most important factor after the SAT at all grid points, while the explained variances in the detrended SST amount to 30–50%. The third most important atmospheric variable explaining the SST variability differs spatially. The wind component parallel to the coastline is important in most of the coastal areas. These areas are known to be affected by wind-induced coastal upwelling. The other areas, mainly located in the open sea and in eastern areas, are dominated by cloudiness, that is, solar radiation. However, the variances explained by wind and cloudiness are very small (below 4%), while that explained by upwelling areas is the largest.

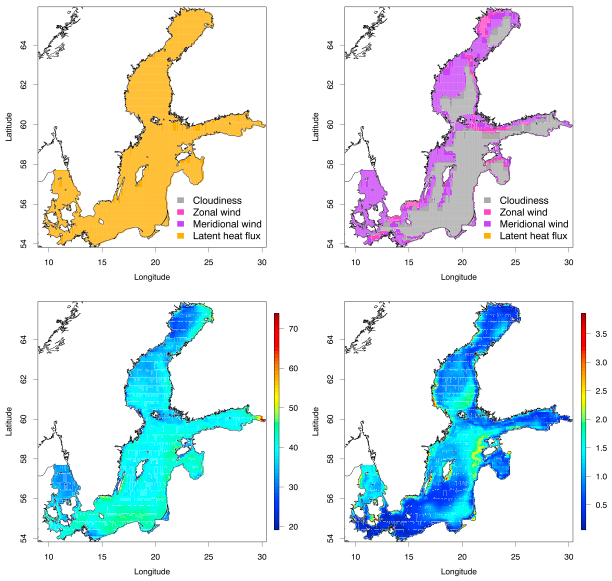

Figure 11. Results of the cross-correlation analysis of the detrended sea surface temperature (2-day output of the RCO model is used) with the wind components, latent heat flux, and cloudiness. Maps of atmospheric drivers (top row) with the highest (left column) and second highest (right column) cross correlations and related explained variances (in percent; bottom row).

3.5. Attribution to the NAO and AMO Climate Indices

In Figure 12, detrended and normalized time series for Baltic Sea mean SST (simulated by the RCO model) and the NAO and AMO climate indices are shown for 1901–2008. Since the winter NAO is the most prominent large-scale circulation pattern for Northern Europe (Lehmann et al., 2011), winter mean values (DJF) are considered. The main conclusions for the AMO are the same for the winter and annual means; hence, the annual mean values are considered for the AMO. Unfortunately, the AMO time series has many missing values before 1901, which is the reason the shorter time period is used. The explained variance amounts to 14% for the winter NAO index, while that for air temperature is much higher (25%). At an annual scale, the explained variance of AMO is quite small (5%). However, considering the long-term variability using the low-pass-filtered time series with a cutoff frequency of 10 years, 58% of the variability in the Baltic Sea mean SST can be explained by the AMO, while the NAO explains only 7%.

4. Discussion

4.1. Evaluation of SAT and SST

Comparing reconstructed and observed trends in Stockholm air temperature (Figure 5), we conclude that HiResAFF provide a good reconstructed air temperature over the Baltic Sea region but fails to resolve the high variability and slightly underestimates the trends in air temperature. We assume that the forcing data underestimate severe winters before 1958, as the analogues for the whole simulation period originate from a period that is already affected by a warmer climate. Thus, forcing fields for cold winters are scarce in the analogues. This assumption is supported by Table 1, which shows that the root-mean-square errors for simulated sea ice as well as the correlation are much better for the analogue pool period (1958–2007) than for the reconstructed period (1850–1957). Hence, the temperature variability and trends are presumably underestimated in the atmospheric forcing.

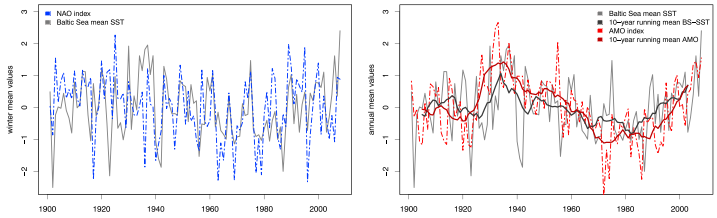

Figure 12. Detrended and normalized time series of the Baltic Sea annual mean SST and two climate indices. (left) Winter (December–February) mean NAO. (right) Annual and 10-year running mean AMO and SST. SST = sea surface temperature; NAO = North Atlantic Oscillation; AMO = Atlantic Multidecadal Oscillation.

The differences in simulated SST and sea ice can be explained by the different heat flux parameterizations and ice albedo values used in the models. Calculating the annual maximum sea ice extent using monthly mean values is an additional source of uncertainty because the observed time series is based on real-time observations with a higher temporal resolution (daily sea ice charts during winter; Baltic Sea ice data (FMI), 2017). Additionally, it should be mentioned that the models use different temperature outputs. The RCO model uses potential temperature, which is comparable to the in situ temperature in a shallow basin such as the Baltic Sea. In this simulation, the MOM applies the conservative temperature leading to a constant offset in comparison to the RCO model. Nonetheless, the correlation between measured air temperatures and reconstructed air temperatures is quite high, and the simulated SST trends fit quite well to the observations. In this manner, the simulations used in this study can be used to analyze the long-term variability in water temperature.

The profiles in Figure 2 show that both models mainly reproduce the vertical structure of temperature but do not meet the exact location and strength of the thermocline, especially in the Bothnian Sea. In addition, the SST is underestimated, presumably due to lack of observations in the winter.

Trend estimates from different publications using satellite SST data in different periods and spatial means of the Baltic Sea are reproduced with our data and compared in Figure 13. Generally, the simulated trends are consistent with the trends in the observations and in former publications, except for in the period 1990–2004 (Siegel et al., 2006). The trends of recent decades are generally slightly underestimated by both models. In Figure 4, higher variability in the HadISST1 data can be seen, which leads to lower temperatures during the colder period in approximately 1980 and higher temperatures in 2008. Since the forcing is not able to reproduce the large temporal variability, the large temperature increase since the 1980s is underestimated. In the

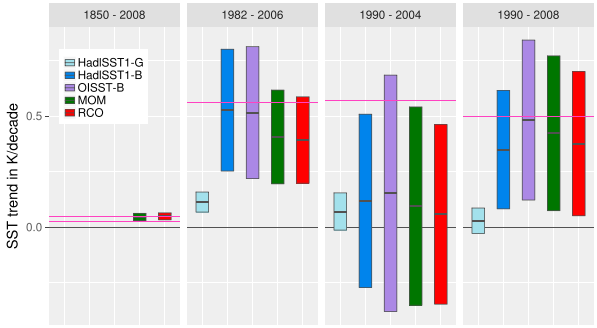

Figure 13. SST trends of the Baltic Sea in different data sets and publications (pink lines, from left to right: Gustafsson et al., 2012, Belkin, 2009, Siegel et al., 2006, and Lehmann et al., 2011). SST = sea surface temperature.

bottom panel of Figure 4, the global SST variability is additionally shown, emphasizing that the Baltic Sea follows the global trend but exhibits much higher variability, that is, stronger trends but also higher uncertainties. The periods of several previous studies were relatively short (15–30 years), although temperature trends in a varying system such as the Baltic Sea are very sensitive to the chosen start and end year. Regarding the high variability, small changes in the time period can lead to large differences in trend estimates, for example, results from the time period 1987–2001 fit well to the results of Siegel et al. (2006). All publications used different areas of the Baltic Sea, for example, Siegel et al. (2006) included Kattegat and Skagerrak, which could lead to different results. This assumption is confirmed by the comparison of OISST and HadISST1, which show similar results compared to the simulations performed in this study in all periods. In this manner, the analysis in this study is based on consistent basin boundaries and focuses on longer time periods of at least 30 years to increase the reliability of the results. Estimates from MacKenzie and Schiedek (2007a) were based on local observations, including observations from the North Sea, and therefore are not comparable to our results.

4.2. Processes Affecting Bottom Temperature

In contrast to the SST, the temperature variability at the bottom of the deeper parts of the Baltic Sea is mainly driven by inflowing water from the North Sea and mixing with upper layers. The strongest SST trends can be found in the shallow Danish straits in the southwestern part of the Baltic Sea (cf. Figure 6). The water in this area arrives at the bottom of the Baltic Sea during inflow events. Since the Danish straits are very shallow, the strong SST trends are projected to the deeper parts of the Baltic Sea. The inflows follow the bathymetry of the Baltic Sea, spread out from subbasin to subbasin, and accumulate at the bottom of the Baltic Sea. Presumably, due to mixing in the relatively shallow Arkona Basin, the trends in the Bornholm Basin are stronger.

Since there are only a few major Baltic inflows (MBIs) bringing surface water to the bottom of the Baltic Sea, the bottom water temperature changes abruptly during these events. During stagnation periods, mixing occurs mainly with the cold intermediate water layer (cf. Figure 2), and the bottom water temperature slowly decreases until the next MBI occurs. In this manner, the choice of the period for trend estimation is crucial and could lead to artificial temperature trends during relatively short time periods, which is why the bottom temperature trends in Figure 7 are different in the simulations.

4.3. Processes Affecting SST

The SST in the Baltic Sea is mainly driven by the air temperature, that is, the sensible heat flux. The smaller explained variances in Figure 9 can be explained by wind-induced upwelling and the seasonal formation of sea ice.

In Figure 6, the trends in annual mean SST during 1856-2005 show higher values in the southwestern parts of the Baltic Sea, with maxima along the Swedish coastline. This is a well-known upwelling area, which leads to the assumption that either the upwelling decreases due to changes in wind or the upwelled water from deeper layers (not necessarily from the bottom) is warmer. In this manner, the strong bottom temperature trends during 1856–2005 could explain the strong SST trends in the upwelling area. In contrast, the bottom temperature trends were weaker during 1978–2007 and could explain the weaker SST trends in the coastal upwelling area along the Swedish coast during 1978–2007 (Figure 7). The effect of the cold water brought from deeper layers to the sea surface leads to lower annual mean SST values in the affected coastal areas (not shown). In addition, the autocorrelation of SST in upwelling areas was quite high (not shown), which led to less accuracy in the statistical analyses. This analysis was performed for the whole time series; therefore, periods without upwelling were included and may have altered the results and reduced the explained variance.

The weaker SST trends and lower explained variances due to SAT in the northern areas can be explained by sea ice cover, which isolates the water column during winter, when the increase in air temperature is greatest. This result can also be seen in Figure 8. In winter and spring, when the water is frozen, the large increase in air temperature has no effect on the SST as long as the water temperature is still at the freezing point. However, the variability in the annual maximum sea ice extent can be explained by local winter mean values of the air temperature (Tinz, 1996).

The difference between SAT and SST, as a measure of the sensible heat flux, is decreasing with climate change in most seasons and basins (not shown). Presumably less sea ice cover and the shortening of the

sea ice season led to a closer relation between the atmosphere and ocean because the decoupling of their variabilities due to the freezing point vanishes with global warming. In accordance with the ice-albedo feedback, the effects are greatest in the melting season (JJA in Bothnian Bay, cf. Figure 8). As the sea ice vanishes earlier in the year, the SST in summer can increase faster than before because the time when radiative and sensitive heat fluxes are both directed to the ocean (cf. Figure 10) is extended. This mechanism explains the strong summer SST trends (cf. Figure 8) as well as the faster strengthening of annual SST trends in the northern basins (cf. Figures 6 and 7).

The MOM generally simulates higher SST trends than the RCO model. It has been discussed before that the sea ice extent is larger in the MOM than in the RCO model, leading to weaker trends in SST toward north in winter. This effect was also observed here, although the effect was reversed in summer. Nevertheless, the qualitative conclusions that could be drawn from the models are the same.

Furthermore, the 1-D simulation in Gotland Deep (MOMBox) without horizontal advection and a constant salinity profile (presented in Figure 4) shows that the long-term variability in SST is not affected by inflows from the North Sea and corresponding changes in stratification. Differences in Figure 4 are caused by the use of different spatial means (whole Baltic Sea and Gotland Deep). Since the vertical stratification of the Baltic Sea is highly variable, an additional simulation using time-dependent salinity profiles from the fully resolved simulation was performed. Figures S1 and S2 in the supporting information compare the box simulations to the original simulation.

Figure 12 attributes the SST variability of the Baltic Sea to the large-scale climate variability indices NAO and AMO. The variance explained by the NAO index is greater on an annual scale (winter mean) than that explained by the AMO. Hence, in the short term, the NAO is the dominant climate index explaining the Baltic Sea mean SST, especially in winter. It was previously shown that the winter NAO describes 40–50% of the sea level pressure patterns over the Baltic Sea area (Lehmann et al., 2011) and 27% of the annual maximum ice extent (Omstedt & Chen, 2001; Tinz, 1996). In this manner, the explained variances in the winter SAT and SST of 40% and 14%, respectively, seem reasonable since the correlation between SST and SAT is weaker during winter due to sea ice cover. In contrast, the AMO explains less than 10% of the variability in both SST and SAT on an annual scale but almost 60% on longer time scales. Analysis of the low-pass-filtered time series suggests that the high SST values in the 1930s and the low SSTs during the 1980s can be explained by the AMO. Variations in heat transport via ocean currents are much slower than atmospheric oscillations such as the NAO (Peixoto & Oort, 1992, scale analyses on pages 37–40). This difference is why the NAO exhibits strong correlations on an annual scale and the AMO exhibits strong correlations on a longer time scale with low-pass-filtered data with a cutoff period of 10 years.

As we have shown, air temperature is the most important forcing variable of SST in the Baltic Sea and thus leads to similar strong trends in water temperature. In this manner, the shift toward a positive phase in the AMO index since the 1980s enhanced the effect of the changing climate over Northern Europe and led to the strongest air temperature trends observed there during 1978–2005 (IPCC AR4, 2007b). Presumably, the trends will weaken when the AMO mode turns negative again. This weakening may already have been the case before the 1980s since the short-term temperature trends during the 1940s–1980s were negative. Unfortunately, the HiResAFF forcing data are only available until 2009; therefore, the following years, with a slight decrease in the rate of global warming, were not included, and the results of this study could not be compared with those in the latest IPCC report. However, a comparison with the prolonged time series ending in 2012 in the IPCC AR5 (2013) reveals that the strongest air temperature trends are no longer in Northern Europe. This result could indicate that the global warming hiatus is also caused by the AMO.

Belkin (2009) identified the North Sea, which is located in the same region in Northern Europe as the Baltic Sea, as the second fastest warming coastal sea worldwide. This identification emphasizes that the warming in this region was generally enhanced and supports our hypothesis that the AMO has an impact on the warming of the region. In comparison with the North Sea, the Baltic Sea is quite shallow, stratified, and almost completely surrounded by land, where global warming is generally more pronounced. In addition, higher latitudes have a higher sensitivity to a warming climate due to polar amplification (Holland & Bitz, 2003; Manabe & Stouffer, 1980). The combination of these factors may have enhanced the heating of the Baltic Sea even more.

4.4. Uncertainties

Sources of uncertainty include deficiencies in the analogue data due to biases of the used regional climate model and discontinuities due to the daily resolution and changing climate not represented by the observations used as analogue data. The impact of advection on temperature trends might be biased due to the coarse grid resolution of the models. In addition, we discussed saltwater inflows from the North Sea as a possible factor affecting bottom water temperature variability but did not analyze the effect of MBIs and small saltwater inflows statistically. In this study, it was assumed that the long-term variability in in situ and satellite measurements and model simulations were comparable.

5. Conclusions

From our results, we can draw the following conclusions:

1. The reconstructed annual mean SAT over the Baltic Sea during 1856–2005 increased by 0.06 and 0.08 K/decade in the central Baltic Sea and in Bothnian Bay, respectively. The strongest trends were identified during winter, including 0.09 K/decade in southwestern and 0.13 K/decade in northeastern basins.
2. During 1856–2005, the simulated (by both the MOM and the RCO model) Baltic Sea annual mean SST increased by 0.03 and 0.06 K/decade in northeastern and southwestern areas, respectively. In comparison to 1856–2005, during 1978–2007, the annual mean SST trends strengthened tenfold, with a mean value of 0.4 K/decade, while the trends in northeastern areas strengthened faster than those in southwestern areas. The strongest SST trends during 1856–2005 were found in the summer season in Bothnian Bay, including 0.09 and 0.12 K/decade in the RCO and MOM model, respectively. These trends exceed the corresponding trends in air temperature.
3. For 1856–2005, the strongest bottom temperature trends were found in Bornholm Basin, where the trends amounted to 0.13 and 0.15 K/decade in the MOM and RCO model, respectively.
4. The seasonal sea ice cover plays an important role in the Baltic Sea as it decouples the variability of the ocean and the atmosphere during winter and spring. Hence, in winter, the strong trends in air temperature were not recognized by the SST because the air temperature was below the freezing point. In contrast, during summer, the ice-albedo feedback led to stronger SST than SAT trends because the length of the warming period of the SST was extended.
5. The most important driver of the Baltic Sea SST variability during 1850–2008 was the SAT, with explained variances between 80% and 93% in the central areas of the Baltic Sea, directly followed by the latent heat flux, with 30–50% explained variances for the detrended SST. The third most important factors were wind-induced upwelling in coastal areas and cloud cover over the open sea. The long-term variability in the Baltic Sea SST was not affected by variability in stratification.
6. The strong SST trends since the 1980s can be explained by the superposition of global warming and a change from the cold to the warm phase of the AMO, while the polar amplification and higher sensitivity of shallow coastal seas enclosed by land may also have contributed to the stronger SST trends.

Acknowledgments

The research presented in this study is part of the Baltic Earth programme (Earth System Science for the Baltic Sea region; see http://www.baltic.earth). We wish to thank Torsten Seifert, who helped convert the RCO model results into netcdf format, as well as Marvin Lorenz, who helped organize additional simulations. Special thanks go to Aurélien Ribes (Toulouse, France) for help with the state-of-the-art trend analysis and its application in R. The authors acknowledge the North-German Supercomputing Alliance (HLRN) for providing high-performance computing (HPC) resources that contributed to the research results reported in this paper. Observational data used for model validation were taken from the Leibniz Institute for Baltic Sea Research Warnemünde (IOW), UK Meteorological Office Hadley Center, the National Oceanographic and Atmospheric Administration (NOAA), the European Environmental Agency (EEA), the Swedish Meteorological and Hydrological Institute (SMHI), and the Bolin Centre for Climate Research in Stockholm. Detailed information and weblinks are provided in section 2.3. The model data used in this study are available at the website (https://doi.io-warnemuende.de/10.12754/data-2018-0006). Finally, we would like to thank the reviewers for their comments and suggestions for the manuscript.

References

Almroth-Rosell, E., Eilola, K., Hordoir, R., Meier, H. E. M., & Hall, P. O. (2011). Transport of fresh and resuspended particulate organic material in the Baltic Sea—A model study. *Journal of Marine Systems*, *87*(1), 1–12.

BACC Author Team (2008). *Assessment of climate change for the Baltic Sea basin* (pp. 474). Verlag Berlin Heidelberg: Springer Science & Business Media.

BACC II Author Team (2015). *Second assessment of climate change for the Baltic Sea basin* (pp. 501). Verlag Berlin Heidelberg: Springer Science & Business Media..

Baltic Sea ice data (FMI) (2017). Maximum annual extent of ice cover in the Baltic Sea since 1720, MERI-Report Series by Finnish Meteorological Institute (FMI), EEA.

Belkin, I. M. (2009). Rapid warming of large marine ecosystems. *Progress in Oceanography*, *81*(1), 207–213.

Berliand, M., & Berliand, T. (1952). Measurement of the effective radiation of the Earth with varying cloud amounts. *Izvestiya Akademii Nauk SSSR, Seriya Geofizicheskaya*, *1*, 64–78.

Bodin, S. (1979). A predictive numerical model of the atmospheric boundary layer based on the turbulent energy equation. SMHI reports meteorology and climatology No. RMK 13, Swedish Meteorological and Hydrological Institute, Norrköping, Sweden.

Börgel, F., Frauen, C., Neumann, T., Schimanke, S., & Meier, H. E. M. (2018). Impact of the Atlantic Multidecadal Oscillation on Baltic Sea variability. *Geophysical Research Letters*, *45*, 9880–9888. https://doi.org/10.1029/2018GL078943

CDO (2015). Climate data operators. http://www.mpimet.mpg.de/cdo

Döscher, R., Willén, U., Jones, C., Rutgersson, A., Meier, H. E. M., Hansson, U., & Graham, L. P. (2002). The development of the regional coupled ocean-atmosphere model RCAO. *Boreal Environment Research*, *7*(3), 183–192.

Eilola, K., Meier, H. E. M., & Almroth, E. (2009). On the dynamics of oxygen, phosphorus and cyanobacteria in the Baltic Sea; a model study. *Journal of Marine Systems*, *75*(1), 163–184.
Fonselius, S., & Valderrama, J. (2003). One hundred years of hydrographic measurements in the Baltic Sea. *Journal of Sea Research*, *49*(4), 229–241.
Griffies, S. M. (2004). *Fundamentals of ocean climate models* (Vol. 518). Citeseer.
Gustafsson, B. G., Schenk, F., Blenckner, T., Eilola, K., Meier, H. E. M., Müller-Karulis, B., et al. (2012). Reconstructing the development of Baltic Sea eutrophication 1850–2006. *Ambio*, *41*(6), 534–548.
Holland, M. M., & Bitz, C. M. (2003). Polar amplification of climate change in coupled models. *Climate Dynamics*, *21*(3-4), 221–232.
Hurrell, J. W. (1995). Decadal trends in the North Atlantic Oscillation: Regional temperatures and precipitation. *Science*, *269*(5224), 676–678.
IPCC AR4 (2007a). *Contribution of Working Group I to the Fourth Assessment Report of the Intergovernmental Panel on Climate Change*. Cambridge, UK and New York: Cambridge University Press.
IPCC AR4 (2007b). Faq 3.1, figure 1, how are temperatures on earth changing?, climate change 2007: Working group i: The physical science basis.
IPCC AR5 (2013). *Climate change 2013: The physical science basis. Contribution of Working Group I to the Fifth Assessment Report of the Intergovernmental Panel on Climate Change*. Cambridge, UK and New York: Cambridge University Press. https://doi.org/10.1017/CBO9781107415324
Jones, P. D., Jonsson, T., & Wheeler, D. (1997). Extension to the North Atlantic Oscillation using early instrumental pressure observations from Gibraltar and south-west Iceland. *International Journal of Climatology: A Journal of the Royal Meteorological Society*, *17*(13), 1433–1450.
Kanoshina, I., Lips, U., & Leppänen, J.-M. (2003). The influence of weather conditions (temperature and wind) on cyanobacterial bloom development in the Gulf of Finland (Baltic Sea). *Harmful Algae*, *2*(1), 29–41.
Kauker, F., & Meier, H. E. M. (2003). Modeling decadal variability of the Baltic Sea: 1. Reconstructing atmospheric surface data for the period 1902–1998. *Journal of Geophysical Research*, *108*(C8), 3267. https://doi.org/10.1029/2003JC001797
Kennedy, J. J., Rayner, N. A., Smith, R. O., Parker, D. E., & Saunby, M. (2011). Reassessing biases and other uncertainties in sea surface temperature observations measured in situ since 1850: 2. Biases and homogenization. *Journal of Geophysical Research*, *116*, D14104. https://doi.org/10.1029/2010JD015220
Knight, J. R., Folland, C. K., & Scaife, A. A. (2006). Climate impacts of the Atlantic multidecadal oscillation. *Geophysical Research Letters*, *33*, L17706. https://doi.org/10.1029/2006GL026242
Kondratyev, K. Y. (1969). *Radiation in the atmosphere* (pp. 915). New York, NY; London.
Laamanen, M., Fleming, V., & Olsonen, R. (2004). Water transparency in the Baltic Sea between 1903 and 2004. HELCOM Indicator fact sheets,257–265.
Lehmann, A., Getzlaff, K., & Harlaß, J. (2011). Detailed assessment of climate variability of the Baltic Sea area for the period 1958–2009. *Climate Research*, *46*, 185–196.
Lehmann, A., & Myrberg, K. (2008). Upwelling in the Baltic Sea—A review. *Journal of Marine Systems*, *74*, S3–S12.
Leppäranta, M., & Myrberg, K. (2009). *Physical oceanography of the Baltic Sea*. Verlag Berlin Heidelberg: Springer Science & Business Media.
Lindkvist, T., & Lindow, H. (2006). Fyrskeppsdata: Resultat och bearbetningsmetoder med exempel från Svenska Björn 1883–1892.
Löptien, U., & Meier, H. E. M. (2011). The influence of increasing water turbidity on the sea surface temperature in the Baltic Sea: A model sensitivity study. *Journal of Marine Systems*, *88*(2), 323–331.
MacKenzie, B. R., & Köster, F. W. (2004). Fish production and climate: Sprat in the Baltic Sea. *Ecology*, *85*(3), 784–794.
MacKenzie, B. R, & Schiedek, D. (2007a). Daily ocean monitoring since the 1860s shows record warming of northern European seas. *Global Change Biology*, *13*(7), 1335–1347.
MacKenzie, B. R., & Schiedek, D. (2007b). Long-term sea surface temperature baselines—Time series, spatial covariation and implications for biological processes. *Journal of Marine Systems*, *68*(3), 405–420.
Manabe, S., & Stouffer, R. J. (1980). Sensitivity of a global climate model to an increase of CO_2 concentration in the atmosphere. *Journal of Geophysical Research*, *85*(C10), 5529–5554.
Matthäus, W., & Franck, H. (1992). Characteristics of major Baltic inflows: A statistical analysis. *Continental Shelf Research*, *12*(12), 1375–1400.
Meier, H. E. M. (2001). On the parameterization of mixing in three-dimensional Baltic Sea models. *Journal of Geophysical Research*, *106*(C12), 30,997–31,016.
Meier, H. E. M. (2002). Regional ocean climate simulations with a 3D ice-ocean model for the Baltic Sea. Part 1: Model experiments and results for temperature and salinity. *Climate Dynamics*, *19*(3), 237–253.
Meier, H. E. M. (2007). Modeling the pathways and ages of inflowing salt-and freshwater in the Baltic Sea. *Estuarine, Coastal and Shelf Science*, *74*(4), 610–627.
Meier, H. E. M., Andersson, H. C., Arheimer, B., Blenckner, T., Chubarenko, B., Donnelly, C., et al. (2012). Comparing reconstructed past variations and future projections of the Baltic Sea ecosystem—First results from multi-model ensemble simulations. *Environmental Research Letters*, *7*(3), 34005.
Meier, H. E. M., Döscher, R., Coward, A. C., Nycander, J., & Döös, K. (1999). *RCO - Rossby Centre regional Ocean climate model: Model description (version 1.0) and first results from the hindcast period 1992/93*. Norrköping, Sweden: SMHI, Swedish Meteorological and Hydrological Institute.
Meier, H. E. M., Döscher, R., & Faxén, T. (2003). A multiprocessor coupled ice-ocean model for the Baltic Sea: Application to salt inflow. *Journal of Geophysical Research*, *108*(C8), 3273. https://doi.org/10.1029/2000JC000521
Meier, H. E. M., Eilola, K., Almroth-Rosell, E., Schimanke, S., Kniebusch, M., Höglund, A., et al. (2018). Disentangling the impact of nutrient load and climate changes on Baltic Sea hypoxia and eutrophication since 1850. *Climate Dynamics*, 1–22. https://doi.org/10.1007/s00382-018-4296-y
Meier, H. E. M., Feistel, R., Piechura, J., Arneborg, L., Burchard, H., Fiekas, V., et al. (2006). Ventilation of the Baltic Sea deep water: A brief review of present knowledge from observations and models. *Oceanologia*, *48*(S), 133–164.
Meier, H. E. M., & Kauker, F. (2003). Modeling decadal variability of the Baltic Sea: 2. Role of freshwater inflow and large-scale atmospheric circulation for salinity. *Journal of Geophysical Research*, *108*(C11), 3368. https://doi.org/10.1029/2003JC001799
Moberg, A., Bergström, H., Krigsman, J. R., & Svanered, O. (2002). Daily air temperature and pressure series for Stockholm (1756–1998). In *Improved understanding of past climatic variability from early daily European instrumental sources* (pp. 171–212). Springer.

Mohrholz, V., Dutz, J., & Kraus, G. (2006). The impact of exceptionally warm summer inflow events on the environmental conditions in the Bornholm Basin. *Journal of Marine Systems*, *60*(3), 285–301.
Neumann, T. (2000). Towards a 3D-ecosystem model of the Baltic Sea. *Journal of Marine Systems*, *25*(3), 405–419.
Neumann, T., Eilola, K., Gustafsson, B., Müller-Karulis, B., Kuznetsov, I., Meier, H. M., & Savchuk, O. P. (2012). Extremes of temperature, oxygen and blooms in the Baltic Sea in a changing climate. *Ambio*, *41*(6), 574–585.
Neumann, T., Radtke, H., & Seifert, T. (2017). On the importance of major Baltic inflows for oxygenation of the central Baltic Sea. *Journal of Geophysical Research: Oceans*, *122*, 1090–1101. https://doi.org/10.1002/2016JC012525
Omstedt, A., & Chen, D. (2001). Influence of atmospheric circulation on the maximum ice extent in the Baltic Sea. *Journal of Geophysical Research*, *106*(C3), 4493–4500.
Omstedt, A., & Rutgersson, A. (2000). Closing the water and heat cycles of the Baltic Sea. *Meteorologische Zeitschrift*, *9*(1), 59–60.
Peixoto, J. P., & Oort, A. H. (1992). *Physics of climate*. New York, NY: American Institute of Physics.
Pinheiro, J., Bates, D., DebRoy, S., Sarkar, D., & R Core Team (2016). nlme: Linear and nonlinear mixed effects models, R package version 3.1-128.
Pohlmann, H., Sienz, F., & Latif, M. (2006). Influence of the multidecadal Atlantic meridional overturning circulation variability on European climate. *Journal of Climate*, *19*(23), 6062–6067.
R Core Team (2015). *R: A language and environment for statistical computing*. Vienna, Austria: R Foundation for Statistical Computing.
Rayner, N. A., Parker, D. E., Horton, E. B., Folland, C. K., Alexander, L. V., Rowell, D. P., et al. (2003). Global analyses of sea surface temperature, sea ice, and night marine air temperature since the late nineteenth century. *Journal of Geophysical Research*, *108*(D14), 37. https://doi.org/10.1029/2002JD002670
Reynolds, R. W., Smith, T. M., Liu, C., Chelton, D. B., Casey, K. S., & Schlax, M. G. (2007). Daily high-resolution-blended analyses for sea surface temperature. *Journal of Climate*, *20*(22), 5473–5496.
Ribes, A., Corre, L., Gibelin, A.-L., & Dubuisson, B. (2016). Issues in estimating observed change at the local scale—A case study: The recent warming over France. *International Journal of Climatology*, *36*(11), 3794–3806.
Samuelsson, P., Jones, C. G., Willén, U., Ullerstig, A., Gollvik, S., Hansson, U., et al. (2011). The Rossby Centre Regional Climate model RCA3: Model description and performance. *Tellus A*, *63*(1), 4–23.
Schenk, F., & Zorita, E. (2012). Reconstruction of high resolution atmospheric fields for northern Europe using analog-upscaling. *Climate of the Past*, *8*, 819–868.
Schimanke, S., Dieterich, C., & Meier, H. E. M. (2014). An algorithm based on sea-level pressure fluctuations to identify major Baltic inflow events. *Tellus A*, *66*, 23452.
Siegel, H., Gerth, M., & Tschersich, G. (2006). Sea surface temperature development of the Baltic Sea in the period 1990–2004. *Oceanologia*, *48*(S), 119–131.
Stramska, M., & Białogrodzka, J. (2015). Spatial and temporal variability of sea surface temperature in the Baltic Sea based on 32-years (1982–2013) of satellite data. *Oceanologia*, *57*(3), 223–235.
Sutton, R. T., & Hodson, D. L. R. (2005). Atlantic Ocean forcing of North American and European summer climate. *Science*, *309*(5731), 115–118.
Tinz, B. (1996). On the relation between annual maximum extent of ice cover in the Baltic Sea and sea level pressure as well as air temperature field. *Geophysica*, *32*(3), 319–341.
Trenberth, K. E., & Shea, D. J. (2005). Atlantic hurricanes and natural variability in 2005. *Geophysical Research Letters*, *33*, L12704. https://doi.org/10.1029/2006GL026894
Uppala, S. M., Kållberg, P. W., Simmons, A. J., Andrae, U., Bechtold, V. d., Fiorino, M., et al. (2005). The ERA-40 re-analysis. *Quarterly Journal of the Royal Astronomical Society*, *131*(612), 2961–3012.
Visbeck, M. H., Hurrell, J. W., Polvani, L., & Cullen, H. M. (2001). The North Atlantic Oscillation: Past, present, and future. *Proceedings of the National Academy of Sciences*, *98*(23), 12,876–12,877.
Wickham, H. (2009). *ggplot2: Elegant graphics for data analysis*. Verlag New York: Springer.
Wilks, D. S. (2011). *Statistical methods in the atmospheric sciences* (Vol. 100). Oxford; Waltham, MA: Academic Press.
Winsor, P., Rodhe, J., Omstedt, A., et al. (2001). Baltic Sea ocean climate: An analysis of 100 yr of hydrographic data with focus on the freshwater budget. *Climate Research*, *18*(1/2), 5–15.

Supporting Information for "Temperature variability of the Baltic Sea since 1850 and attribution to atmospheric forcing variables"

Madline Kniebusch[1], **H.E. Markus Meier**[1,2], **Thomas Neumann**[1], **Florian Börgel**[1]

[1]Leibniz Institute for Baltic Sea Research Warnemünde, Rostock, Germany

[2]Swedish Meteorological and Hydrological Institute, Norrköping, Sweden

Additional Supporting Information about the box simulations

The figures of the Supplementary material compare the results of the reference MOM simulation as used in the publication (MOM (original)) with results of the two box simulations. MOMBox is the simulation shown in Figure 4 in the paper and uses constant salinity profiles from 1850 for each year. MOMBox2 uses time-dependent annual salinity profiles. Figure S1 shows the temporal evolution of SSS in all simulations at Gotland Deep and Figure S2 shows a scatter plot of the SST of the box simulations over the original simulation for Gotland Deep.

Since the initialization profile from 1850 shows lower SSS, MOMBox generally has lower SSS values. However, the different initializations regarding the salinity profile do not change the simulated SST significantly.

Corresponding author: Madline Kniebusch, madline.kniebusch@io-warnemuende.de

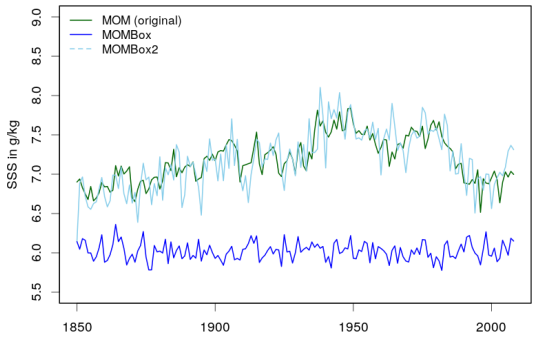

Figure S1. Annual mean of simulated SSS at the station Gotland Deep (lon: 20E, lat: 57.3N) from MOM, MOMBox and MOMBox2

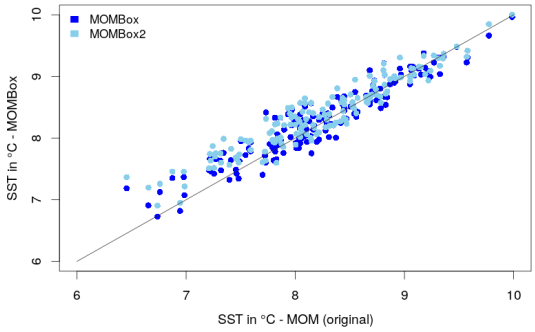

Figure S2. Annual mean of simulated SST at the station Gotland Deep (lon: 20E, lat: 57.3N) from MOM, MOMBox and MOMBox2